Tissue signals regulating commensal-specific $CD8^+$ T cells

Tayla M. Olsen

A dissertation
submitted in partial fulfillment of the
requirement for the degree of

Doctor of Philosophy

University of Washington
2026

Reading Committee:
Oliver J. Harrison, Chair
Meghan Koch
Jessica Hamermam

Program Authorized to Offer Degree:
Molecular and Cellular Biology

©Copyright 2026
Tayla M. Olsen

University of Washington

Abstract

Tissue signals regulating commensal-specific $CD8^+$ T cells

Tayla M. Olsen

Chair of the Supervisory Committee:

Oliver J. Harrison

Department of Immunology; Molecular and Cellular Biology

A central challenge of host-microbiota mutualism is the need to balance antigen-specific immune recognition with durable tolerance. Commensal-specific T cells must be restrained under homeostatic conditions to prevent inappropriate tissue damage, while retaining the capacity to respond during infection or tissue injury. The intestinal epithelium harbors a large population of microbiota-dependent $CD8\alpha\beta^+$ T cells whose antigen specificity and regulation are ill-defined. Furthermore, how epithelial signals are integrated to maintain antigen-experienced $CD8^+$ T cells in a non-pathogenic state, particularly in the context of commensal colonization and continuous microbial antigen exposure, remains an open question. Despite their increasing implication in intestinal-immune pathologies, $CD8^+$ IEL have remained understudied largely due to lack of tools to track this enigmatic population. My thesis research aimed to gain mechanistic understanding of how commensal-specific $CD8^+$ T cell responses are induced, regulated, and maintained. To do this, I identified and cloned a $CD8^+$ T cell receptor (TCR) specific to a gut microbe, enabling granular characterization of the mechanisms by which commensal-specific $CD8^+$ IEL are restrained in the healthy gut, and how this restraint is lost during chronic intestinal inflammation.

By identifying MHCIa-restricted TCRs and generating tetramers against the gut commensal Segmented Filamentous Bacteria, I was able to demonstrate that a single commensal species drives a clonally expanded, antigen-specific CD8αβ$^+$ T cell population within the intraepithelial lymphocyte (IEL) compartment. Mechanistically, the intestinal epithelium coordinates coincident signals governing this population: peptide:MHC-dependent TCR engagement drives IEL accumulation, while αvβ6-mediated TGFβ activation restrains effector cell differentiation. Perturbation of epithelial cell-mediated TGFβ activation diverts commensal-specific CD8$^+$ T cells toward inflammatory differentiation states transcriptionally convergent with those observed in ulcerative colitis. The intestinal epithelium thus functions as a dual-signal organizer of commensal-specific CD8$^+$ T cell responses, coupling differentiation to restraint through spatially coincident molecular cues. Altogether, these findings reframe intestinal tolerance not as an absence of commensal-specific immunity, but as epithelially enforced restraint of commensal-specific CD8$^+$ T cells and identify the αvβ6-TGFβ axis as a critical checkpoint whose disruption tips the balance from homeostasis to inflammation.

“We cannot fully understand the lives of animals without understanding our microbes and our symbiosis with them…They contribute to our lives in profound and wide-ranging ways: no corner of our biology is untouched. If we ignore them, we are looking at our lives through a keyhole.”

-Ed Yong

I Contain Multitudes

Table of Contents

Dedication

To the small moments in life. The in-between times that are often forgotten and overlooked in the busyness and noise. Life happens in these moments and they should be treasured. Stop and smell the roses or at least look at the birds.

Acknowledgements

When I started graduate school, I had plans to use my ample experience to complete a project quickly and move to the next steps in my career. This was folly. Not because my experience did not aid in advancing my project but because I decided to answer a hard question and I thought it would be easy (or easier, anyway). I underestimated the convolutions of scientific pursuit, thinking instead that by willing it so, steady progress would be made on one project from the start. In fact, several well-conceived projects did not bear fruit, and the project that "stuck" was stumbled upon almost by chance – though in retrospect, I think Ollie knew what he was doing and knew to have me look in the right place. Graduate school demands the belief in success with simultaneous adaptability and resiliency in the face of almost constant failure. This mindset and drudgery demand bull-headed stubbornness, something I excel at, and a supervisor that has patience with same, something Ollie excels at.

Through his support and dry English humor, Ollie has made this all possible. Not just by inviting me into his lab to pursue my PhD by rote, but by partnering with me to explore something about whose ending we were unsure and by being a source of reassurance, encouragement, and guidance in all aspects of this journey. I cannot understate how important these qualities are in a mentor; to be able to guide without control, shape without force, and listen without judgement are marks of true mentorship and I was so fortunate to experience that in Ollie's lab. Thank you!

I would also not be where I am without the scientific environment that the rest of the lab provides. Collaboration, sharing of ideas and musings are all integral parts of what makes science enjoyable and possible, and I need to thank members of the lab for that. Sheenam who has

offered her opinion and her ear on enumerable occasions when I just needed to bounce something off someone or share an exciting or puzzling piece of data. We have been partners in SFB-crime the last 5+ years and it has been an absolute pleasure to be her friend and colleague. Sam, Viviana, and Addie who have been powerhouses of genotyping have made my project immeasurably easier by doing the tedious and critical tasks of animal husbandry and who have all helped me learn to be a better mentor and teacher myself. To Hannah who is always willing to listen to my rambling thoughts. And to all past and present members of the Harrison lab who have helped me grow and have taught me a lot about myself, though you may not know it: Thank you!

I would be remiss if I did not thank everyone at BRI for their feedback over the years and for sharing reagents, their time, and expertise. They make science easier and more enjoyable. A thanks to my committee for being supportive through all the iterations of my PhD project, especially to Josh, who is probably sick of hearing about T cells. And to my reading committee for taking their time to give me feedback on this manuscript. To the MCB administrators and directors who make it the wonderful Program it is. I also need to acknowledge the mice, who give their lives for science and are the reason we know so much about immunology. We should always respect their sacrifice and contribution.

I, of course, need to thank my past mentors, Drs. Michael Cox, Angela Gruber, Sean Murphy, and Anthony Rongvaux who have all supported me as an independent scientist and have taught me so much about what it takes. Some of you believed in me before I did, thank you.

I also need to thank my gal pals “The Coven”, for being such smart and supportive women, who know what grad school is like and who have cheered me on throughout. And to friends I’ve met at the climbing gym, who have helped me keep everything in perspective and kept me grounded when science was hard. I need to also thank my family: my mom and cousin Jennifer, and especially my sister, Tannis, who always lifts my spirits and listens with compassion. And to my husband’s family, especially Susie, who makes life better and whose support has meant the world to me.

I want to thank my dog, Rufus, for being a constant companion and for reminding me to enjoy life's small moments and to treasure each day. It is easier to shrug off a bad day of experiments, when you have a warm dog to snuggle. And finally, I need to thank my husband, Andrew. I would not be here without his love and partnership. I am so grateful to have him in my life. It is hard to articulate all the ways in which he makes life wonderful; by making me coffee every morning to tolerating me coming home late from a day that got away from me and having dinner and a hug waiting, he demonstrates his support every day.

List of Figures and Tables

Chapter 1

Chapter 2

Chapter 3

List of common abbreviations

IEC: intestinal epithelial cell
IEL: intraepithelial lymphocytes; nIEL: natural IEL; pIEL: peripherally-induced IEL
LP: lamina propria
MLN: Mesenteric lymph node
TCR: T cell receptor
DC: dendritic cell
APC: antigen presenting cell
MHC: major histocompatibility complex; HLA: human leukocyte antigen
TL: thymic leukemia-antigen (an MHCIb molecule)
IBD: inflammatory bowel disease
SNPs: short nucleotide polymorphisms
SFB: segmented filamentous bacteria
scRNAseq: single-cell RNA sequencing

CHAPTER 1: Introduction

Bacteria appeared on Earth an estimated 3.5 billion years ago, consequently all eukaryotic life has evolved in the presence of microbes. In fact, it is an accepted hypothesis that all eukaryotes exist due to the merging of bacteria with archaea which became the first organelle, the mitochondria, around 2 billion years ago[1]. And of course, aside from this amalgamation event, microbes interact in all environments with both unicellular and multicellular organisms in a variety of capacities to exploit resources for survival. Mammals, having arisen from the first common eukaryotic ancestor surrounded by microbes, have evolved close relationships with symbionts throughout the billions of years of divergence. Some ancient relationships with microbes are even integral to our identity as placental mammals[2,3]. Through evolutionary history, these interactions take on various flavors, depending on the organisms in question and the degree of inter-reliance, but they all fall under the umbrella of symbiosis; mutualism results when both organisms benefit, commensalism results when neither organism is harmed nor helped, and parasitism results when one organism benefits at the expense of the other[4–6]. These can be further classified into obligate symbiosis or facultative symbiosis.

The term “microbiota” is the symbioses found in all multicellular organisms and includes bacteria, viruses, fungi, and protists and was originally coined in 2001[7]. In relation to mammalian microbiota, for simplicity, I will use this term to refer generally to the ecology of bacterial species that we play host to. Many of these species are either mutualists or commensals and I will refer to these microbes as commensals to remain agnostic of their interactions with the host and what benefit they might, in turn, receive. This inherent ecology and the interconnectedness of the microbiota add a layer of difficulty in studying it. Additionally, some of these microbes can be isolated and grown in a pure liquid culture while many others cannot grow without the nutrients provided by other microbes or the intestinal epithelium that furthers this difficulty.

Accompanying the increased complexity of multicellular organisms is a complex system of molecular and cellular mechanisms whose function is to distinguish “self” from “non-self” on

the molecular level to maintain meta-organismal health and, through billions of years of evolutionary history, has become the immune system as we understand it today. As you can imagine, the immune system's role in distinguishing self from non-self is complicated where bacterial symbionts are concerned and maintains a careful balance between immunity and tolerance[8]. In fact, as the microbiota inhabit all barrier surfaces of the body, including the skin, lung, and gut, they have been described as "extended self"[9]. So rather, one could reframe the immune system's role in this regard as distinguishing "harmful" from "not-immediately harmful" and tuning the magnitude of the immune response against non-invasive, potentially beneficial microbes to maintain tissue health and avert immune pathology. Thus, it is likely that the immune system evolved to support and maintain these commensal bacteria for their benefits. Though much of our understanding of immunity is through the lens of pathogen infection, there is only an estimated 500 to 1000 species of bacteria that cause significant clinical human disease and these encounters are generally rare and transient[10,11], whereas commensal bacteria species are estimated to be around 10,000 and are encountered constantly[12]. I offer these musings because it is important to keep these aspects of immunity and bacterial commensalism in mind when thinking about how immunity against the microbiota could become pathogenic and lead to chronic inflammation – where the line between self and non-self gets blurred.

Overview of immunity – with a focus on T cell diversity and selection

The immune system is composed of two pillars, the innate and the adaptive, which work together in all aspects of organismal biology to achieve homeostasis – in the truest sense of the word, meaning to maintain stable conditions for survival. Detecting potential pathogens, clearing infection, repairing tissues, and exerting tolerance to the microbiota or chronic infection are all shared responsibilities of the immune system. A major arm of the innate immune system is made up of myeloid cells that express a suite of pattern-recognition-receptors (PRRs) that recognize microbe-associated molecular patterns (MAMPs) and damage-associated molecular patterns

(DAMPs), which sense both non-eukaryotic structures (like lipopolysaccharide in bacterial cell walls) and ectopic locations of shared molecules (like cytoplasmic DNA or extracellular ATP) as a first line of defense to detect and clear invasive microbes or sense tissue damage[13]. Specialized myeloid cells of the innate immune system called dendritic cells (DCs) take up foreign proteins from the site of detection, migrate to lymph nodes, and present processed peptides on MHC molecules to activate naïve T cells, thus initiating activation or "priming" and expansion of the adaptive pillar of the immune system. There will be more discussion on this process in Chapter 3, so for now, suffice it to say that the innate immune system first responds to alterations in homeostasis and alerts adaptive responses to amplify the response according to the magnitude of inflammation or damage initially detected[13].

Adaptive immunity consists of B cells and T cells that both express highly variable receptors whose diversity is not genetically encoded but arises through several random processes, including gene recombination and conversion, base editing, and random pairing of receptor subunits, together enabling highly specific detection of a given protein antigen or peptide[14]. B cells, responsible for producing antibodies, will not be covered further but are nonetheless an integral part of the immune response. Conventional T cells express the T cell receptor (TCR) that consists of an alpha and a beta chain that recognize cognate peptide in the context of MHC molecules[14–16]. Both TCR and MHC molecules allow for a dramatic diversity of possible interactions that enable the immune system to distinguish self from non-self with surprising accuracy, though of course not perfectly[14]. Diversity in the TCR repertoire is gained by somatic rearrangement and base additions in the variable region of the TCR alpha and beta loci during T cell development, resulting in an estimated 10^{15} to 10^{20} possible T cell clonotypes[15]. During development in the thymus, TCRs undergo positive and negative selection, in which TCRs are screened for MHC-restriction/functionality and self-reactivity, respectively, and diversity is reduced to 2.5×10^{7}, which is nevertheless an impressive breadth[15,17]. A portion of this diversity is thought to be germline encoded, while others believe it is set during TCR selection during thymic

development and somatic rearrangement and base addition[14]; no doubt reality sits somewhere between these theories. MHC molecules certainly contribute to the reduction in diversity and bias of TCR sequences that are possible, as the sequences of the peptides presented on these molecules are constrained by the MHC sequences themselves[14]. Similarly, certain MHC haplotypes are strong risk alleles in autoimmune diseases where particular T cell self-specificities are more common[18].

During negative selection, T cells expressing self-reactive TCRs are deleted via interactions with medullary thymic epithelial cells (mTECs) that are specialized APCs capable of expressing virtually any gene encoded in the genome enabled by the transcription factor Aire or Fezf2[19,20]. Notably, microbe-specific $CD4^+$ T cell education has also been shown to take place in the thymus in early life, where intestine-derived DCs migrate while carrying microbe-derived antigens[21], potentially adding to the breadth of "extended-self" derived peptides encountered in the thymus and contributing to microbial tolerance during TCR negative selection. Some intestine-resident T cell populations arise from thymic development and undergo positive, agonist selection through the CD8αα homodimer and self-derived peptides presented by unconventional MHCIb molecules before they migrate to the intestine where they play a tolerogenic role as intraepithelial lymphocytes (IEL)[22,23]. These IEL make up the majority of the lymphocytes found in the intestine at birth and are supplanted by conventionally induced/restricted $TCR\alpha\beta^+$ T cells during commensal-colonization and exposure to food antigens. Whether conventional MHCIa-restricted commensal-specific $CD8^+$ T cells are also educated in the thymus in early life remains unexplored. However, as you will see later in Chapter 2 and 3, this need not be the case as tolerance to the microbiota can be induced within the tissue after colonization in adulthood. Myriad other mechanisms exist that help shape microbiota tolerization by the immune system during development or during tissue residency[24,25]. And indeed, this redundancy underscores the importance and scale of our symbiosis with the microbiota, where many layered events need to

take place to trigger loss of tolerance to the microbiota or acquisition of autoimmune/autoinflammatory disease.

Modulation of host physiology by gut commensal bacteria

Our intestine harbors trillions of beneficial bacteria and is where the largest biomass of our microbiota resides and is also an entry point for pathogens. The intestines themselves, of course, absorb ingested nutrients that resident microbes extract for their survival while supporting gastrointestinal (GI) function[26]. Our GI microbiota protects against infection, strengthens barrier integrity and enhances tissue repair, and modulates immune responses to vaccines and cancer immunotherapy. They also help digest nutrients, improve gut motility, and promote synthesis of essential fatty acids, amino acids, vitamins, and hormones that can modulate whole-body metabolism and immunity[27–34]. Recent research is also uncovering the ways in which the microbiota can influence behavioral or neurological systems[35].

As individuals, we first encounter significant commensal colonization the moment we are born. In a vaginal birth, our skin and GI tract is colonized with vaginal and intestinal microbes from our mother that help prevent infection and prime the neonatal immune system[26,36,37]. Throughout the early months of life, maternal breastmilk acts as a prebiotic, supporting the growth of beneficial microbes as well as providing nutrients for the infant[26]. Furthermore, antibodies found in breastmilk help shape the neonatal immune response to colonizing bacteria, which can have long-term health consequences[38]. Through further development and microbial colonization, the neonatal microbiota is cultivated and eventually resembles an adult microbiota by about 3 years of age, as cessation of breast feeding makes way for solid foods that support a wider array of bacterial species and the neonatal immune system matures to shape the composition of commensal microbes in a predictable and well described colonization cascade[26,37].

The importance of the intestinal microbiota in mammals is perhaps best understood experimentally by observing changes in germ-free mice, that is, mice borne into an abiotic

environment free of bacterial commensals or pathogens. Notably, germ-free mice have functionally immature immune, endocrine and exocrine, respiratory, and digestive systems accompanied by behavioral and learning deficits[35,39,40]. Interestingly, only some of these deficits are rescued by bacterial colonization in later life indicating that at least some of the influences of commensal bacteria take place during sensitive windows of development, enforcing the notion that optimizing organismal health depends on timely commensal microbial colonization.

As methods to detect bacteria at the strain level become cheaper and more robust, work to determine individual bacterial strains' effects on the host are ever more granular[41]. Accompanying bacterial strain identification, whole genome sequencing of the microbiota provides a deeper look into specific bioactive bacterial metabolites and products responsible for such system-wide influence[42–44]. The recent emphasis on describing active compounds and their mechanistic function is driving new therapeutic paradigms and will surely be a continued source of discoveries in how the microbiota can influence health and disease, opening new avenues of therapeutic intervention[45]. Beyond simple metabolite production, the microbiome can engage the adaptive immune system, leading to production of systemically disseminated antibodies, as well as circulating and tissue-resident T cells capable of modulating the immune response to a variety of insults or stimuli, not all of which are strictly beneficial[46,47]. Thus, our commensal microbiome can systemically alter our biology both through production of metabolites and/or induction of hormone secretion, as well as through inducing adaptive immunity.

Adaptive immunity to intestinal commensal microbes

To reconcile the paradox that we have an immune system that is evolved to distinguish self from non-self with the observation that a healthy individual is colonized with trillions of microbes, it was historically thought that our immune system simply ignored these microbes by virtue of physical separation between our luminal bacteria and the rest of our tissues. However, it is becoming ever clearer that whether our immune system is engaged by microbial colonization

depends entirely on the properties of the bacteria itself. This engagements manifests on a spectrum depending primarily on the invasive properties of the microbe, namely how closely it can interact with, or attach to, our intestinal epithelial cells (IECs) and penetrate the mucus layer of our gut lining; most microbes are physically separated by this thick mucus layer, which is rich in antimicrobial peptides and antibodies produced by enterocytes and resident B cells, respectively. Indeed, timing of colonization also matters as infants' mucus layer is thinner and tight junctions between IECs are weaker, leading to increased bacterial translocation to the mesenteric lymph node (MLN) in early life, which is important for maturation of the infant immune system[48]. So called "immunogenic" microbes are those that can circumvent intestinal barrier defenses, like mucus and antibodies, and go on to engage adaptive immunity. Thus, myriad microbial species including Segmented Filamentous Bacteria (SFB), *Clostridia*, *Helicobacter*, *Bacteroidetes*, and *Akkermansia muciniphila*, among others, have been shown to induce both B and T cell responses to varying degrees[49–60]. Here, I will focus on the role of T cells in intestinal immunity though will not discount the importance of B cell responses in microbial symbiosis.

The intestinal epithelial lining is a single-cell layer separating the luminal intestinal contents and microbes from blood and internal organs, and where adaptive immune responses keep hyperproliferation and systemic dissemination of microbes at bay[61,62]. This epithelial layer is replaced and renewed in a conveyor-belt fashion from crypt stem cells to fully differentiated epithelial cells at the villus tip every 4 to 5 days in a remarkable feat of cellular proliferation[63]. Intraepithelial lymphocytes (IEL) are imbedded in, and in close contact with, the epithelial layer and it has been estimated that the intestinal epithelium contains one T cell for every 10 epithelial cells, making it the most lymphocyte-rich barrier tissue[64]. These IEL are a large heterogeneous population consisting broadly of cells present at birth, natural IEL (nIEL), and those arising from exogenous antigens like food, pathogens, or microbial colonization, peripherally induced IEL (pIEL), that eventually replace nIEL over time[22,64].

T cell populations in the IEL, comprising both TCR$\gamma\delta^+$ and TCR$\alpha\beta^+$ T cells, are functionally and phenotypically diverse but share core features: tissue adaptation, innate-like properties, limited TCR diversity, and cytotoxic potential coupled with high activation threshold[22]. Another feature common among IEL is expression of CD8$\alpha\alpha$ homodimers that interact with the molecule TL on epithelial cells and whose ligation sequesters TCR-signaling machinery conferring some of their heightened activation threshold[22]. TCR$\gamma\delta^+$ T cells primarily express the CD8$\alpha\alpha$ homodimer, while TCR$\alpha\beta^+$ T cells can variably express CD4 or CD8$\alpha\beta$ co-receptors in addition to the CD8$\alpha\alpha$ homodimer[22,64]. Additionally, the MHC restriction of the TCR$\alpha\beta^+$CD8$^+$ IEL can either be by unconventional MHCIb molecules, like MR1, CD1d, Qa-2 or H2-M3, or conventional MHCIa molecules like H2-K and H2-D, in C57Bl/6 mice[22,65]. TCR$\alpha\beta^+$CD4$^+$ and TCR$\alpha\beta^+$CD4$^+$CD8$\alpha\alpha^+$ IEL are restricted by MHCII molecules. Together, this panoply helps illustrate the varied developmental and ontological origins of T cells within the IEL compartment.

T cells are also found in abundance within the lamina propria (LP), a layer of loose connective tissue immediately beneath the intestinal epithelium. Interestingly, the IEL primarily contains CD8$^+$ T cells, while the LP largely consists of CD4$^+$ T cells[22]. Both CD4$^+$ and CD8$^+$ T cells found in the LP have a much more conventional phenotype and are largely TCR$\alpha\beta^+$ T cells. Though some populations of intestinal T cells are food antigen-specific, it is clear from studies in germ-free mice that much of the pIEL and LP lymphocytes are microbe-dependent and accumulate in the intestine due to bacterial colonization[49].

Of the few characterized antigen-specific commensal T cell responses in the intestine, CD4$^+$ T cell responses predominate; from T regulatory (Tregs) cells controlling immune responses to *Helicobacter* spp*.* and *Akkermansia*, Th17 cells that aid in barrier defense against *Clostridia* spp., SFB, and fungi*,* to regulatory CD4$^+$CD8$\alpha\alpha^+$ T cells induced by *Bacteroides* spp.[49]. And while several species of microbes have been shown to elicit TCR$\alpha\beta^+$CD8$^+$ IEL responses including several pathogens (e.g. *Yersinia* and *Listeria*) as well as some human commensal microbes[66],

commensal-*specific* $CD8^+$ IEL have remained understudied largely due to lack of tools to track this population. Consequently, the role of commensal-specific potentially cytotoxic $CD8^+$ IEL have not been well described. Likewise, potential functional differences between pathogen- or commensal-specific $CD8^+$ IEL have not been explored.

When things go wrong - dysbiosis and disease in the intestine

What happens when our immune system gets it wrong? When the distinction between self and non-self breaks down or tolerance to our extended-self is lost? Often it is not one event that leads to this breakdown but rather a combination of genetic predispositions (particular HLA haplotypes, SNPs in risk alleles, etc.) and environmental factors (composition of the microbiota, diet, etc.) that compound, eventually leading to disease onset and progression. In the case of inflammatory bowel disease (IBD) and many autoimmune disorders, inflammatory T cells are a robust biomarker of disease in an otherwise healthy individual unencumbered by ongoing infection – though infection can sometimes be a trigger-event. These inflammatory T cells then enter the tissue and cause tissue destruction where they should otherwise remain tolerant and non-inflammatory. In type 1 diabetes, for instance, it is well known that islet specific $CD4^+$ and $CD8^+$ T cells lead to destruction of the insulin producing β-cells of the pancreas[67]. In the context of IBD, $CD4^+$ T cells activated in the context of perturbed immune tolerance can drive colitis and are enriched in inflamed intestinal tissue[68]. Similarly, there has been recent interest in the role of $CD8^+$ T cells in IBD as inflammatory $CD8^+$ T cells are also found increased in both circulation and in inflamed intestinal tissue of patients with IBD[69,70]. It has been shown that colitogenic bacteria are highly coated with IgA in models of experimental IBD[71] and functional alterations in $CD4^+$ T cells specific to the microbiome have also been identified in IBD patient samples[72–74]. However, the specificity of inflammatory $CD8^+$ T cells has not been directly linked to microbes in human IBD, though it is highly suspected given the fact that IBD is also associated with intestinal microbial dysbiosis[75–77].

Conventional TCRαβ$^+$ T cells are, by virtue of their TCR, able to recognize short linear peptides that enable highly specific effector responses against those peptides in the context of MHC. However, this does not preclude T cells from cross-reactivity with similar peptides, and in fact these can contribute significantly to intestinal disease as some microbial protein sequences are conserved across distinct species[78,79]. I mention this now to highlight the shortcomings of studying polyclonal, that is, of many antigen-specificities, T cell responses in intestinal diseases like IBD and emphasize the importance of identifying immunogenic microbes that modulate T cell immunity. More broadly, characterizing antigen-specific responses is important for studies of intestinal homeostasis, immunity, and inflammation, and for future work to develop therapies to manipulate these cells or microbes in the context of inflammatory disorders such as IBD and other gut-related pathologies where aberrant T cell responses have been implicated in disease progression **(Schematic 1).**

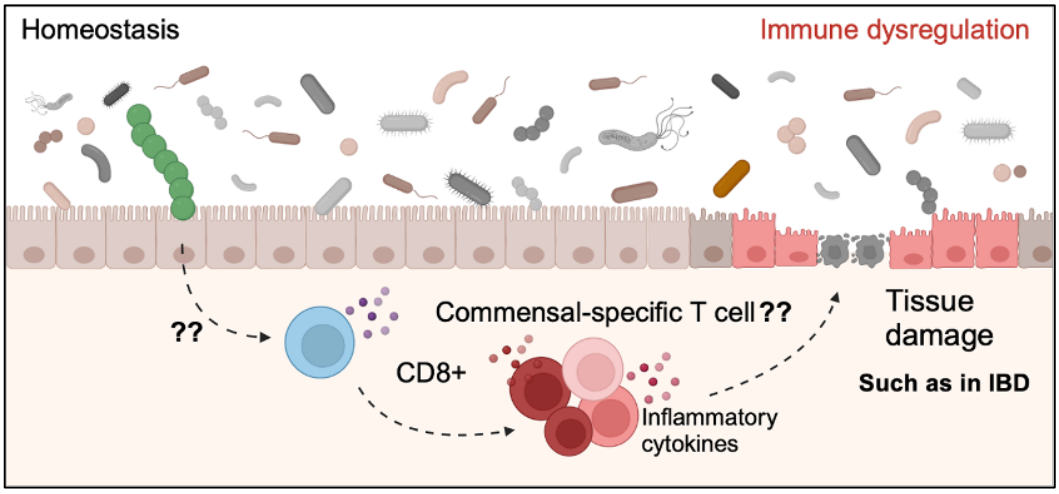

Schematic 1: CD8αβ$^+$ T cells as potential drivers of intestinal damage stemming from dysregulated commensal-specific immunity

Moreover, despite their increasing implication in intestinal-immune pathologies, commensal-specific CD8$^+$ IEL have remained understudied. Through my dissertation research, I aimed to gain a mechanistic understanding of how commensal-specific CD8$^+$ T cell responses are induced, regulated, and maintained. To do this, I focused on identifying a CD8$^+$ TCR specific to an immunogenic intestinal microbe, segmented filamentous bacteria (SFB), enabling granular

characterization of the mechanisms by which commensal-specific $CD8^+$ IEL effector functions are restrained in the healthy gut, and how this restraint is lost during chronic intestinal inflammation like IBD. These findings are laid out in **Chapter 2** and describe my approach to identifying and validating commensal-specific TCRs, and the critical mechanisms that help restrain the effector function of this population. In **Chapter 3**, I will provide discussion on outstanding questions, other mechanisms by which commensal-specific $CD8^+$ T cells may be induced and regulated, and potential future directions that my work here enables.

References

1. Kay CJ, Spang A, Szöllősi GJ, Pisani D, Williams TA, Donoghue PCJ. Dated gene duplications elucidate the evolutionary assembly of eukaryotes. *Nature*. 2026;650(8100):129-140. doi:10.1038/S41586-025-09808-Z
2. Imakawa K, Kusama K, Kaneko-Ishino T, et al. Endogenous Retroviruses and Placental Evolution, Development, and Diversity. *Cells*. 2022;11(15). doi:10.3390/CELLS11152458
3. Chuong EB. The placenta goes viral: Retroviruses control gene expression in pregnancy. *PLoS Biol*. 2018;16(10). doi:10.1371/JOURNAL.PBIO.3000028
4. Wiesmann CL, Wang NR, Zhang Y, Liu Z, Haney CH. Origins of symbiosis: shared mechanisms underlying microbial pathogenesis, commensalism and mutualism of plants and animals. *FEMS Microbiol Rev*. 2023;47(6). doi:10.1093/FEMSRE/FUAC048
5. Dimijian GG. Evolving together: the biology of symbiosis, part 1. *Proc (Bayl Univ Med Cent)*. 2000;13(3):381-390. doi:10.1080/08998280.2000.11927712
6. Dimijian GG. Evolving together: the biology of symbiosis, part 2. *Proc (Bayl Univ Med Cent)*. 2000;13(4):381-390. doi:10.1080/08998280.2000.11927712
7. Lederberg J, Mccray AT. COMMENTARY 'Ome Sweet 'Omics-A Genealogical Treasury of Words. Accessed August 15, 2026. www.-ics.com
8. Tian K, Jing D, Lan J, Lv M, Wang T. Commensal microbiome and gastrointestinal mucosal immunity: Harmony and conflict with our closest neighbor. *Immun Inflamm Dis*. 2024;12(7). doi:10.1002/IID3.1316
9. Rees T, Bosch T, Douglas AE. How the microbiome challenges our concept of self. *PLoS Biol*. 2018;16(2). doi:10.1371/JOURNAL.PBIO.2005358
10. Bartlett A, Padfield D, Lear L, Bendall R, Vos M. A comprehensive list of bacterial pathogens infecting humans. *Microbiology (Reading)*. 2022;168(12). doi:10.1099/MIC.0.001269
11. McFall-Ngai M. Care for the community. *Nature 2007 445:7124*. 2007;445(7124):153-153. doi:10.1038/445153A
12. Huttenhower C, Gevers D, Knight R, et al. Structure, function and diversity of the healthy human microbiome. *Nature*. 2012;486(7402):207-214. doi:10.1038/NATURE11234

13. Pradeu T, Thomma BPHJ, Girardin SE, Lemaitre B. The conceptual foundations of innate immunity: Taking stock 30 years later. *Immunity*. 2024;57(4):613-631. doi:10.1016/J.IMMUNI.2024.03.007
14. La Gruta NL, Gras S, Daley SR, Thomas PG, Rossjohn J. Understanding the drivers of MHC restriction of T cell receptors. *Nat Rev Immunol*. 2018;18(7):467-478. doi:10.1038/S41577-018-0007-5
15. Szeto C, Lobos CA, Nguyen AT, Gras S. TCR Recognition of Peptide-MHC-I: Rule Makers and Breakers. *Int J Mol Sci*. 2020;22(1):1-26. doi:10.3390/IJMS22010068
16. Turner SJ, La Gruta NL, Kedzierska K, Thomas PG, Doherty PC. Functional implications of T cell receptor diversity. *Curr Opin Immunol*. 2009;21(3):286-290. doi:10.1016/J.COI.2009.05.004
17. Arstila TP, Casrouge A, Baron V, Even J, Kanellopoulos J, Kourilsky P. A direct estimate of the human alphabeta T cell receptor diversity. *Science*. 1999;286(5441):958-961. doi:10.1126/SCIENCE.286.5441.958
18. Sartoris S, Del Pozzo G. Exploring the HLA complex in autoimmunity: From the risk haplotypes to the modulation of expression. *Clin Immunol*. 2024;265. doi:10.1016/J.CLIM.2024.110266
19. Takaba H, Morishita Y, Tomofuji Y, et al. Fezf2 Orchestrates a Thymic Program of Self-Antigen Expression for Immune Tolerance. *Cell*. 2015;163(4):975-987. doi:10.1016/J.CELL.2015.10.013
20. Nitta T, Suzuki H. Thymic stromal cell subsets for T cell development. *Cell Mol Life Sci*. 2016;73(5):1021-1037. doi:10.1007/S00018-015-2107-8
21. Zegarra-Ruiz DF, Kim D V., Norwood K, et al. Thymic development of gut-microbiota-specific T cells. *Nature*. 2021;594(7863):413-417. doi:10.1038/s41586-021-03531-1
22. Lockhart A, Mucida D, Bilate AM. Intraepithelial Lymphocytes of the Intestine. *Annu Rev Immunol*. 2024;42(1):289-316. doi:10.1146/ANNUREV-IMMUNOL-090222-100246
23. Hayday A, Gibbons D. Brokering the peace: The origin of intestinal T cells. *Mucosal Immunol*. 2008;1(3):172-174. doi:10.1038/mi.2008.8
24. Harrison OJ, Powrie FM. Regulatory T cells and immune tolerance in the intestine. *Cold Spring Harb Perspect Biol*. 2013;5(7). doi:10.1101/CSHPERSPECT.A018341
25. Yoo E, Jo Y, Park J, Hong SW. Immune tolerance to foreign antigens in the intestine: mechanisms mediated by CD4＋ T cells. *BMB Rep*. 2025;58(4):158-168. doi:10.5483/BMBRep.2025-0009
26. Senn V, Bassler D, Choudhury R, et al. Microbial Colonization From the Fetus to Early Childhood-A Comprehensive Review. *Front Cell Infect Microbiol*. 2020;10. doi:10.3389/FCIMB.2020.573735
27. Abt MC, Pamer EG. Commensal bacteria mediated defenses against pathogens. *Curr Opin Immunol*. 2014;29(1):16-22. doi:10.1016/J.COI.2014.03.003
28. Hayes CL, Dong J, Galipeau HJ, et al. Commensal microbiota induces colonic barrier structure and functions that contribute to homeostasis. *Sci Rep*. 2018;8(1). doi:10.1038/S41598-018-32366-6
29. Round JL, Mazmanian SK. The gut microbiota shapes intestinal immune responses during health and disease. *Nat Rev Immunol*. 2009;9(5):313-323. doi:10.1038/NRI2515

30. Dimidi E, Christodoulides S, Scott SM, Whelan K. Mechanisms of Action of Probiotics and the Gastrointestinal Microbiota on Gut Motility and Constipation. *Adv Nutr*. 2017;8(3):484-494. doi:10.3945/AN.116.014407
31. Hoverstad T, Midtvedt T. Short-chain fatty acids in germfree mice and rats. *J Nutr*. 1986;116(9):1772-1776. doi:10.1093/JN/116.9.1772
32. Jiménez E, Fernández L, Marín ML, et al. Isolation of commensal bacteria from umbilical cord blood of healthy neonates born by cesarean section. *Curr Microbiol*. 2005;51(4):270-274. doi:10.1007/S00284-005-0020-3
33. Gustafsson BE, Daft FS, Mcdaniel EG, Smith JC, Fitzgerald RJ. Effects of vitamin K-active compounds and intestinal microorganisms in vitamin K-deficient germfree rats. *J Nutr*. 1962;78(4):461-468. doi:10.1093/JN/78.4.461
34. Martin AM, Sun EW, Rogers GB, Keating DJ. The Influence of the Gut Microbiome on Host Metabolism Through the Regulation of Gut Hormone Release. *Front Physiol*. 2019;10(MAR). doi:10.3389/FPHYS.2019.00428
35. Delgado-Ocaña S, Cuesta S. From microbes to mind: germ-free models in neuropsychiatric research. *mBio*. 2024;15(10). doi:10.1128/MBIO.02075-24
36. Martin R, Makino H, Yavuz AC, et al. Early-Life Events, Including Mode of Delivery and Type of Feeding, Siblings and Gender, Shape the Developing Gut Microbiota. *PLoS One*. 2016;11(6). doi:10.1371/JOURNAL.PONE.0158498
37. Walker RW, Clemente JC, Peter I, Loos RJF. The prenatal gut microbiome: are we colonized with bacteria in utero? *Pediatr Obes*. 2017;12 Suppl 1(Suppl 1):3-17. doi:10.1111/IJPO.12217
38. Patnode CD, Henrikson NB, Webber EM, Blasi PR, Senger CA, Guirguis-Blake JM. Breastfeeding and Health Outcomes for Infants and Children: A Systematic Review. *Pediatrics*. 2025;156(1). doi:10.1542/PEDS.2025-071516
39. Eberl G, Boneca IG. Bacteria and MAMP-induced morphogenesis of the immune system. *Curr Opin Immunol*. 2010;22(4):448-454. doi:10.1016/J.COI.2010.06.002
40. Fiebiger U, Bereswill S, Heimesaat MM. Dissecting the Interplay Between Intestinal Microbiota and Host Immunity in Health and Disease: Lessons Learned from Germfree and Gnotobiotic Animal Models. *Eur J Microbiol Immunol (Bp)*. 2016;6(4):253-271. doi:10.1556/1886.2016.00036
41. Kim N, Ma J, Kim W, Kim J, Belenky P, Lee I. Genome-resolved metagenomics: a game changer for microbiome medicine. *Exp Mol Med*. 2024;56(7):1501-1512. doi:10.1038/S12276-024-01262-7
42. Tang J. Microbial metabolomics. *Curr Genomics*. 2011;12(6):391-403. doi:10.2174/138920211797248619
43. Vernocchi P, Del Chierico F, Putignani L. Gut Microbiota Profiling: Metabolomics Based Approach to Unravel Compounds Affecting Human Health. *Front Microbiol*. 2016;7(JUL). doi:10.3389/FMICB.2016.01144
44. Krishnamurthy HK, Pereira M, Bosco J, et al. Gut commensals and their metabolites in health and disease. *Front Microbiol*. 2023;14. doi:10.3389/FMICB.2023.1244293
45. Zhou P, Chen C, Patil S, Dong S. Unveiling the therapeutic symphony of probiotics, prebiotics, and postbiotics in gut-immune harmony. *Front Nutr*. 2024;11. doi:10.3389/FNUT.2024.1355542

46. James EA. From Mouth to Joint: Citrullinated Bacteria in Driving Synovial Autoimmunity. *J Rheumatol*. 2026;53(8):jrheum.2026-0410. doi:10.3899/JRHEUM.2026-0410
47. Zeng Q, Liu JC, Yang C, et al. Gut microbiota-driven pathogenic Th17 cells mediated autoimmune epididymo-orchitis in a mouse model of colitis. *iScience*. 2025;28(5). doi:10.1016/J.ISCI.2025.112508
48. Weström B, Arévalo Sureda E, Pierzynowska K, Pierzynowski SG, Pérez-Cano FJ. The Immature Gut Barrier and Its Importance in Establishing Immunity in Newborn Mammals. *Front Immunol*. *Frontiers Media S.A.* 2020;11. doi:10.3389/fimmu.2020.01153
49. Ansaldo E, Farley TK, Belkaid Y. Control of Immunity by the Microbiota. doi:10.1146/annurev-immunol-093019
50. Earley ZM, Lisicka W, Sifakis JJ, et al. GATA4 controls regionalization of tissue immunity and commensal-driven immunopathology. *Immunity*. 2023;56(1):43-57.e10. doi:10.1016/J.IMMUNI.2022.12.009
51. Nutsch KM, Hsieh CS. T cell tolerance and immunity to commensal bacteria. *Curr Opin Immunol*. 2012;24(4):385-391. doi:10.1016/J.COI.2012.04.009
52. Ostadmohammadi S, Nojoumi SA, Fateh A, Siadat SD, Sotoodehnejadnematalahi F. Interaction between Clostridium species and microbiota to progress immune regulation. *Acta Microbiol Immunol Hung*. 2022;69(2):89-103. doi:10.1556/030.2022.01678
53. Nishio J, Honda K. Immunoregulation by the gut microbiota. *Cell Mol Life Sci*. 2012;69(21):3635-3650. doi:10.1007/S00018-012-0993-6
54. Xu M, Pokrovskii M, Ding Y, et al. c-MAF-dependent regulatory T cells mediate immunological tolerance to a gut pathobiont. *Nature*. 2018;554(7692):373-377. doi:10.1038/NATURE25500
55. Matharu KS, Mizoguchi E, Cotoner CA, et al. Toll-like receptor 4-mediated regulation of spontaneous Helicobacter-dependent colitis in IL-10-deficient mice. *Gastroenterology*. 2009;137(4). doi:10.1053/J.GASTRO.2009.07.004
56. Bousbaine D, Fisch LI, London M, et al. *A Conserved Bacteroidetes Antigen Induces Anti-Inflammatory Intestinal T Lymphocytes*. https://www.science.org
57. Bilate AM, London M, Castro TBR, et al. T Cell Receptor Is Required for Differentiation, but Not Maintenance, of Intestinal CD4+ Intraepithelial Lymphocytes. *Immunity*. 2020;53(5). doi:10.1016/j.immuni.2020.09.003
58. Ansaldo E, Slayden LC, Ching KL, et al. Akkermansia muciniphila induces intestinal adaptive immune responses during homeostasis. *Science (1979)*. 2019;364(6446):1179-1184. doi:10.1126/science.aaw7479
59. Bae M, Cassilly CD, Liu X, et al. Akkermansia muciniphila phospholipid induces homeostatic immune responses. *Nature*. 2022;608(7921):168-173. doi:10.1038/s41586-022-04985-7
60. Overacre-Delgoffe AE, Hand TW. Regulation of tissue-resident memory T cells by the Microbiota. *Mucosal Immunol*. *Springer Nature*. 2022;15(3):408-417. doi:10.1038/s41385-022-00491-1
61. Cheroutre H, Lambolez F, Mucida D. The light and dark sides of intestinal intraepithelial lymphocytes. *Nat Rev Immunol*. 2011;11(7):445-456. doi:10.1038/nri3007

62. Olivares-Villagómez D, Van Kaer L. Intestinal Intraepithelial Lymphocytes: Sentinels of the Mucosal Barrier. *Trends Immunol*. *Elsevier Ltd*. 2018;39(4):264-275. doi:10.1016/j.it.2017.11.003
63. Van Der Flier LG, Clevers H. Stem cells, self-renewal, and differentiation in the intestinal epithelium. *Annu Rev Physiol*. 2009;71:241-260. doi:10.1146/ANNUREV.PHYSIOL.010908.163145
64. McDonald BD, Jabri B, Bendelac A. Diverse developmental pathways of intestinal intraepithelial lymphocytes. *Nat Rev Immunol*. *Nature Research*. 2018;18(8):514-525. doi:10.1038/s41577-018-0013-7
65. Park SH, Guy-Grand D, Lemonnier FA, Wang CR, Bendelac A, Jabri B. Selection and expansion of CD8alpha/alpha(1) T cell receptor alpha/beta(1) intestinal intraepithelial lymphocytes in the absence of both classical major histocompatibility complex class I and nonclassical CD1 molecules. *J Exp Med*. 1999;190(6):885-890. doi:10.1084/JEM.190.6.885
66. Tanoue T, Morita S, Plichta DR, et al. A defined commensal consortium elicits CD8 T cells and anti-cancer immunity. *Nature*. 2019;565(7741):600-605. doi:10.1038/s41586-019-0878-z
67. Burrack AL, Martinov T, Fife BT. T Cell-Mediated Beta Cell Destruction: Autoimmunity and Alloimmunity in the Context of Type 1 Diabetes. *Front Endocrinol (Lausanne)*. 2017;8(DEC). doi:10.3389/FENDO.2017.00343
68. Gomez-Bris R, Saez A, Herrero-Fernandez B, Rius C, Sanchez-Martinez H, Gonzalez-Granado JM. CD4 T-Cell Subsets and the Pathophysiology of Inflammatory Bowel Disease. *Int J Mol Sci*. 2023;24(3). doi:10.3390/IJMS24032696
69. Boland BS, He Z, Tsai MS, et al. Heterogeneity and clonal relationships of adaptive immune cells in ulcerative colitis revealed by single-cell analyses. *Sci Immunol*. 2020;5(50). doi:10.1126/SCIIMMUNOL.ABB4432
70. Lin YH, Duong HG, Limary AE, et al. Small intestine and colon tissue-resident memory CD8+ T cells exhibit molecular heterogeneity and differential dependence on Eomes. *Immunity*. 2023;56(1):207-223.e8. doi:10.1016/J.IMMUNI.2022.12.007
71. Palm NW, De Zoete MR, Cullen TW, et al. Immunoglobulin A coating identifies colitogenic bacteria in inflammatory bowel disease. *Cell*. 2014;158(5):1000-1010. doi:10.1016/J.CELL.2014.08.006
72. Hegazy AN, West NR, Stubbington MJT, et al. Circulating and Tissue-Resident CD4+ T Cells With Reactivity to Intestinal Microbiota Are Abundant in Healthy Individuals and Function Is Altered During Inflammation. *Gastroenterology*. 2017;153(5):1320-1337.e16. doi:10.1053/J.GASTRO.2017.07.047
73. Uchida AM, Boden EK, James EA, Shows DM, Konecny AJ, Lord JD. Escherichiacoli-Specific CD4+ T Cells Have Public T-Cell Receptors and Low Interleukin 10 Production in Crohn's Disease. *Cell Mol Gastroenterol Hepatol*. 2020;10(3):507-526. doi:10.1016/J.JCMGH.2020.04.013
74. Pedersen TK, Brown EM, Plichta DR, et al. The CD4+ T cell response to a commensal-derived epitope transitions from a tolerant to an inflammatory state in Crohn's disease. *Immunity*. 2022;55(10):1909-1923.e6. doi:10.1016/J.IMMUNI.2022.08.016

75. Britton GJ, Contijoch EJ, Mogno I, et al. Microbiotas from Humans with Inflammatory Bowel Disease Alter the Balance of Gut Th17 and RORγt+ Regulatory T Cells and Exacerbate Colitis in Mice. *Immunity*. 2019;50(1):212-224.e4. doi:10.1016/J.IMMUNI.2018.12.015
76. Casalegno Garduño R, Däbritz J. New Insights on CD8+ T Cells in Inflammatory Bowel Disease and Therapeutic Approaches. *Front Immunol*. 2021;12. doi:10.3389/FIMMU.2021.738762
77. Larmonier CB, Shehab KW, Ghishan FK, Kiela PR. T Lymphocyte Dynamics in Inflammatory Bowel Diseases: Role of the Microbiome. *Biomed Res Int*. 2015;2015. doi:10.1155/2015/504638
78. Chiaranunt P, Tometich JT, Ji J, Hand TW. T Cell Proliferation and Colitis Are Initiated by Defined Intestinal Microbes. *J Immunol*. 2018;201(1):243-250. doi:10.4049/JIMMUNOL.1800236
79. Martini GR, Tikhonova E, Rosati E, et al. Selection of cross-reactive T cells by commensal and food-derived yeasts drives cytotoxic TH1 cell responses in Crohn's disease. *Nat Med*. 2023;29(10):2602-2614. doi:10.1038/S41591-023-02556-5

CHAPTER 2: Coincident epithelial signals restrain commensal-specific CD8αβ$^+$ T cells in the intestine

The contents of this chapter were adapted from the following manuscript:

Olsen, T. M., Dufort, M. J., Verma, S., Makani, V. K. K., Cameron, B., Gralen, A. R., Johnson, A. J., Joglekar, A. V., Byrd, A. L., Lacy-Hulbert, A., & Harrison, O. J. (2026). Coincident epithelial signals restrain commensal-specific CD8αβ+ T cells in the intestine. bioRxiv: the preprint server for biology, 2026.04.29.720676. https://doi.org/10.64898/2026.04.29.720676

Conceptualization: TMO, OJH; Formal analysis: TMO, MJD, ALB, OJH; Methodology: TMO, SV, VKKM, BC, ARG, AJJ, AVJ; Investigation: TMO, MJD; Funding acquisition: TMO, SV, ALH, OJH; Project administration: OJH; Writing-original draft: TMO, OJH; Writing-review & editing: TMO, OJH

Introduction

The microbiota is essential for development and education of the immune system and tissue homeostasis, yet poses a persistent challenge to the host: commensal-specific immune recognition must be tightly restrained to prevent inflammation at barrier surfaces.[1–3] In the intestine, diverse bacterial taxa, including Segmented Filamentous Bacteria (SFB), *Clostridia*, *Helicobacter*, *Bacteroidetes*, and *Akkermansia muciniphila* among others elicit robust antigen-specific CD4$^+$ T cell responses that shape intestinal immunity,[1–14] demonstrating that commensals actively instruct adaptive immune differentiation programs. Beyond lamina propria CD4$^+$ T cells, the intestinal epithelium contains a specialized compartment of T cell receptor (TCR)αβ$^+$ peripherally induced intraepithelial lymphocytes (pIEL) positioned in intimate contact with intestinal epithelial cells (IECs). CD8αβ$^+$ pIEL are nearly absent in germ-free mice and accumulate markedly upon colonization,[4,15,16] yet unlike their CD4$^+$ counterparts, far less is known about which defined commensal species elicit cognate CD8αβ$^+$ pIEL responses, and the cellular and molecular mechanisms governing such responses remain undefined.

A central challenge of host-microbiota mutualism is the need to balance antigen-specific immune recognition with durable tolerance.[17] Commensal-specific T cells must be restrained under homeostatic conditions to prevent inappropriate tissue damage, while retaining the capacity to respond during infection or tissue injury.[1,18–20] When such restraint fails, pathological immune activation ensues, a hallmark of chronic inflammatory disorders including inflammatory bowel disease (IBD), in which inflammatory pIEL have been observed.[21–24]

Tissue-resident lymphocytes are shaped by local cues reflecting the unique structural, metabolic, and microbial features of each barrier site.[25–29] In the intestinal epithelium, CD8αβ$^+$ pIEL are exposed to epithelial-derived signals distinct from those in lymphoid organs or the lamina propria, which critically determine their differentiation, function, and tolerance.[14,21,30,31] Among these, the MHCIb molecule Thymic Leukemia (TL) antigen, highly expressed on IECs, raises the threshold for TCR activation through its interaction with CD8αα.[32,33] How epithelial signals are integrated to maintain antigen-experienced CD8$^+$ T cells in a non-pathogenic state, particularly in the context of commensal colonization and continuous microbial antigen exposure, remains an open question. Locally derived immunoregulatory signals within the epithelial microenvironment must play a central role in this process, yet their identity and cellular source are poorly understood. TGFβ is a central immunoregulatory cytokine essential for immune tolerance and limiting immunopathology, particularly in the intestine;[34–37] and a compelling candidate for such a role. Unlike freely diffusible cytokines, it is produced as a latent complex requiring spatially controlled activation. Which cell types locally activate TGFβ within the intestinal microenvironment, and how this signal is directed toward CD8αβ$^+$ pIEL remains to be determined. Here, by developing commensal-specific MHCIa-restricted TCRs and tetramers we identify SFB as a driver of antigen-specific CD8αβ$^+$ pIEL responses in the small intestine and show that cognate peptide MHC (pMHC) interactions with IECs are required for their differentiation and continuous TCR stimulation within the epithelium. Despite harboring potent effector potential, SFB-specific

CD8αβ$^+$ pIEL are actively restrained, a state whose epithelial and cell-intrinsic basis we define here.

Results

SFB colonization induces accumulation of clonally expanded CD8αβ$^+$ pIEL

To determine how the commensal microbiota influences the CD8αβ$^+$ pIEL compartment, we compared C57BL/6 mice harboring distinct microbial communities. Wild-type (WT) mice from Taconic Biosciences (Tac) exhibited increased frequencies and total numbers of CD8αβ$^+$ pIEL relative to their counterparts from Jackson Laboratories (Jax) **(Fig. 1A)**. This expansion arose post-weaning, was vertically transmissible, and unlike the transient accumulation of lamina propria (LP) CD8αβ$^+$ T cells following weaning, was stable and persisted into adulthood **(Fig. S1A-B)**.

Segmented Filamentous Bacteria (SFB) colonizes mice from Tac but not Jax[38] **(Fig. S1C)** and elicits robust CD4$^+$ T cell and B cell responses in the gut.[38–42] We therefore tested whether SFB colonization alone induced CD8αβ$^+$ pIEL accumulation using fecal transfer from enriched SFB (eSFB) donors.[39,40] De novo colonization with eSFB flora promoted CD8αβ$^+$ pIEL accumulation in the small intestinal ileum **(Fig. 1B, S1D)**, as did colonization with SFB monoassociated feces of SPF Jax and germ-free C57BL/6 or Swiss Webster mice **(Fig. 1C-D, S1E)**, demonstrating that a single commensal is sufficient to drive establishment of intestinal epithelial-resident CD8$^+$ T cells in genetically distinct mouse strains. Consistent with these cells being SFB-specific, mesenteric lymph node (MLN)-derived CD8αβ$^+$ T cells from eSFB-colonized mice produced IFN-ɣ in response to SFB antigens ex vivo **(Fig. S1F)**, corroborating recent reports.[4] To directly assess antigen specificity of SFB-induced CD8αβ$^+$ pIEL, we conducted single-cell RNA (scRNAseq) and V(D)J sequencing. Given that microbe-specific MHCIb-restricted CD8$^+$ T cells contribute to tissue repair and intestinal immunity,[18,43,44] we assessed CD8αβ$^+$ pIEL

from WT and *H2-M3*$^{-/-}$ mice.[45] Robust clonal expansion in both genotypes indicated that H2-M3-restricted cells are not major contributors to the SFB-induced CD8αβ^{+} pIEL pool **(Table S1)**. We then retrovirally expressed the ten most clonally expanded TCRαβ heterodimers in WT CD8^{+} T cells and adoptively transferred them into congenic recipients subsequently colonized with control or eSFB flora **(Fig. 1E, S1G, Table S1)**. Two TCRs, TCR1 and TCR3, drove robust CD8αβ^{+} pIEL accumulation in SFB colonized hosts, which we prioritized for further study **(Fig. S1H-I)**.

To enable further investigation of TCR1 and TCR3 and their ability to differentiate into CD8αβ^{+} pIEL, we generated TCR retrogenic (TCR^{Rg}) mice using a modified "On Time" system that produces naive CD8αβ^{+} T cells expressing a TCR of interest and a truncated Thy1.1 marker.[46,47] Upon adoptive transfer, naive TCR1^{Rg} and TCR3^{Rg} CD8αβ^{+} T cells became activated in hosts de novo colonized with eSFB, and accumulated in the spleen, MLN, LP and intestinal epithelium, with the latter harboring the highest frequency of TCR3^{Rg} CD8αβ^{+} T cells **(Fig. 1F-G)**. TCR3^{Rg} CD8αβ^{+} pIEL, but not LP cells, were further enriched within the ileum **(Fig. 1H-I, S1K)**, consistent with the restricted anatomic niche of SFB at this site.[38] Located primarily in small intestinal villi, TCR3^{Rg} cells progressively acquired a CD69^{+}CD103^{+} phenotype from 7 days post-colonization (d.p.c.) and remained a significant fraction of the pIEL compartment for up to 2 months, detectable by both flow cytometry and imaging **(Fig. 1J-L)**. CD69^{+}CD103^{+} differentiation was accompanied by upregulation of CD8αα, detectable by TL-tetramer staining **(Fig. S1L)**, a hallmark of pIEL differentiation.[11,21,30,33] Together, these data establish that a single commensal species can drive clonal expansion and epithelial residency of antigen-specific CD8αβ^{+} T cells, a previously uncharacterized arm of the adaptive immune response to the intestinal microbiota.

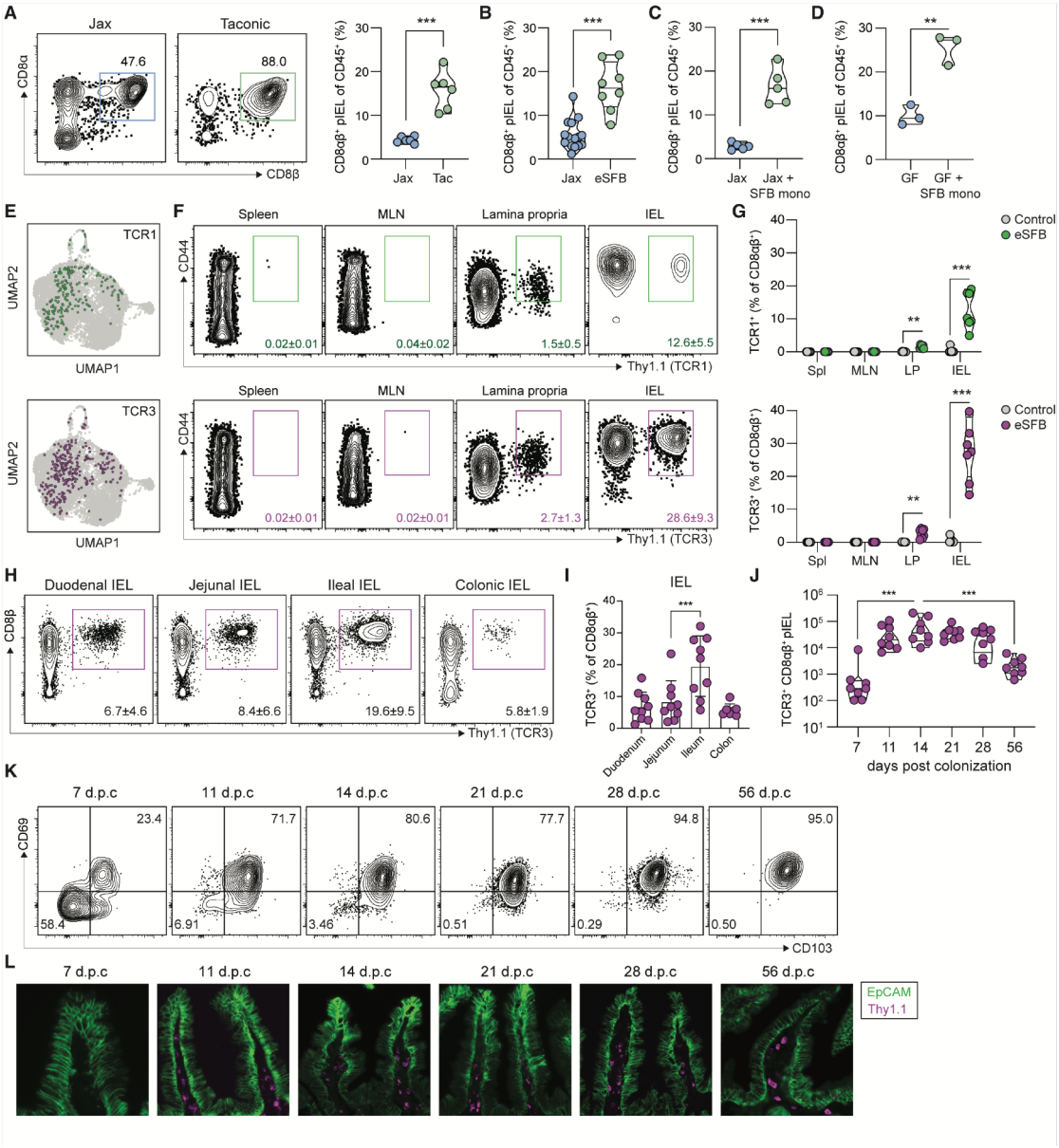

Fig. 1 SFB colonization induces accumulation of clonally expanded CD8αβ⁺ pIEL. **(A)** Representative flow plots of CD8αβ⁺ pIEL pre-gated on live CD45⁺Thy1.2⁺TCRβ⁺CD4⁻ and violin plot of CD8αβ⁺ T cells as a percent of total live CD45⁺ cells from the IEL fraction of the last 10cm of the small intestine of mice from Jax and Tac, n=6 pooled from two independent experiments. **(B)** Violin plot of CD8αβ⁺ T cells as a percent of total live CD45⁺ cells from Jax mice and Jax mice colonized with eSFB 28 days post colonization (d.p.c.), n=8-15 per group pooled from three independent experiments. **(C)** Violin plot of CD8αβ⁺ T cells as a percent of total live CD45⁺ cells from Jax mice and Jax mice colonized with SFB from monoassociated feces 28 d.p.c., n=5 per group. **(D)** Violin plot of CD8αβ⁺ T cells as a percent of total live CD45⁺ cells from germ-free B6 mice colonized with SFB from monoassociated feces 28 d.p.c., n=3 per group. **(E)** Uniform manifold approximation and projection (UMAP) plot highlighting the cluster position and frequency of TCR clonotypes TCR1 and TCR3 from 10x single cell V(D)J sequencing of CD8αβ⁺ pIEL from two Jax mice and two H2-M3$^{-/-}$ mice 28 d.p.c. with eSFB. **(F)** Representative flow plots from eSFB colonized Jax mice and **(G)** violin plot of retrogenic cells as a frequency of total CD8αβ⁺ T cells from Jax mice receiving 10,000 naive TCR1^{Rg} (green) and TCR3^{Rg} CD8⁺ T cells (pink) with or without eSFB analyzed 14 d.p.c and T cell transfer, n=7-8 per group from two independent experiments. **(H)** Representative flow plots and **(I)** Bar graph of TCR3^{Rg} CD8⁺ T cells as a frequency of total CD8αβ⁺ T cells from Jax mice receiving 10,000 naive cells with eSFB analyzed 14 d.p.c. and T cell transfer. The small intestine was segmented in thirds, and the colon was taken along with the cecum, n=9 mice per group from two independent experiments. **(J)** Violin plot of total TCR3^{Rg} CD8⁺ T cells and **(K)** their flow plots showing CD69 by CD103 from Jax mice receiving 10,000 naive cells with eSFB analyzed over time, n=8 per group from two independent experiments. **(L)** Small intestine imaging from Swiss Rolls of TCR3^{Rg} CD8⁺ T cells from Jax mice receiving 10,000 naive cells with eSFB analyzed over time, stained with anti-Thy1.1 (magenta) and Ep-CAM (green). P values were calculated using (A-D) unpaired t test (G-J) ordinary one-way ANOVA with Tukey's multiple comparisons, and (K) quadrant frequencies plus/minus the standard deviation are shown. Statistical significance denoted as ** P <0.01, *** P <0.001, and **** P <0.0001.

SFB-specific CD8αβ⁺ pIEL are MHCIa-restricted and recognize a unique SFB epitope

To determine the antigen specificity of TCR1^{Rg} and TCR3^{Rg} cells, we co-cultured them with purified antigen-presenting cells (APCs) and SFB-derived antigens. Both TCRs were activated by FACS-purified SFB, but not germ-free or Jax feces **(Fig. 2A, S2B)**,[38] confirming that responses were driven by SFB-derived peptide antigens. Furthermore, TCR activation was dependent upon MHCIa-mediated antigen presentation, as *H2-Kb*$^{-/-}$*H2-Db*$^{-/-}$ APCs failed to activate either TCR **(Fig. 2A, S2B)**. Using DC2.4 cell lines deficient for individual MHCIa molecules,[48] we determined that TCR1 is H2-Db-restricted, whereas TCR3 is H2-Kb-restricted **(Fig. 2B, S2A, S2C, S2D)**, demonstrating that both MHCIa molecules in C57BL/6 mice can present SFB antigens to drive commensal-specific CD8αβ$^+$ pIEL differentiation.

Given the magnitude of TCR3 responses relative to TCR1, we focused on TCR3 for epitope identification. Using an H2-Kb signaling and antigen-presenting bifunctional receptor (SABR) platform **(Fig. 2C, S2E)**[49–51], we screened a library of 15,769 in-silico-predicted H2-Kb-binding peptides derived from the SFB-Mouse-NYU proteome against TCR3-expressing Jurkat cells (Methods for full details). This approach identified a single high-confidence epitope, SGLIYVTL **(Fig. 2D-E)**, derived from SFBNYU_003240, a putatively secreted protein containing a domain of unknown function (DUF4214) implicated in cell surface-anchoring.[52,53] TCR3 specificity for SGLIYVTL was confirmed using a single SGLIYVTL-H2-Kb-SABR construct and in vitro stimulation of naive TCR3^{Rg} CD8$^+$ T cells with recombinant SGLIYVTL or control SIINFEKL peptides **(Fig. 2G, 2H)**. TCR3^{Rg} CD8$^+$ T cells were also detectable by H2-Kb:SGLIYVTL tetramer staining **(Fig. 2I)** and, following SFB colonization in vivo, H2-Kb:SGLIYVTL tetramer positive cells accumulated in the intestinal epithelium of SFB colonized mice where they recapitulated the CD69$^+$CD103$^+$ phenotype of TCR3^{Rg} CD8αβ$^+$ pIEL **(Fig. 2J-K, S2F)**. Together, these data establish SGLIYVTL as an H2-Kb-restricted SFB epitope, validate the H2-Kb:SGLIYVTL tetramers for tracking endogenous commensal-specific CD8$^+$ T cells in vivo, and now incorporate

MHCIa-restricted CD8$^+$ T cell responses into the suite of adaptive immune responses elicited by the commensal microbiota.

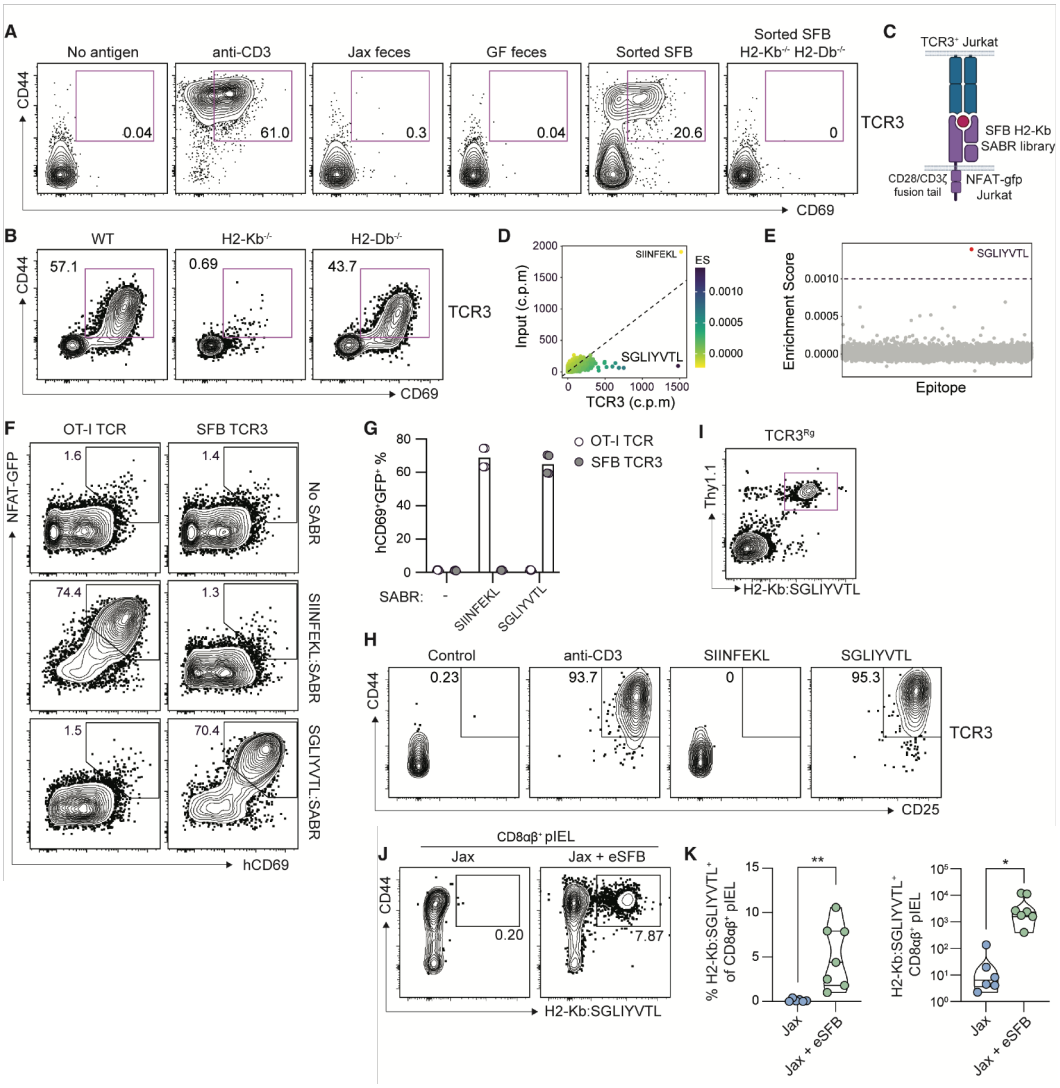

Fig. 2 SFB-specific CD8αβ$^+$ pIEL are MHCIa-restricted and recognize a unique SFB epitope. **(A)** Representative flow plots from co-cultured naive TCR3^{Rg} CD8$^+$ T cells and purified CD11c$^+$ WT or MHCIa$^{-/-}$ antigen-presenting cells (APCs) treated with either anti-CD3, feces from Jax or germ-free mice, or FACS-purified SFB from monoassociated feces and incubated for 72 hours. Data are representative of two independent experiments. **(B)** Representative flow plots from co-cultured naive TCR3^{Rg} CD8$^+$ T cells and DC2.4 APC cell lines WT or deficient for individual MHCIa molecules treated with eSFB feces and incubated for 72 hours. Data were confirmed with two independent experiments. **(C)** Schematic of Signaling and antigen-presenting bifunctional receptors (SABRs) epitope screening in Jurkat cells. **(D)** Scatter plot comparing normalized counts per million (cpm) epitope sequence reads from both SABR input library and sorted SABR cells cultured with Jurkat cells expressing TCR3. Calculated enrichment score is expressed as a heatmap statistic and **(E)** scatter plot of enrichment score versus each 15,769 epitopes from SFB-H2-Kb-SABR library sorted alphabetically. (D) and (E) were calculated from two independent library transduction events with sorted cells from triplicate co-cultures; SGLIYVTL appeared in all library samples. **(F)** Representative flow plots for single SABR co-cultures of OTI -and TCR3-expressing Jurkat cells and SABR-SIINFEKL and SABR-SGLIYVTL Jurkat cells and **(G)** the bar graphs of 2 replicates from two independent experiments from (F). **(H)** Representative flow plots from co-cultured naive TCR3^{Rg} CD8$^+$ T cells and purified CD11c$^+$ WT APCs treated with either anti-CD3 or 1μg/mL of each peptide and incubated overnight. Data were confirmed with two independent experiments. **(I)** Flow cytometry plot of splenic CD8$^+$ T cells from SFB-free Thy1.1$^+$ TCR3 retrogenic mice stained with SGLIYVTL-tetramer and analyzed by flow cytometry. **(J)** Representative flow plots and **(K)** violin plots of total numbers of CD44$^+$SGLIYVTL-tetramer$^+$ CD8αβ$^+$ T cells and as a frequency of total CD8αβ$^+$ T cells from Jax mice receiving 10,000 naive cells with eSFB, analyzed 14 d.p.c. and T cell transfer, n=7 per group pooled from two independent experiments. P values were calculated using (G) ordinary one-way ANOVA with Tukey's multiple comparisons and (K) unpaired t test. Statistical significance denoted as * P <0.05, ** P <0.01, and *** P <0.001.

SFB-specific CD8αβ⁺ pIEL accumulation is dependent upon epithelial cell antigen presentation

SGLIYVTL-specific TCR3^{Rg} and polyclonal endogenous CD8^{+} T cells accumulated in the intestinal epithelium in an SFB-dependent manner **(Fig. 1F, 2J-K)**. SFB colonization promoted IEC expression of H2-Kb **(Fig. S3A)**,[54,55] raising the possibility that local TCR stimulation by IECs drives microbiota-specific CD8αβ^{+} pIEL expansion or retention. To test this, we adoptively transferred naïve Nur77^{GFP} TCR3^{Rg} CD8^{+} T cells and colonized mice with SFB. At 10 days post colonization (d.p.c.), SFB-specific CD8^{+} T cells expressed Nur77^{GFP} equivalently across the MLN, LP and IEL, consistent with recent TCR stimulation of clonally expanding cells **(Fig. S3B, S3C)**. By contrast, 28 d.p.c., when CD8αβ^{+} pIEL accumulation had stabilized **(Fig. 1J)**, Nur77^{GFP} expression was selectively enriched in pIEL relative to MLN- and LP-derived cells **(Fig. 3A-C)**, demonstrating ongoing TCR stimulation within the epithelial compartment, even in CD8αα-expressing cells. Notably, this distinguishes MHCIa-restricted SFB-specific CD8αβ^{+} pIEL from MHCII-restricted CD4^{+}CD8αα^{+} pIEL which progressively lose TCR-responsiveness upon epithelial entry,[11] and pathogen-specific pIEL, in which TCR signaling after pathogen clearance is not observed.[37,56] EdU incorporation confirmed ongoing proliferation of TCR3^{Rg} pIEL, consistent with receipt of sufficient TCR stimulation to drive cell cycle entry **(Fig. 3D)**.

To determine whether IEC antigen presentation was required for these responses, we generated bone marrow chimeras in which WT hematopoietic cells were transplanted into WT or MHCIa$^{-/-}$ hosts. Loss of MHCIa on radio-resistant cells, including IECs, almost entirely ablated TCR3^{Rg} CD8αβ^{+} pIEL accumulation, and the few remaining pIEL lacked Nur77^{GFP} expression entirely **(Fig. 3E-H)**, demonstrating that CD8αβ^{+} pIEL accumulation and homeostatic TCR signaling both require IEC-derived MHCIa expression. To confirm this finding, we used inducible epithelial-specific H2-Kb deletion, by generating mice in which H2-Kb is the sole MHCIa molecule, that can be conditionally deleted from IECs by tamoxifen-mediated Villin^{CreERT2} activation (H2-Kb$^{Tg\text{-}flox}$ x MHCIa$^{-/-}$ x Villin$^{CreERT2/+}$ mice).[57] Epithelial H2-Kb-deletion both prior to and during eSFB

colonization impaired TCR3^{Rg} CD8αβ^{+} pIEL accumulation relative to H2-Kb-competent controls **(Fig. 3I)**. Thus, IEC MHCIa antigen presentation is required for commensal-specific CD8αβ^{+} pIEL accumulation.

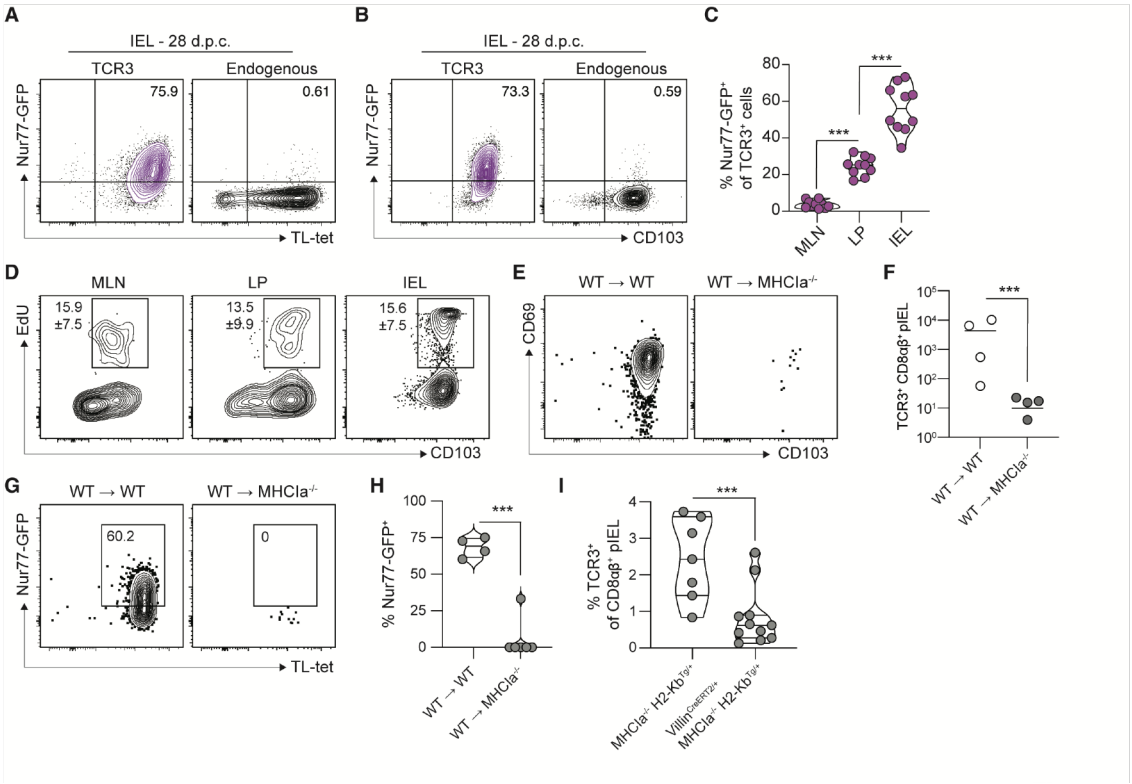

Fig. 3 SFB-specific CD8αβ^{+} pIEL differentiation is dependent upon epithelial cell antigen presentation. **(A)** Representative flow plots showing TL-tetramer (CD8αα) staining and **(B)** CD103 staining of Nur77^{GFP} TCR3^{Rg} CD8^{+} or endogenous CD8αβ^{+} T cells from ileum of eSFB colonized Jax mice 28 d.p.c. and T cell transfer, n=8-10 per group pooled from two independent experiments. **(C)** Violin plot of Nur77^{GFP} as a frequency of TCR3^{Rg} CD8^{+} T cells from (A). **(D)** Representative flow plots of EdU incorporation in TCR3^{Rg} CD8^{+} T cells as frequency of total TCR3^{Rg} CD8^{+} T cells from mice 24 hours post EdU administration (0.5mg/mouse) analyzed 28 d.p.c. and T cell transfer, n=8 per group pooled from three independent experiments. **(E)** Representative flow plots showing CD69 and CD103 staining and **(F)** dot plot of total numbers of TCR3^{Rg} CD8^{+} pIEL, and TCR3^{Rg} CD8^{+} pIEL frequency of total T cells, and **(G)** representative flow plots showing Nur77^{GFP} by TL-tetramer (CD8αα), and **(H)** violin plot of Nur77^{GFP+} TCR3^{Rg} CD8^{+} T cells as a frequency of total TCR3^{Rg} CD8^{+} T cells present in WT or MHCIa$^{-/-}$ bone marrow chimeras that received WT transplantation. Mice were analyzed 28 d.p.c. and T cell transfer (administered 2 months post chimerism), n=4-5 per group. **(I)** Violin plot of TCR3^{Rg} CD8^{+} pIEL as frequency of total CD8^{+} T cells in H2-Kb$^{Tg\text{-}fl/fl}$ (MHCIa$^{-/-}$) crossed to *Villin*$^{CreERT2/+}$ administered with 4mg tamoxifen orally 4 and 1 day prior to T cell transfer and eSFB colonization, then 2, 5, and 8 d.p.c and T cell transfer. Mice were analyzed 14 d.p.c. and T cell transfer, n=7-11 per group pooled from two independent experiments. P values were calculated using (C and D) ordinary one-way ANOVA with Tukey's multiple comparisons and (F, H and I) unpaired t test. Statistical significance denoted as not significant (ns), * P<0.05, ** P <0.01, *** P <0.001, and **** P <0.0001.

Epithelial entry imprints a restrained phenotype on commensal-specific CD8αβ⁺ pIEL

At odds with blunted TCR responses in MHCII-restricted CD4⁺CD8αα⁺ pIEL, and those CD8αβ⁺ pIEL elicited by pathogen infection,[21,35,37,56,58–60] SFB-specific CD8αβ⁺ pIEL demonstrate robust TCR-signaling under homeostasis **(Fig. 3A-D)**. Yet TCR3^{Rg} cells isolated from the IEL, unlike those from the LP, were more refractory to ex vivo TCR driven cytokine production with agonistic anti-CD3, despite retaining strong IFN-ɣ production capacity upon PMA/Ionomycin stimulation that bypasses proximal TCR signaling **(Fig. 4A)**. This dissociation between homeostatic TCR activity and ex vivo TCR responsiveness suggested that the epithelial microenvironment qualitatively remodels TCR signaling in commensal-specific pIEL. To identify the underlying signals contributing to this local immune regulation, we performed scRNAseq of TCR3^{Rg} CD8αβ⁺ T cells from the spleen, MLN, LP, and IEL of SFB-colonized mice. Louvain clustering resolved 10 transcriptionally distinct clusters **(Fig. 4B-C),** with spleen and MLN cells predominating in clusters 1-2 and IEL-enriched cells segregating into clusters 6, 7 and 8 **(Fig. 4D)**. Slingshot pseudo-time inference[61] revealed five differentiation trajectories consistent with progressive tissue entry from secondary lymphoid organs through LP into IEL **(Fig. 4E)**. Splenic and MLN cells were enriched for lymphoid egress genes (*Sell*, *Klf2*, *S1pr1*), while LP and IEL cells upregulated gut homing and retention programs (*Itga4*, *Ccr9*, *Hic1*, *Cd69*) **(Fig. S4A-B)**, reflecting gut imprinting defined in other experimental systems.[29,62–64] Within tissue-derived cells, pIEL expressed higher levels of *Gzmb* and *Itgae* than their LP counterparts, consistent with being pIEL markers in infectious settings **(Fig. S4C)**,[29] along with canonical pIEL effector and residency genes (*Gzma, Gzmk, Ccl5*, *Itga1*, *Cd101*, *Cxcr6*)[29,65] **(Fig. S4D)**.

SFB-specific CD8αβ⁺ pIEL expressed transcription factors and coinhibitory molecules associated with terminally differentiated and/or exhausted T cells (*Tox, Prdm1*, *Lag3*, *Havcr2*, *Pdcd1*, *Tigit*, *Ctla4*, *Cd160*, *Cd244a*, *Cd39*, *Cd73*, *CD200R,* and *Cish*),[66–71] of which only a subset were shared with LP-derived cells **(Fig. 4F-G, S4E-F),** pointing to compartment specific regulatory signals. Despite this profile, SFB-specific CD8αβ⁺ pIEL were not enriched for a canonical T cell

exhaustion signature **(Fig. 4H)**.[72] Instead, they bore the transcriptional signature of "restrained" autoreactive islet-specific $CD8^+$ T cells, that maintain functional potential despite coinhibitory receptor expression **(Fig. 4I-J)**.[72] This restraint signature was largely confined to pIEL, implicating local epithelial signals in its induction. While Lag3 promoted functional restraint in autoreactive pancreatic $CD8^+$ T cells,[72] *Lag3* deletion did not impact $CD8\alpha\beta^+$ pIEL phenotype **(Fig. S4G)**.

Among candidate epithelial signals, pIEL were selectively enriched for a TGFβ-response gene signature **(Fig. 4K)**, and retained low-level expression of T stem-cell memory (Tscm) transcripts (*Tcf7*, *Slamf6*, *Lef1*) **(Fig. S4H-I)**, consistent with recent evidence that TGFβ and retinoic acid cooperate to protect pathogen-elicited pIEL from terminal effector differentiation.[73] As such, in addition to myriad roles for TGFβ-signaling in establishment, maintenance, and local positioning of intestinal $CD8^+$ T cells elicited by pathogen infection,[74–77] these data point to epithelial TGFβ as a central enforcer of the restrained pIEL program and raise the question of how local TGFβ activation impacts commensal-specific $CD8^+$ T cells within the epithelium.

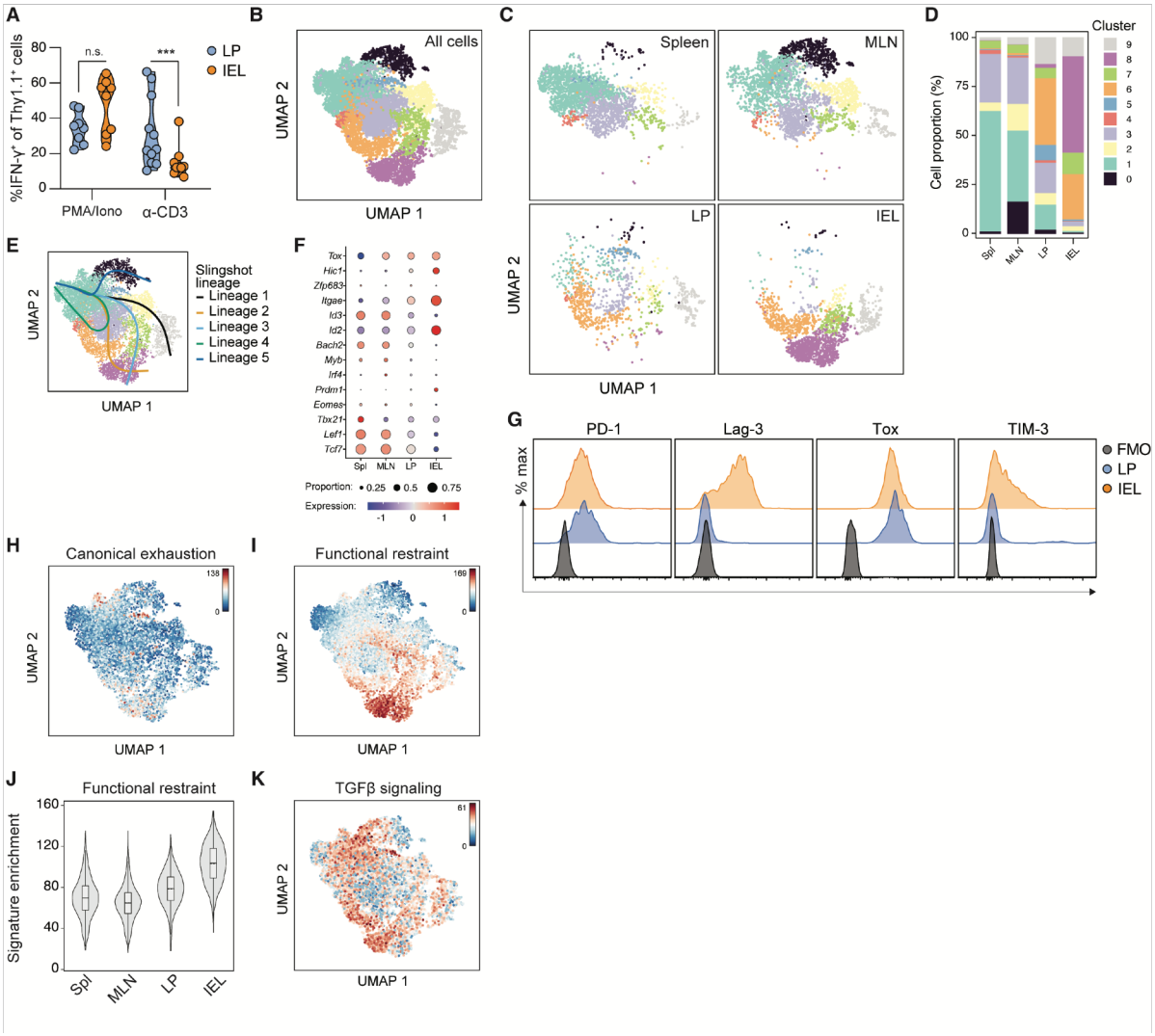

Fig. 4 Epithelial entry imprints functional restraint on commensal-specific CD8αβ⁺ pIEL. **(A)** Violin plot of IFN-γ^{+} TCR3^{Rg} CD8^{+} T cells following *ex vivo* restimulation with PMA/ionomycin (2.5 hours) or anti-CD3 (5 hours) of cells from the ileum of Jax mice 14 d.p.c. and T cell transfer. **(B and C)** UMAP projection and **(D)** tissue Cluster distribution of 10x scRNAseq analysis of sorted TCR3^{Rg} CD8^{+} T cells from the spleen, MLN, ileum LP and IEL of Jax mice 11 d.p.c. and T cell transfer. Data were generated from cells pooled from 10 mice. **(E)** Slingshot cell lineage and pseudo-time inference analysis of differentiation trajectories of cells and **(F)** heatmap and proportion analysis of selected genes across tissues in cells from (B). **(G)** Protein expression of selected inhibitory receptors on TCR3^{Rg} CD8^{+} T cells from LP and IEL cells from Jax mice 14 d.p.c. and T cell transfer. **(H)** Canonical exhaustion and **(I)** functional restraint gene set enrichment projected on 10x scRNAseq data from (B) and **(J)** enrichment score violin plot for functional restraint gene set from projection in (I) plotted for spleen, MLN, LP and IEL. **(K)** TGFβ signaling gene set enrichment score projected on 10x scRNAseq data from (B). P values were calculated using (A) two-way ANOVA with Šídák's multiple comparisons. Statistical significance denoted as not significant (ns), *** P <0.001.

Epithelial cell αvβ6-dependent TGFβ activation restrains commensal-specific CD8αβ$^+$ T cell effector function and reinforces pIEL differentiation

To determine the T cell-intrinsic requirement for TGFβ-receptor signaling in restraint of SFB-specific CD8αβ$^+$ pIEL effector functions, we performed CRISPR-Cas9-mediated *Tgfbr2* deletion in TCR3^{Rg} CD8$^+$ T cells prior to adoptive transfer and eSFB colonization. This resulted in accumulation of aberrant CD103$^-$KLRG1$^+$ CD8$^+$ T cells in the MLN, LP, and IEL which was not observed in *Cd19* or *Itgae* targeting controls, consistent with reports that impaired TGFβ signaling during tissue entry drives terminal effector differentiation, and that CD103-E-cadherin ligation alone is not required for conventional pIEL differentiation **(Fig. 5A)**.[36,73,74,78] Aberrant adaptive immune responses to commensal microbes are a hallmark of IBD.[23,79–81] Notably, patients with ulcerative colitis (UC) harbor autoantibodies targeting epithelial integrin αvβ6, a key pathway for activation of latent TGFβ in vivo.[82–87] To define how this epithelial axis impacts commensal-specific CD8αβ$^+$ pIEL differentiation, we adoptively transferred TCR3^{Rg} CD8$^+$ T cells into *Itgav*$^{fl/fl}$ Villin$^{Cre/+}$ mice, which lack αv-dependent integrins on IECs, prior to eSFB colonization. Epithelial *Itgav* deletion reduced CD103 expression in ~50% of TCR3^{Rg} CD8αβ$^+$ pIEL, consistent with TGFβ-dependent *Itgae* regulation **(Fig. 5B)**.[36,88] Transcriptional changes extended well beyond *Itgae*, however, as both CD103$^+$ and CD103$^-$ cells in *Itgav*$^{fl/fl}$ *Villin*$^{Cre/+}$ mice exhibited elevated expression of effector associated genes, including *Klrg1*, *Eomes*, *Ifng*, *Bhlhe40* and *Il12rb2*, relative to CD103$^+$ pIEL from *Itgav*$^{fl/fl}$ *Villin*$^{Cre/-}$ controls **(Fig. S5A-B)**. Additionally, aberrant CD103$^-$ KLRG1$^-$ and CD103$^-$KLRG1$^+$ TCR3^{Rg} CD8$^+$ T cells accumulated to higher levels in MLN, LP and IEL of *Itgav*$^{fl/fl}$ *Villin*$^{Cre/+}$ mice **(Fig. 5C, S5C)**. Epithelial *Itgav* deletion also drove TCR3^{Rg} CD8$^+$ T cell hyperplasia in the MLN and LP and resulted in alterations in terminal ileum villi architecture consistent with intestinal inflammation resembling that found in human IBD patient samples **(Fig. 5D, S5D).**[22]

Loss of epithelial *Itgav* gave rise to two transcriptionally distinct CD103^{-} populations, CD103^{-}KLRG1^{+} and CD103^{-}KLRG1^{-} cells, whose developmental origins were unclear. Since TGFβ signaling suppresses KLRG1 expression during effector differentiation,[89] these populations could represent either cells that had previously acquired CD103 and subsequently downregulated it, or cells that had never initiated conventional pIEL differentiation. To distinguish between these possibilities, we used a fate-mapping approach to trace the origin of CD103^{-} pIEL, we adoptively transferring TCR3-transduced CD8^{+} T cells from CD103 fate-mapping mice (*Itgae*$^{CreERT2/+}$ x *Rosa26*$^{LSL\text{-}tdTomato/+}$)[56] into *Itgav*$^{fl/fl}$ or *Itgav*$^{fl/fl}$ *Villin*$^{Cre/+}$ mice. Ex-CD103^{+} (CD103^{-}tdTomato^{+}) cells were enriched in the LP and IEL but not MLN of *Itgav*$^{fl/fl}$ *Villin*$^{Cre/+}$ mice, accounting for ~30% of CD103^{-}KLRG1^{-} cells, whereas this population was not observed in control recipients **(Fig. 5E-F, S5E)**. By contrast, CD103^{-}KLRG1^{+} cells were almost entirely tdTomato^{-} **(Fig. 5G, S5F)**, identifying them as a lineally distinct population that never acquired CD103, likely failing to initiate conventional pIEL differentiation in the absence of epithelial TGFβ. These cells accumulated not only in the IEL but also in the MLN and LP **(Fig. S5C)**, suggesting systemic dissemination of aberrantly differentiated commensal-specific CD8^{+} T cells. Together, these fate-mapping data reveal that impaired IEC αvβ6-dependent TGFβ activation subverts SFB-specific CD8^{+} T cells into divergent inflammatory lineages.

Loss of epithelial *Itgav* also unleashed effector function within SFB-specific CD8αβ^{+} pIEL: more TCR3^{Rg} CD8^{+} T cells from the IEL, but not LP, of *Itgav*$^{fl/fl}$ *Villin*$^{Cre/+}$ mice produced IFN-ɣ upon TCR restimulation, pIEL exhibited elevated Nur77^{GFP} expression in CD103^{+} cells and exhibited increased cellular proliferation, indicating heightened TCR responsiveness and loss of functional restraint **(Fig. 5H-J, S5G-H)**. ScRNAseq analysis of TCR3^{Rg} CD8αβ^{+} pIEL from *Itgav*$^{fl/fl}$ *Villin*$^{Cre/+}$ mice revealed a transcriptionally distinct cluster, Cluster 3, that was strongly enriched compared to *Itgav*$^{fl/fl}$ controls **(Fig. 5K-L)**, and aligned transcriptionally with inflammatory CD8^{+} T cell subsets identified in human UC patients samples **(Fig. 5M)**,[22] suggesting that loss of epithelial αvβ6-mediated TGFβ activation in mice recapitulates features of human intestinal inflammation

associated with dysregulated CD8$^+$ T cell responses. Together, these findings identify the intestinal epithelium as an active controller of antigen-specific CD8$^+$ T cell responses to the microbiota, in which coincident pMHC presentation and αvβ6-mediated TGFβ activation restrain cells induced by commensal colonization, and whose dysregulation is associated with intestinal inflammation in both mice and humans.

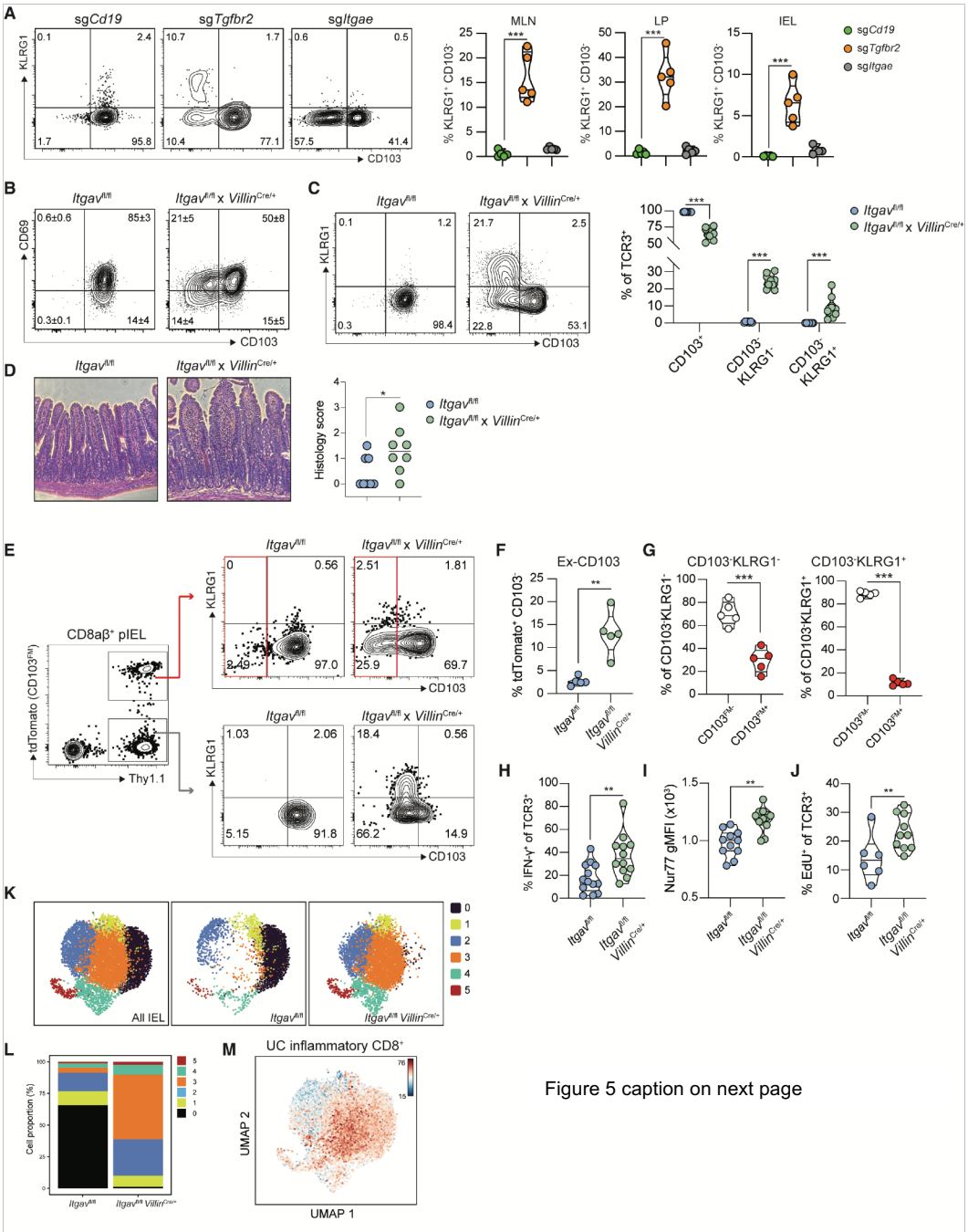

Figure 5 caption on next page

Fig. 5 Epithelial cell αvβ6-dependent TGFβ activation restrains commensal-specific CD8αβ+ T cell effector function and reinforces pIEL differentiation. (A) Representative flow plots showing staining of KLRG1 by CD103 in $TCR3^{Rg}$ pIEL knocked down with CRISPR-Cas9 RNPs of indicated gene and violin plots of $CD103^{-}KLRG1^{+}$ $TCR3^{Rg}$ $CD8^{+}$ T cells as a frequency of total $TCR3^{Rg}$ cells in MLN, LP and IEL from Jax mice 14 d.p.c. and T cell transfer, n=10 per group pooled from two independent experiments. **(B)** Representative flow plots showing CD69 and CD103 staining on $TCR3^{Rg}$ $CD8^{+}$ pIEL from *Itgav*$^{fl/fl}$ *Villin*$^{Cre/+}$ or *Itgav*$^{fl/fl}$ littermate control mice 28 d.p.c. and T cell transfer, n=7-10 per group pooled from two independent experiments. **(C)** Representative flow plots of KLRG1 and CD103 staining in $TCR3^{Rg}$ pIEL and violin plot of CD103 and KLRG1populations of $TCR3^{Rg}$ pIEL in mice from (B). **(D)** Representative images of hematoxylin and eosin staining of the last 1cm of the terminal ileum and dot plot of pathology scores in *Itgav*$^{fl/fl}$ *Villin*$^{Cre/+}$ or *Itgav*$^{fl/fl}$ littermate control mice 28 d.p.c. and $TCR3^{Rg}$ $CD8^{+}$ T cell transfer, n=8 per group from two independent experiments. **(E)** Flow gating scheme and representative plots pre-gated $CD44^{+}CD8\alpha\beta^{+}$ T cells from CD103-CreERT2 fate mapping $CD8^{+}$ T cells transduced *ex vivo* with TCR3 prior to transfer into *Itgav*$^{fl/fl}$ *Villin*$^{Cre/+}$ or *Itgav*$^{fl/fl}$ littermate control mice. Mice were given 4mg tamoxifen every other day starting 12 d.p.c. and T cell transfer and analyzed day 21, n=5 per group. **(F)** Violin plot of $CD103^{-}$tdTomato^{+} cells from *Itgav*$^{fl/fl}$ *Villin*$^{Cre/+}$ or *Itgav*$^{fl/fl}$ littermate control mice from (E) as a frequency of total $TCR3^{Rg}$ pIEL. **(G)** Violin plot of frequency of $CD103^{-}KLRG1^{+}$ $TCR3^{Rg}$ $CD8^{+}$ pIEL that are tdTomato^{-} or tdTomato^{+} from *Itgav*$^{fl/fl}$ *Villin*$^{Cre/+}$ mice from (E). **(H)** Violin plot of IFN-γ^{+} $TCR3^{Rg}$ $CD8^{+}$ pIEL following *ex vivo* restimulation with 1μg/mL anti-CD3 (5 hours) from the ileum of *Itgav*$^{fl/fl}$ *Villin*$^{Cre/+}$ or *Itgav*$^{fl/fl}$ littermate control mice 14 d.p.c. and T cell transfer, n=12-13 per group pooled from three independent experiments. **(I)** Violin plot of the geometric mean fluorescence intensity (gMFI) of GFP from $Nur77^{GFP}$ $TCR3^{Rg}$ $CD8^{+}$ pIEL of *Itgav*$^{fl/fl}$ *Villin*$^{Cre/+}$ or *Itgav*$^{fl/fl}$ littermate control mice 28 d.p.c and T cells transfer, n=11-12 per group pooled from two independent experiments. **(J)** Violin plot of EdU^{+} $TCR3^{Rg}$ $CD8^{+}$ pIEL as a frequency of total $TCR3^{Rg}$ $CD8^{+}$ T cells from *Itgav*$^{fl/fl}$ *Villin*$^{Cre/+}$ or *Itgav*$^{fl/fl}$ littermate control mice 28 d.p.c and T cells transfer, n=7-9 per group pooled from two independent experiments. **(K)** UMAP projection and **(L)** tissue Cluster distribution of 10x scRNAseq analysis of sorted $TCR3^{Rg}$ $CD8^{+}$ T cells from the pIEL of *tgav*$^{fl/fl}$ *Villin*$^{Cre/+}$ or *Itgav*$^{fl/fl}$ littermate control mice 28 d.p.c. and T cell transfer. Data were generated from cells pooled from 3 mice for each genotype. **(M)** Functional restraint gene set enrichment projected on 10x scRNAseq data from (K). P values were calculated using (A) ordinary one-way ANOVA with Tukey's multiple comparisons, (B) quadrant frequencies plus/minus the standard deviation are shown, (C, E, F, and G) two-way ANOVA with Šídák's multiple comparisons, and (H-J) unpaired t test. Statistical significance denoted as * P<0.05, ** P <0.01, *** P <0.001.

Discussion

Intraepithelial $CD8\alpha\beta^{+}$ T cells expand in response to microbial colonization, yet whether specific commensals elicit cognate, antigen-driven responses in this compartment, and how such responses are regulated, has remained unknown. Here, using commensal-specific MHCIa-restricted TCRs and tetramers we reveal that SFB colonization drives a clonally expanded, antigen-specific $CD8\alpha\beta^{+}$ T cell population of intraepithelial lymphocytes, establishing that a defined commensal species elicits a cognate $CD8^{+}$ T cell response within the intestinal epithelium. These tools further reveal that the epithelium itself is a key regulator of this response: IEC pMHC presentation is required for pIEL accumulation and continuous TCR engagement, while coincident αvβ6-activated TGFβ enforces compartment-specific functional restraint. That both signals originate from the same cell type ensures that differentiation and restraint are spatially and mechanistically coupled, a logic that, when disrupted, results in inflammatory effector programs in commensal-specific $CD8^{+}$ T cells transcriptionally aligned with those found in patients with IBD. A key finding is that commensal-specific $CD8\alpha\beta^{+}$ pIEL actively signal through their TCR under homeostasis, evidenced by $Nur77^{GFP}$ expression and basal proliferation, yet are refractory to ex

vivo restimulation. This uncoupling of TCR signaling from effector output distinguishes these cells from both exhausted and conventionally resting T cells. Strikingly, this homeostatic TCR activity is entirely IEC-dependent: loss of MHCIa on IECs nearly abolished TCR3^{Rg} pIEL differentiation and eliminated Nur77^{GFP} expression entirely. Cognate interactions with IECs are therefore required to establish the commensal-specific CD8αβ^{+} pIEL compartment. Thus, IEC pMHC presentation serves a dual purpose, driving differentiation and retaining commensal-specific CD8^{+} T cells within the epithelium, while simultaneously positioning them in proximity to epithelial signals that enforce restraint. How, then, do commensal-specific CD8αβ^{+} pIEL integrate opposing signals, continuous TCR engagement alongside potent coinhibitory and regulatory cues, to preserve tissue homeostasis while retaining functional potential? Part of the answer may lie in cell-intrinsic feedback: CD8αα and Nur77 are both upregulated downstream of TCR engagement and act to dampen further activation, providing a self-limiting brake that operates alongside coinhibitory receptors such as Lag3, Tim-3, and PD-1.[21,32,33,35,58–60,90,91] Though some amount of IEC-directed cytotoxicity by commensal-specific pIEL may occur without overt pathology, the continuous presentation of microbial products likely necessitates the potent redundancy of restraint mechanisms observed here, where *Lag3* deletion alone is insufficient to break tolerance.[92,93] Whether commensal-specific pIEL can be reactivated during infection or inflammation is an important open question; Type I interferons can lower TCR activation thresholds in intestinal T cells,[94] raising the possibility that inflammatory conditions may license these cells to respond.

TGFβ signaling adds a further layer of restraint, potentially protecting pIEL from terminal effector differentiation.[73,74] The low-level expression of stem-like markers (*Tcf7*, *Slamf6*, *Lef1*, *Id3*) in SFB-specific CD8αβ^{+} pIEL is consistent with this interpretation, though their functional significance remains to be determined. The requirement for both TCR and TGFβ signals to originate from the same cell is a critical feature of this model. Dendritic cell-mediated peripheral regulatory T cell induction requires coincident pMHCII presentation and αvβ8-dependent TGFβ

activation by the same DC,[95,96] a mechanism that ensures tolerogenic signals are delivered exclusively to cells receiving cognate antigen. Our findings extend this principle to the intestinal epithelium: IECs provide both the pMHCI signal that drives commensal-specific CD8$^+$ T cell differentiation and αvβ6-activated TGFβ that enforces their functional restraint, ensuring that the cells most capable of epithelial cytotoxicity are precisely those most exposed to the signal that restrains them. That commensal colonization drives low-level local epithelial activation rather than systemic inflammation,[97,98] likely also limits progression to exhaustion, preserving the long-term functional potential of these cells. The epithelial checkpoint identified here thus operates at multiple levels, shaping differentiation, enforcing restraint, and preserving long-term T cell fitness. Prior studies have documented elevated CD8αβ$^+$ T cell frequencies in the intestine of SFB-colonized mice;[4,16,99–101] our work now identifies SFB as a major driver of antigen-dependent TCRαβ$^+$CD8αβ$^+$ pIEL expansion and establishes their antigen-specificity and epithelial regulation through development of a gut commensal-specific MHCIa-restricted TCR and tetramer. Although SFB has been largely characterized as a mouse commensal, recent studies reveal its presence in the human intestine.[102–104] More broadly, we propose that the immunoregulatory mechanisms identified here are not SFB-specific but likely operate for any epithelium-adherent or mucus-penetrating member of the microbiota capable of eliciting continual presentation of pMHC complexes on IECs. As such, an important open question remains to identify other commensal microbes capable of eliciting CD8αβ$^+$ pIEL responses. The clinical significance of this axis is underscored by the presence of anti-αvβ6 autoantibodies in UC,[82,83,87] which would selectively disable the epithelial TGFβ checkpoint identified here.[85] Loss of this restraint drives enhanced TCR sensitivity, cytokine production, and divergent inflammatory cell lineages in commensal-specific CD8$^+$ T cells, transcriptionally aligned with IBD patient samples,[22] suggesting that dysregulated pIEL responses to the microbiota may contribute to disease pathogenesis rather than simply accompany it. Together, these findings reframe intestinal tolerance not as an absence of commensal-specific immunity, but as an active, epithelially enforced restraint of commensal-

specific $CD8^+$ T cells and identify the αvβ6-TGFβ axis as a critical checkpoint whose disruption tips the balance from homeostasis to inflammation.

Materials and Methods

Ethics statement:

All experiments were approved by the Institutional Animal Care and Use Committee of Benaroya Research Institute and performed according to their guidelines. All experimental work was performed with approval of the BRI Institutional Biosafety Committee.

Mice:

C57BL/6 (Jax 000664), CD45.1 Pep Boy (Jax 002014), CD45.1 JAXBoy (Jax 033076), B6 Vil1-Cre (Jax 004586), B6 Vil1-CreERT2 (Jax 020282), *Itgav-fl* (Jax 032297), *Rag2*$^{-/-}$ *Il2rg*$^{-/-}$ (Jax 014593), Nur77-GFP (Jax 16617), *Tcra*$^{-/-}$ (Jax 002116), CD4-Cre (Jax 02217), Ai14 (TdTomato fate-mapper; Jax 007914), B6 $Thy1^a$ (Jax 000406) mice were purchased from Jackson Laboratory. C57BL/6 mice were also purchased from Taconic Biosciences (Tac B6 B6-MPF) sourced from Germantown, NY as our SFB-colonized group. *H2-M3*$^{-/-}$ mice were provided by Dr. Chyung-Ru Wang (University of Chicago, Chicago, IL).[45] *H2-Kb transgene-fl* x $MHCIa^{-/-}$ mice[57] and H2-$Kb^{-/-}$ H2-$Db^{-/-}$ mice[43,48] were generously provided by Dr. Aaron Johnson (Mayo Clinic Rochester, Minnesota) and Dr. Ellen Robey (University of California Berkeley, Berkeley, CA), respectively. All mice were housed at the Benaroya Research Institute in specific pathogen-free (SPF) conditions and were *Helicobacteraceae*-free as determined by PCR of fecal DNA (see below). Germ-free Swiss Webster mice were purchased internally from the University of Washington's Gnotobiotic Animal Core (GNAC) and germ-free C57BL/6 mice were purchased from Charles River Laboratories; All germ-free mice and SFB-monoassociated mice were housed in the University of Washington Gnotobiotic Animal Core. Mice used in experiments were between 6 and 14 weeks of age at time of sacrifice unless specified. Both female and male mice were used

for experiments and no sex differences were noted during analysis. Littermate controls were used to limit the variability and effects of microbiome. Mice were maintained at a temperature between 18°C and 23°C with 40–60% humidity and a 12 h-12 h light-dark cycle.

In vivo treatments:

Colonization:

Segmented Filamentous Bacteria-containing fecal pellets from SFB-monoassociated gnotobiotic mice were a gift from Dr. Dan Littman (New York University Grossman School of Medicine, New York, NY). SFB-monoassociated feces were stored at -80°C until use. For colonization of germ-free mice or Jax mice, frozen fecal pellets were sterilely mashed and resuspended in sterile PBS and put through a 70µm cell strainer. The resultant slurry was used for oral gavage for fecal material transfer (FMT) – approximately 1 pellet/mouse was administered. To generate fecal donors for enriched-SFB (eSFB) flora, *Rag2*$^{-/-}$ *Il2rg*$^{-/-}$ (R2G2) mice were housed under SPF conditions and colonized using SFB-monoassociated fecal pellets as above. Fresh fecal pellets were collected from R2G2 mice and processed as above for de novo colonization with eSFB flora of SFB-free mice – for fresh feces, approximately 0.5 pellets/mouse was administered.

Tamoxifen administration:

For activation of inducible Vil1-CreERT2, mice were given 4mg tamoxifen in corn oil by oral gavage 4 and 1 day prior to T cell transfer, then 2, 5, and 8 days post T cell transfer followed by euthanasia at day 14. Note: for SFB-specific T cell transfer experiments into *H2-Kb*$^{Tg\text{-}flox}$ x MHCIa$^{-/-}$ mice, T cells were nucleofected with *H2-d1* Cas9-RNPs to avoid allograft rejection due to H2-Db expression on the transferred T cells (see nucleofection Method below). Knock down of H2-Db was confirmed by flow cytometry and knock down of H2-Kb on epithelial cells was also confirmed by flow cytometry on the CD45- fraction of the IEL samples.

For fate-mapping with CD103-CreERT2 and Ai14, mice were given 4mg tamoxifen in corn oil by oral gavage every other day starting at day 12 post T cell transfer and SFB colonization followed by euthanasia on day 21.

EdU administration and staining:

To track proliferation and DNA synthesis, 0.5mg or 0.2mg EdU was injected i.p. in 200µL PBS. Mice were euthanized 24 hours later, and cell suspensions were prepared as described below. EdU staining was performed using the Click-iT EdU staining kit (ThermoFisher C10337 AF488), per manufacturer's instructions with the following modifications/notes: permeabilization and fixation was performed using BD Cytofix/Cytoperm kit (BD 554655), Click-iT staining was performed in 100µL using half the amount of recommended Alexa Fluor Azide, and PE-based dyes were stained after Click-iT EdU staining (PE and PE-Cy7).

ELISPOT:

The mesenteric lymph nodes of Jax mice or from mice colonized with eSFB 10 days prior were harvested and mashed with 3% FBS complete RPMI through a 70µm cell strainer and $CD8^+$ T cells were isolated using untouched EasySep™ Mouse $CD8^+$ T Cell Isolation Kit (Stemcell Technologies 19853) per manufacturer's instructions. $CD11c^+$ antigen presenting cells (APCs) from spleens of SFB-free mice were isolated using mouse CD11c MicroBeads UltraPure (Miltenyi Biotec 130-125-835) after 25 min of enzymatic digestion with 100µg/mL Liberase TL (Sigma 5401020001) and 500µg/mL DNase I (Sigma DN25). 250,000 enriched CD8+ T cells and 250,000 enriched $CD11c^+$ APCs were plated on a MultiScreen 96-well ELISPOT plate (Millipore MAIPS4510) that was coated with Mouse IFNγ ELISPOT Pair (BD 551881) per manufacturer's instruction with 150µL/well in 10% complete RPMI. For treatments, anti-CD3 was used at 1µg/mL final concentration; one fecal pellet from SFB monoassociated gnotobiotic mice were resuspended in 200µL PBS and boiled for 1hr at 95°C and clarified at 100xg for 1 min and used

at a final dilution of 1:250 or 1:500 in each well. Cells were incubated overnight before spots were developed per manufacturer's instructions and read on an ImmunoSpot C.T.L. Analyzer and quantitated using ImmunoSpot.

Quantification of bacterial DNA:

Quantification of fecal DNA was performed as described.[40] Briefly, fecal DNA was prepared using QIAGEN DNeasy PowerSoil Pro Kit (Qiagen 47016) according to the manufacturer's instructions. For generating a standard curve of qPCR, SFB 16S rRNA gene fragment was cloned into the pCR™2.1-TOPO™ vector (ThermoFisher) and serial 10-fold dilutions from 10^9 copies/reaction of plasmid DNA was used. PCR containing primers (SFB736F 5′-GACGCTGAGGCATGAGAGCAT-3′ and SFB844R 5′- GACGGCACGGATTGTTATTCA-3′), 50ng of purified fecal DNA or plasmid standard, and PowerUp SYBR Green Master Mix in a 10µL reaction were mixed and the PCR was performed in a 7500 Fast Real-Time PCR System (Life Technologies). Fecal DNA from SPF mice was also screened for *Helicobacteraceae* by PCR (Pan *Helico* F: 5'-GCTATGACGGGTATCC-3' and Pan *Helico* R: 5'-GATTTTACCCCTACACCA-3')[105] and all mice used in the present study were negative.

SABR epitope discovery:

TCR3 epitope discovery was enabled by using a signaling and antigen-presenting bifunctional receptors to encode MHC-I molecules presenting covalently linked peptides (SABR-I) for $CD8^+$ T cell antigen discovery.[51] H2-Kb SABRs were constructed using gene synthesis (Twist Biosciences) similar to the HLA-A0201 SABRs described previously. Retroviral vectors presenting LNGFR-2A-Stuffer-H2-Kb SABR were generated and used to clone epitope libraries. The H2-Kb SFB peptidome was predicted in silico by entering the SFB-Mouse-NYU (ncbitaxon:1073972) proteome into NetMHCI4.0 with predictions for 8-mer and 9-mer epitope lengths. The result was a pool of 456,594 8-mers and 455,129 9-mer peptides. This pool was

further selected on peptides predicted to bind with a dissociation constant less than 500nM. The final pool was a library of 7,295 8-mer and 8,474 9-mer peptides covering 93% of the SFB proteome (theoretical max of predicted H2-Kb peptidome) as well as positive and negative control peptides. The libraries were encoded in single stranded oligonucleotide pools containing the following sequences (tggttacaggagggctcggca – reverse-translated-epitope – ggatgcggaggttccggcggg). The SABR backbone was digested with BsbI-HF (NEB R3539) to remove the stuffer fragment.[49–51] The oligonucleotide library was cloned using NEBuilder HiFi DNA Assembly (NEB E5520S) at over 30X coverage at the DNA level. Library quality control was performed by confirming the presence of epitopes in 24 colonies by Sanger sequencing (Azenta). The cloned library was used to transduce NFAT-GFP-Jurkat cells. NFAT-GFP, NFAT-GFP with SABR-SIINFEKL, and murine-CD8αβ-Jurkats and murineCD8αβ-Jurkats with OT-I TCR. Jurkats expressing TCR3 were made in-house using the mp71-TCR3 construct described for $CD8^+$ T cells transduction. Retroviral production for Jurkat transduction and epitope discovery was performed as previously described.[63–65] Briefly, VSV-G pseudo-typed retrovirus was produced by transfecting 293T with pHIT60, pMD2-G (VSV-G), and library transfer vectors using TransIT 293 (Mirus Bio MIR 2700) transfection reagent per manufacturer's instructions. Jurkat cells were transduced as described using RetroNectin-coated plates (Takara T100A) and 4μg/ml protamine sulfate (MedChem Express HY-107911), virus was harvested 48hours later and filtered through a 45μm syringe filter and used directly without concentration, or frozen in -80°C[51,107(chap2)] cells were co-cultured with TCR3 (in addition to control co-cultures) and human$CD69^+GFP^+$ cells were sorted using a BD FACSAria Fusion. Genomic DNA was extracted as described using AMPure XP SPRI-beads (Beckman Coulter A63881) after cellular lysis with ChIP lysis buffer containing 1% SDS, 10mM EDTA in 50mM Tris-HCL pH8.1.[106] After magnetic purification, 80% ethanol washes, and resuspension in H2O, total gDNA was used as template for serial PCR to amplify the integrated SABR DNA using KOD polymerase (Millipore KMM-101NV) as described.[51,107(chap2)] The first round of PCR amplified the cloned epitope, and the second round of PCR added UDI-

indexes and i5 and i7 adapters (see Table S2 for list of primers). PCR products were purified using AMPure XP SPRI-beads as above and DNA was quantified using a Qubit 4 Fluorometer and ran on a 2% agarose gel to ensure pure product amplification. DNA concentrations were adjusted appropriately and subjected to sequencing using the MiSeq Nano V2 kit (Illumina MS-103-1001) spiked with 25% PhiX DNA (Illumina FC-110-3001) per manufacturer's instructions. Jurkat SABR library co-cultures were sequenced from two independent library transductions each with 3 replicate co-culture wells.

Enrichment scores for putative epitopes were calculated using linear regression models for relative epitope abundance in the cellular input and TCR3-selected human$CD69^+NFAT\text{-}GFP^+$ samples. High confidence hits were selected based on their presence in all technical replicates and enrichment over input. The single SABR construct for SGLIYVTL was cloned from a gBlock purchased from Twist Biosciences using Gibson assembly.

Retroviral production:

Retrovirus for bone marrow and primary $CD8^+$ T cell transduction was produced as described[108] with some modifications – no chloroquine was used for transfection and virus was not concentrated. Briefly, mycoplasma-free 293T cells (ATCC CRL-3216) were cultured at 37°C, 5% CO_2 in RPMI (Fisher cat. SH30027FS) supplemented with 100U/mL penicillin and streptomycin, 2mM glutamine, 10mM HEPES, and 55μM beta-mercaptoethanol with 10% FBS (Sigma 20C132) and plated at 60-70% density on Poly-L-Lysine-coated 15 cm tissue-culture-treated dish. The next day, transfection of pCL-Eco and the transfer vector was performed using 1:3 DNA:PEI (polyethylenimine) mixture. Culture media was changed 6 hours later, and virus was collected 48 hours from change, filtered through a 0.45μm syringe filter and used directly without concentration, or frozen in -80°C for later use. Retroviral transfer vectors for TCR overexpression were gifted to us by Dr. Shivani Srivastava (Fred Hutchinson Cancer Center, Seattle, WA) and

are in the mp71 backbone modified to include a truncated Thy1.1 linked by P2A to track transduction by flow cytometry.

Retroviral transduction of primary mouse CD8$^+$ T cells and adoptive transfer:

Primary mouse CD8$^+$ T cell transduction was performed as described.[109] Briefly, T cells from spleen and lymph nodes of B6 WT mice (Jackson Laboratories), or other strains as indicated, were isolated using untouched EasySep™ Mouse CD8$^+$ T Cell Isolation Kit (Stemcell Technologies 19853) and cultured in 10% mTCM media (RPMI supplemented with 100U/mL penicillin and streptomycin, 2mM glutamine, 1mM sodium pyruvate, 10mM HEPES, and 55μM beta-mercaptoethanol with 10% FBS) with 50U/mL recombinant human IL-2 (Preprotech, AF-200-15) and activated using Mouse T-Activator anti-CD3/CD28 Dynabeads (Thermo Scientific 11452D) and cultured for 24-30 hours at 1 million cells/mL at 37°C (1:1 Dynabeads to T cells). Non-tissue culture treated dishes were coated with 12.5μg/mL Retronectin (Takara T100B) in PBS overnight at 4°C or at 37°C for 30 minutes. Retronectin-coated plates were washed with PBS then blocked with 2% BSA in PBS for 30 minutes at 37°C and coated with viral supernatants for 2 hours while being centrifuged at 3000xg at 32°C in a tabletop centrifuge the day of transduction. T cells and Dynabeads were harvested, counted, and cultured as above then centrifuged at 800xg at 32°C for 30 minutes and returned to the incubator. After 24 hours, T cells were harvested and resuspended in media containing 50 U/mL IL-2 as above. After another 24 hours, T cells were harvested and resuspended in mTCM media containing 10 U/mL recombinant human IL-15 (Preprotech, AF-200-15) and cultured for 48 hours. T cells were then removed from Dynabeads and rested 24 hours and transduction efficiency was determined by flow cytometry by staining for anti-Thy1.1 in the case of TCR overexpression. Between 50,000 and 500,000 transduced cells were adoptively transferred i.v. into recipient mice in PBS.

Retrogenics/On Time:

Retrogenic mice were generated as described with modifications[46] using an "On Time" retroviral transfer vector gifted by Dr. Kristin Hogquist (University of Minnesota, Minneapolis, MN) modified to include P2A linked-expression of truncated Thy1.1 with TCRα under the control of CD4-Cre-mediated deletion of floxed GFP-stop[47]. In some cases, *Tcra*$^{-/-}$ x CD4-Cre^{+} intercrossed with a Nur77-GFP transgene was used as donors to track TCR engagement. Briefly, bone marrow was harvested from *Tcra*$^{-/-}$ x CD4-Cre^{+} donor mice, prepared as described[46] and cultured in DMEM (Thermo Fisher Scientific 11995073) supplemented with 100U/mL penicillin and streptomycin,1X non-essential amino acids, 1mM sodium pyruvate, 10μM HEPES, and 55μM beta-mercaptoethanol with 20% FBS with 50ng/mL recombinant mouse SCF (Biolegend 579704), 50ng/mL recombinant mouse IL-6 (Biolegend 570804), 20ng/mL recombinant mouse IL-3 (Biolegend 575504) overnight at 37°C, 5% CO_2 at about 3 million cells/mL in a petri dish. Non-tissue culture treated dishes were coated with 12.5μg/mL Retronectin (Takara T100B) in PBS overnight at 4°C, or at 37°C for 30 minutes. Retronectin-coated plates were washed with PBS then blocked with 2% BSA in PBS for 30 minutes at 37°C and coated with viral supernatants for 2 hours while being centrifuged at 3000xg at 32°C in a tabletop centrifuge the day of transduction. After 24 hours, cells were harvested, counted, and resuspended in media as above with about 6 million cells/well of a virus-coated plate at about 2 million cells/mL. Cells were then centrifuged at 800xg at 32°C for 30 minutes and returned to the incubator. After another 24 hours, cells were harvested, counted, and 3-5 million cells were injected i.v. into lethally irradiated Jax B6 recipients. A small portion of cells were cultured an additional day to determine transduction efficiency by flow cytometry using GFP as the transduction marker. Mice were bled 6-8 weeks later to determine engraftment of "On Time" transduced bone marrow.

Bone Marrow Chimeras:

Bone marrow was harvested from JAXBoy (CD45.1) mice as above, counted. Before injection, a T cell depletion was performed using anti-Thy1.2 (30-H12),[110] anti-biotin microbead, and MACs columns. Cells were injected i.v., separately, into lethally irradiated H2-Kb$^{-/-}$ H2-Db$^{-/-}$ or Jax B6 recipient mice. For mixed bone marrow chimeras bone marrow was harvested from *Lag3*$^{-/-}$ (CD45.1, CD90.1) bones (a generous gift from Dr. E. John Wherry at the University of Pennsylvania, Philadelphia, PA, Jax: 026644) and B6 Thy1^{a} mice as congenic WT donors. Cells were counted, mixed 1:1 and injected i.v. into lethally irradiated Jax B6 recipients. In both cases, mice were rested for 8 weeks before use.

Adoptive transfer of naive CD8^{+} T cells:

Spleen and lymph nodes (except the mesenteric lymph node) of TCR3 On Time retrogenic mice were harvested and mashed through a 70µm cell strainer and CD8+ T cells were isolated using untouched EasySep™ Mouse CD8^{+} T Cell Isolation Kit (Stemcell Technologies 19853) with the addition of biotinylated anti-CD44 (clone IM7 used at 1:300) to enrich for naive CD8+ T cells (amount of selection cocktail and magnetic beads recommended by manufacturer were halved to enhance yield and purity). The frequency of Thy1.1^{+} cells was determined by flow cytometry and the volume was adjusted in PBS such that 10,000 SFB-specific CD8^{+} T cells were injected i.v. in 100µL in each mouse. On Time donors and recipient mice were CD45.2 unless stated in figure legends. Mice were then colonized with SFB, as described above, up to 24 hours later.

Nucleofection of sgRNAs:

Purified CD8^{+} On Time retrogenic cells were isolated as above or thawed from frozen stock and the frequency of Thy1.1^{+} cells was determined by flow cytometry and nucleofected using the P3 nucleofection kit as described.[35] Predesigned sgRNA guides were purchased from IDT that target *Cd19* (5'-GGUGGAAUGCUUCAGACGUC-3'), *Itgae* (5'-ACAUUGGUCGGGAACCACAA-3' and

5'-CAAGGGAGGCGUUAAUGUCC-3'), *Tgfbr2* (5'-ACGGCCACGCAGACUUCAUG-3' and 5'-GGACUUCUGGUUGUCGCAAG-3'), and *H2-d1* (5'-GGUGACUUCACCUUUAGAUC-3' and 5'-UGUCGGCUAUGUGGACAACA-3'). Briefly, Cas9-RNP complex was made by combining 1-2μL of sgRNA (IDT) at 100μM and 6μg of Cas9 (ThermoFisher A36496) in 5μL of water and incubated at room temperature for 10min. Then 2-5 million cells were resuspended in P3 nucleofection reagent, Cas9-sgRNA RNP complex was added and cells were electroporated using Lonza 4D-Nucleofector system using DN-100 pulse code. Cells were incubated for 10min at 37°C in 5% CO_2 with 100μL of warm completed RMPI, then washed, counted, and resuspended in PBS such that 50,000 $CD8^+$ T cells were injected i.v. in 100μL in each mouse. Mice were then colonized with SFB, as described above, up to 24 hours later.

Cell isolation:

Cells from mesenteric lymph nodes and spleen were collected in 3% FBS complete media (RPMI supplemented with 100U/mL penicillin and streptomycin, 1X non-essential amino acids, 2mM glutamine, 1mM sodium pyruvate, 10mM HEPES, and 55μM beta-mercaptoethanol with 10% FBS) and mashed through a 70μm cell strainer to generate single cell suspensions (the spleen was subjected to ACK red blood cell lysis during mashing and then quenched with media). For intestinal preparations, where indicated in the text, the ileum was defined as the distal 10cm of the small intestine. Where segmentation was performed, the intestines were sectioned into thirds: duodenum, jejunum, and ileum, and large intestine including the cecal tissue. The lamina propria and IEL were prepared from each segment as follows: the intestine was dissected and collected in cold 3% FBS complete media Peyer's patches and cecal patch was removed before the intestines were opened longitudinally, rinsed in PBS to clean intestinal contents off and incubation in 3% FBS complete media containing 5 mM EDTA (Sigma-Aldrich), 0.145 mg/ml DTT (Sigma-Aldrich) at 37°C for 20 minutes on a stirring platform.

To separate the intestinal epithelial lymphocyte (IEL) and lamina propria (LP) layer, intestinal contents were transferred through a sterile fine-meshed kitchen strainer into a 500mL beaker. Strainer was tapped on beaker several times after straining and pieces of each intestine were transferred to a 50mL conical tube containing 10mL of 0% FBS complete media with 2mM EDTA. After shaking the tube vigorously for 30 seconds, the contents of the tube were strained again through the sieve into the beaker. The process was repeated three times. The tissue was minced finely in digest containing 0% FBS complete media with either 0.1mg/mL Liberase TL (Sigma 5401020001) and 0.5mg/mL DNase I (Sigma-Aldrich) or 1mg/mL Collagenase type VIII (Sigma C2139) and 0.25mg/mL DNase I, with continuous stirring at 37°C for 25 min. The fraction collected in the beaker was passed through a 100µm cell strainer and is the "IEL" fraction. Digested tissue for LP was passed through a 70µm cell strainer. Lymphocytes from each fraction were centrifuged at 550xg on a tabletop centrifuge and further enriched by centrifugation at room temperature at 695xg for 8 min after pellets were resuspended in 37.5% Percoll (GE Healthcare). After washing in 3% FBS complete RPI, cells were resuspended for downstream use.

Ex vivo restimulation:

Single cell suspensions from tissues were stimulated in 48-well, tissue culture-treated dishes in 300µL of 10% FBS complete media. For anti-CD3 restimulation, 1µg/mL final concentration was used and cells were incubated at 37°C, 5% CO_2 for 1 hour before the addition of 1x GolgiPlug (BD BDB555029) and incubated an additional 3 hours. For phorbol myristate acetate (PMA) (Sigma P8139) and ionomycin (Sigma I0634) restimulation, 50ng/mL of PMA was used and 5µg/mL of ionomycin was used with the addition of 1x GolgiPlug and cells were incubated for 2.5 hours at 37°C, 5% CO_2. After stimulation, cells were then washed with cold PBS and moved into a 96-well plate for antibody staining and analysis.

Flow cytometry:

Cells were resuspended in 96-well, U-bottom plates and stained in PBS containing Rat IgG, Fc Block, fixable live/dead (Thermo L23105) and cell surface antibodies (for list of antibodies, see Table S3) and incubated on ice for 25 minutes. Cells were washed with PBS and, where necessary, intracellular protein staining was performed using either a transcription factor staining buffer set (Thermo 00-5523-00) or BD Cytofix/Cytoperm kit (BD 554655). In most cases, counting beads (Polysciences 183285) were used to enumerate total cell counts. All cells were analysed by a BD LSRFortessa.

Tetramers:

TL tetramer staining to identify CD8αα-expressing cells was performed as described at a concentration of 5µg/ml for 30 minutes at 37°C in 3% FBS complete RMPI.[33] Tetramer was procured from the NIH tetramer core. SGLIYVTL tetramer was made using the easYmer H2-Kb MHC tetramer kit (Eagle Biosciences 5004-01) and peptide purchased from Genscript. SGLIYVTL tetramer staining was performed with 10nM tetramer conjugated to PE-streptavidin (Agilent PJRS25-1) for 30 minutes at 37°C in 3% FBS complete RMPI. In both cases, tetramer staining was followed by a PBS wash and other cell surface markers.

In vitro culture:

Spleen and lymph nodes (except the mesenteric lymph node) of On Time retrogenic mice or TCR transgenic mice were harvested and mashed through a 70µm cell strainer and CD8+ T cells were isolated using untouched EasySep™ Mouse $CD8^+$ T Cell Isolation Kit (Stemcell Technologies 19853) with the addition of biotinylated anti-CD44 (clone IM7 used at 1:300) to enrich for naive $CD8^+$ T cells. $CD11c^+$ antigen presenting cells (APCs) from spleens of *Tcra*$^{-/-}$ or *H2-Kb*$^{-/-}$ *H2-Db*$^{-/-}$ mice were isolated using mouse CD11c MicroBeads UltraPure (Miltenyi Biotec 130-125-835) after 25 min of enzymatic digestion with 100µg/mL Liberase TL (Sigma 5401020001) and 500µg/mL

DNase I (Sigma DN25) in 0% FBS complete RPMI. Frozen or fresh 50,000 Thy1.1^{+}CD8^{+} T cells and fresh 100,000 CD11c^{+} APCs were mixed in a 96-well U-bottom plate and cultured in 150µL of 10% FBS complete RPMI with various treatments added: anti-CD3 1µg/mL final concentration; all fecal pellets were resuspended in 200µL PBS and boiled for 1hr at 95C and clarified at 100xg for 1 min, and used at a final dilution of 1:250 or 1:500 in each well. SFB from cecal contents of SFB-monoassociated gnotobiotic mice were density-enriched and sorted as described,[38] where 750,000 FACS events were resuspended in 300µL PBS and boiled for 1hr at 95C, final dilution was used at 1:50 in each well. Cells were incubated for 72 hours at 37°C then analyzed by flow cytometry for activation with antibodies against CD44, CD62L, CD25, and CD69. For peptide stimulation of SGLIYVTL (Genscript) and SIINFEKL (Genscript) were resuspended in DMSO at 10mg/ml and diluted to the indicated concentration in PBS co-cultures were set up as above and incubated overnight prior to analysis by flow cytometry. To determine MHC-restriction, DC2.4 cell lines were used as antigen presenting cells and co-cultures were performed as above in flat-bottom plates. WT and MHC-I KO cell lines were gifts from Dr. Laurent Coscoy (UC Berkeley).[48]

Microscopy and histology:

Staining Swiss rolls was done as previously described.[35] Briefly, the small intestine was dissected then flushed with cold PBS, splayed open and rolled into a Swiss roll, then fixed in 4% paraformaldehyde (PFA) for 4hr then placed in 30% sucrose overnight at 4°C. The next day rolls were shaken gently in 50% OCT in PBS for >2hr and then embedded in OCT and frozen at -80°C. Eight-16 µm sections were cut on a cryotome, dried and then frozen at -20°C. Slides were then fixed in ice-cold acetone for 10 min, dried and then blocked in PBS with 2.5% goat serum and 2.5% Donkey serum at room temperature for 1hr. Sections were stained in primary antibodies overnight at room temperature (anti-Thy1.1-Alexa Fluor 647 (1:200), anti-Ep-CAM FITC (1:800)). Stained slides were washed in PBS then mounted in ProLong Diamond Antifade reagent (Invitrogen P36961). Images were acquired using an SP5 confocal microscope (Leica) or Echo

Revolve. Histology was performed on intestinal clippings fixed in 10% normal buffered formalin before paraffin embedding, slicing, and staining with hematoxylin and eosin and imaged on a Leica DMi1 with iPhone 13 mini through eyepiece. Pathology was scored blind using a modified Marsh-Oberhuber classification.[111]

RNA sequencing:

10x Single cell RNA sequencing:

To sequence CD8αβ^{+} T cells from SFB colonized mice, two Jax B6 and two H2-M3$^{-/-}$ mice were de novo colonized with enriched SFB fecal samples by oral gavage. Four weeks later, the IEL from the last 10cm of the small intestine was prepared and each mouse was stained with oligo-hashtagged antibodies and other surface markers. CD8^{+}CD44^{+}CD62L^{-} T cells from each mouse were FAC sorted using a BD FACSAria Fusion, counted, and pooled equally and 15,000 cells total were loaded onto one channel with a 10x Genomics Chromium Controller per manufacturer's instructions. Gene expression, feature barcode, and TCR libraries were generated with Next GEM 5' v2 reagents and sequenced on an Illumina NextSeq 2000. Base calls were performed using Illumina RTA on the instrument. Libraries were processed to FASTQ files, gene and feature barcode UMI counts, and assembled TCR sequences, using 10x Genomics Cell Ranger v.6.1.1. Reconstruction of full TCR sequences from 10x VDJ outputs was performed using Stitchr software[112] and V(D)J calls from sequencing. The full TCR sequence from the ten most clonally expanded TCRs (genotype agnostic) were used for retroviral re-expression in vitro and subsequent in vivo adoptive transfer. TCR1 was from a Jax B6 mouse and TCR3 was from an *H2-M3$^{-/-}$* mouse **(Table S1)**.

To sequence SFB-specific CD8^{+} T cells from various tissues, 10,000 naïve TCR3^{Rg} cells were transferred into 10 Jax mice and de novo colonized with enriched SFB fecal samples by oral gavage. 11 days later, spleen and MLN were enriched for Thy1.1-APC using MACS column enrichment and anti-APC microbeads (Miltenyi 130-090-855) and the LP and IEL from the last

10cm of the small intestine were prepared without enrichment. All 10 mice were pooled and each tissue was stained with oligo-hashtagged antibodies and other surface markers. $CD8^{+}Thy1.1^{+}$ T cells from each tissue were FAC sorted using a BD FACSAria Fusion, counted, and pooled equally and 14,000 cells total were loaded onto one channel with a 10x Genomics Chromium Controller per manufacturer's instructions. Gene expression and feature barcode libraries were generated with Next GEM 5' v3 reagents, and sequenced on an Illumina NextSeq 2000. Base calls were performed using BCL Convert v.4.2.7 on Illumina BaseSpace. Libraries were processed to FASTQ files and gene and feature barcode UMI counts using 10x Genomics Cell Ranger v.9.0.0.

To sequence SFB-specific $CD8^{+}$ T cells in a setting with perturbed TGFβ signaling, 10,000 naïve TCR3 cells were transferred into three *Itgav*$^{fl/fl}$ and three *Itgav*$^{fl/fl}$ *Villin*$^{Cre/+}$ mice and de novo colonized with enriched SFB fecal samples by oral gavage. 28 days later, IEL from the last 10cm of the small intestine was prepared and each mouse was stained with oligo-hashtagged antibodies and other surface markers. CD8+Thy1.1+ T cells from each mouse were FAC sorted using a BD FACSAria Fusion, counted, and pooled such that 1/3 of the cellular input was from *Itgav*$^{fl/fl}$ mice and 2/3 was from *Itgav*$^{fl/fl}$ *Villin*$^{Cre/+}$ mice to account for enhanced T cell heterogeneity found in *Itgav*$^{fl/fl}$ *Villin*$^{Cre/+}$ mice. Target cell numbers were loaded onto one channel with a 10x Genomics Chromium Controller per manufacturer's instructions. Gene expression and feature barcode libraries were generated with Next GEM 5' v3 reagents, and sequenced on an Illumina NextSeq 2000. Base calls were performed using BCL Convert v.4.2.7 on Illumina BaseSpace. Libraries were processed to FASTQ files and gene and feature barcode UMI counts using 10x Genomics Cell Ranger v.9.0.0.

Quality control, demultiplexing, projection, clustering, and gene expression comparisons were performed using the Seurat toolkit v.5.4.0.[113] Cells were filtered based on empirically determined thresholds for minimum and maximum gene and UMI counts and maximum percent of UMIs derived from mitochondrial, hemoglobin, and ribosomal protein genes. Cells were further

filtered based on expression of genes characteristic of non-T cells, to remove contaminating B cells, monocytes, and intestinal epithelial cells. Cells were assigned to source sample based on empirically determine thresholds for hashtag counts; any cells positive for multiple hashtags were excluded. UMAP parameters were optimized using scDEED.[114] Trajectory analysis was performed using Slingshot v.2.18.0.[61]

Bulk RNA sequencing:

To sequence $CD8^+$ T cells from *Itgav fl/fl* mice, 10,000 naïve TCR3 cells were transferred into four *Itgav*$^{fl/fl}$ and four *Itgav*$^{fl/fl}$ *Villin*$^{Cre/+}$ mice and de novo colonized with enriched SFB fecal samples by oral gavage. 14 days later, IEL from the last 10cm of the small intestine was prepared and stained with surface markers. 400 $CD8^+Thy1.1^+CD103^+$ T cells from *Itgav*$^{fl/fl}$ mice and 400 of each $CD8^+Thy1.1^+CD103^+$ and $CD103^-$ T cells from *Itgav*$^{fl/fl}$ *Villin*$^{Cre/+}$ mice were FAC sorted directly into SMARTseq buffer using a BD FACSAria Fusion. Full-length cDNA was amplified using the SMART-Seq v4 Ultra Low Input RNA kit (Takara Bio, San Jose, CA). Sequencing libraries were constructed using the NexteraXT DNA Library prep kit (Illumina, San Diego, CA). Library concentrations were quantified using a Qubit fluorometer (Thermo Fisher, Waltham, MA), and libraries were pooled based on relative concentration to achieve equal depth, and sequenced on an Illumina NextSeq 2000. Base calling and FASTQ generation was performed on Illumina BaseSpace using BCL Convert v.4.2.7. Reads were trimmed and filtered using fastp v.0.24.0.[115] Trimmed FASTQs were aligned to mouse genome assembly GRCm38.91, using STAR v.2.7.11b.[116] Gene counts were calculated using htseq-count,[117] and quality metrics were calculated using Picard v.3.1.0 (http://broadinstitute.github.io/picard/) and FastQC v.0.12.1.[118]

To sequence $CD8^+$ T cells from *Lag3*$^{-/-}$ mixed bone marrow chimeras, chimeras were de novo colonized with enriched SFB fecal samples by oral gavage. 28 days later, LP and IEL from the last 10cm of the small intestine was prepared and stained with surface markers. 400 $CD8^+CD44^+C62L^-Thy1.1^+CD45.1$ T cells from *Lag3*$^{-/-}$ chimeras and 400 of each $CD8^+CD44^+C62L^-$

Thy1.1^{+}CD45.2 T cells from WT control chimeras were FAC sorted directly into SMARTseq buffer using a BD FACSAria Fusion. Full-length cDNA was amplified using the SMART-Seq v4 Ultra Low Input RNA kit (Takara Bio, San Jose, CA). Sequencing libraries were constructed using the NexteraXT DNA Library prep kit (Illumina, San Diego, CA). Library concentrations were quantified using a Qubit fluorometer (Thermo Fisher, Waltham, MA), and libraries were pooled based on relative concentration to achieve equal depth and sequenced on an Illumina NextSeq 2000. Base calling and FASTQ generation was performed on Illumina BaseSpace using BCL Convert v.3.10.4. Reads were trimmed and filtered using Trimmomatic.[119] Trimmed FASTQs were aligned to mouse genome assembly GRCm38.91, using STAR v.2.7.11a.[116] Gene counts were calculated using htseq-count,[117] and quality metrics were calculated using Picard v.3.1.0 (http://broadinstitute.github.io/picard/) and FastQC v.0.12.1.[118]

Libraries were filtered based on total read counts, percent of reads aligned to genome, and median CV of coverage. Read counts were normalized using the trimmed mean of m-values,[120] and differential gene expression was calculated using the limma package.[121] Gene set enrichment analysis was performed using GSEA as implemented in the GSEA_R package with MSigDB hallmark gene sets.[122,123]

Statistics:

Statistical analysis was performed in Prism (GraphPad Software, v10). Unpaired, two-tailed student's t tests were applied to determine the differences between two individual groups. For multiple group comparisons ANOVA was used. For statistical details of specific experiments, please see respective figure legends.

Data and materials availability:

All data needed to evaluate the conclusions in the paper are present in Chapter 2 or the supplementary materials in Chapter 2.

Supplementary Material

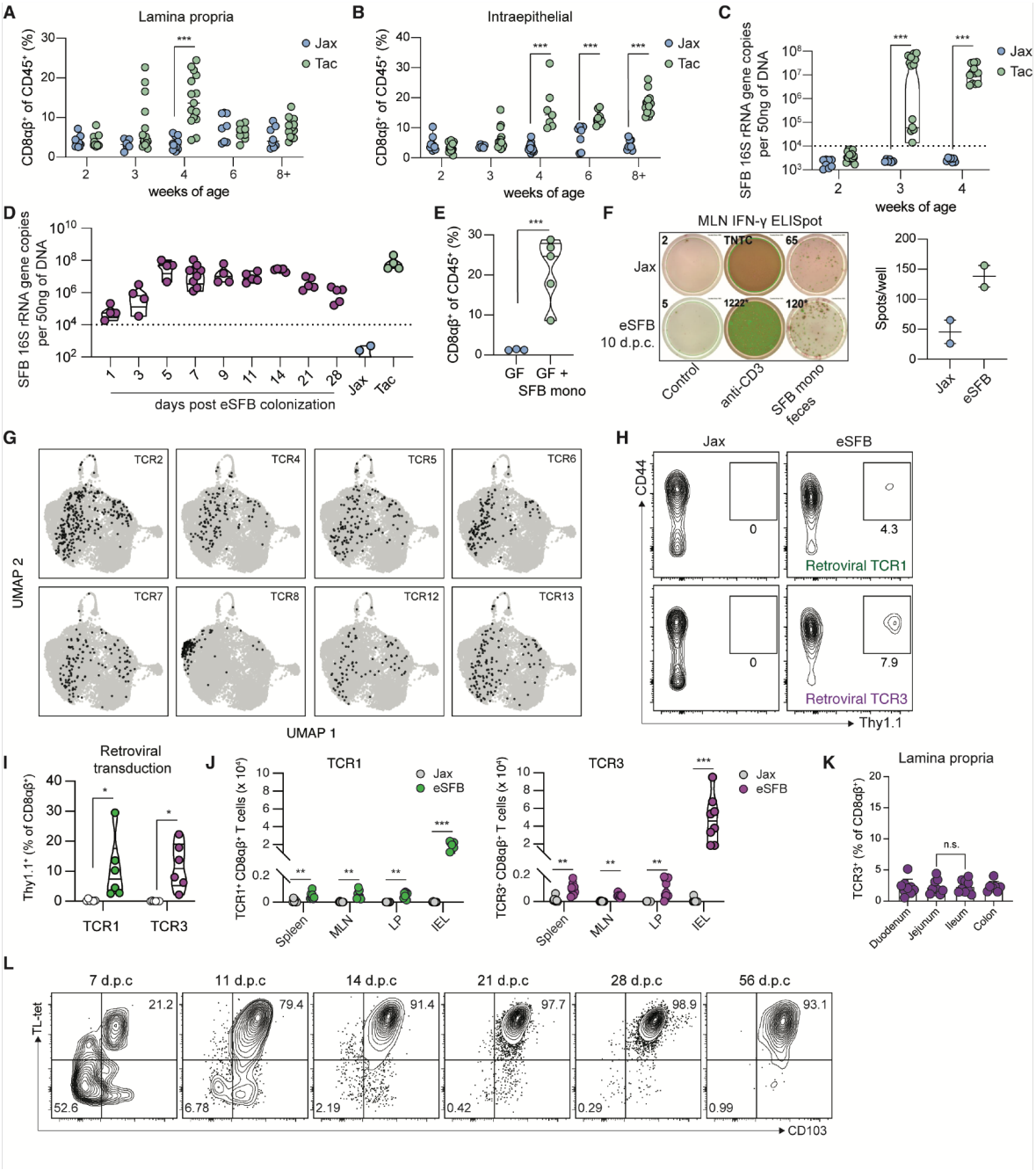

Figure S1 caption on next page

Fig. S1. **(A)** Dot plot of CD8αβ$^+$ T cells as a percent of total live CD45$^+$ cells from the LP and **(B)** IEL fraction of the last 10cm (or, in the case of 2-week-old mice, the entire intestine) of the small intestine of mice originating from Jax and Tac at different age bred in-house. Data were collected from age matched mixed male and female Jax and Tac mice at each time point, n=6-14 per group per timepoint, pooled from five independent experiments. **(C)** Violin plot of qPCR analysis for total SFB load from feces from mice in (A). **(D)** Violin plots of qPCR analysis for total SFB load from feces over time from mice colonized with eSFB, n=4-5 per group. **(E)** Violin plot of CD8αβ$^+$ T cells as a percent of total live CD45$^+$ cells from germ-free Swiss Webster (SWR/J) mice colonized with SFB from monoassociated feces 28 days post colonization (d.p.c.), n=3-5 per group. **(F)** Purified CD8$^+$ T cells from the MLN of mice colonized with SFB for 10 days were incubated with purified CD11c$^+$ APCs with anti-CD3 or feces from SFB monoassociated mice overnight on an IFN-ɣ ELISPOT plate. One representative plate is shown with replicate dot plots, data are from two independent experiments. **(G)** Uniform manifold approximation and projection (UMAP) plot highlighting the cluster position and frequency of TCR clonotypes TCR2, TCR4, TCR5, TCR6, TCR7, TCR8, TCR12, and TCR13 from 10x single cell V(D)J sequencing of CD8αβ$^+$ pIEL from two Jax mice and two H2-M3$^{-/-}$ mice 28 d.p.c. with eSFB. **(H)** Representative flow plots of CD44 and Thy1.1 staining of total CD8αβ$^+$ T cells and **(I)** violin plots of CD44$^+$Thy1.1$^+$CD8αβ$^+$ pIEL as frequency of total CD8αβ$^+$ pIEL from mice adoptively transferred with 500,000 CD8$^+$ T cells transduced *ex vivo* with Thy1.1-TCR1 and Thy1.1-TCR3 retrovirus with or without eSFB 14 d.p.c. and T cell transfer, n=6 pooled from two independent experiments. **(J)** Violin plots of total retrogenic CD8αβ$^+$ T cells from spleen, MLN, LP and IEL of Jax mice receiving 10,000 naive TCR1^{Rg} (green) and TCR3^{Rg} (pink) CD8$^+$ T cells with or without eSFB 14 d.p.c and T cell transfer, n=7-8 per group from two independent experiments. **(K)** Bar graph of total TCR3^{Rg} CD8$^+$ T cells from Jax mice receiving 10,000 naive cells 14 d.p.c. and T cell transfer. The small intestine was segmented in thirds and the colon was taken along with the cecum, n=9 mice per group from two independent experiments. **(L)** Representative flow plots of TCR3^{Rg} CD8$^+$ T cells TL-tetramer (CD8αα) by CD103 from Jax mice receiving 10,000 naive cells with eSFB analyzed over time, n=8 per group from two independent experiments. P values were calculated using (A-D, H and J) ordinary one-way ANOVA with Tukey's multiple comparisons, (E) unpaired t test, and (K) quadrant frequencies plus/minus the standard deviation are shown. Statistical significance denoted as not significant (ns), * P<0.05, ** P <0.01, and *** P <0.001.

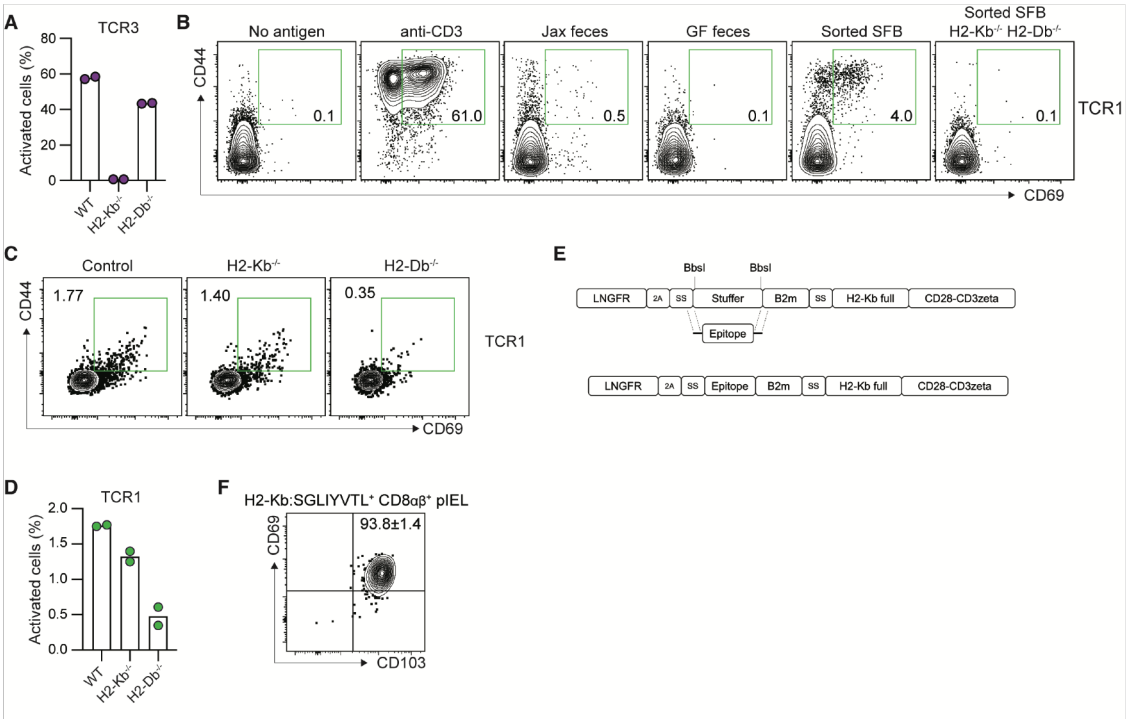

Fig. S2. **(A)** Bar graphs from co-cultured naive TCR3^{Rg} CD8^{+} T cells and DC2.4 APC cell lines WT or deficient for individual MHCIa molecules treated with eSFB feces and incubated for 72 hours. Data are from two independent experiments. (**B)** Representative flow plots from co-cultured naive TCR1^{Rg} CD8^{+} T cells and purified CD11c^{+} WT or MHCIa$^{-/-}$ antigen-presenting cells (APCs) treated with either anti-CD3, feces from Jax or germ-free mice, or FACS-purified SFB from monoassociated feces and incubated for 72 hours. Data were confirmed with two independent experiments. **(C)** Representative flow plots from co-cultured naive TCR1^{Rg} CD8^{+} T cells and DC2.4 APC cell lines WT or deficient for individual MHCIa molecules treated with eSFB feces and incubated for 72 hours. Data were confirmed with two independent experiments. **(D)** Bar graphs from co-cultured naive TCR1^{Rg} CD8^{+} T cells and DC2.4 APC cell lines WT or deficient for individual MHCIa molecules treated with eSFB feces and incubated for 72 hours. Data are from two independent experiments. **(E)** Schematic of Signaling and antigen-presenting bifunctional receptors (SABRs) epitope screening construct. **(F)** Representative flow plot of CD69 and CD103 staining on CD44^{+}SGLIYVTL-tetramer^{+} CD8αβ^{+} pIEL from Jax mice receiving 10,000 naive cells with eSFB, analyzed 14 d.p.c. and T cell transfer, n=7 per group pooled from two independent experiments. Quadrant frequencies plus/minus the standard deviation are shown.

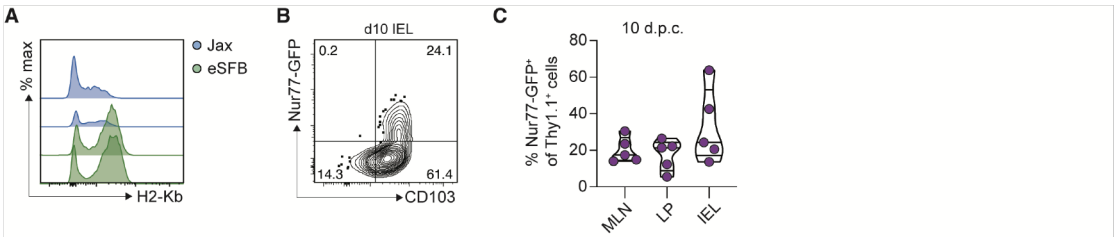

Fig. S3. **(A)** Histograms of H2-Kb staining on live CD45^{-} cells from the IEL fraction of the small intestine with or without eSFB 14 d.p.c. n=2. **(B)** Representative flow plots showing CD103 staining of Nur77^{GFP} TCR3^{Rg} CD8^{+} T cells from ileum of eSFB colonized Jax mice 10 d.p.c. and T cell transfer, n=8-10 per group pooled from two independent experiments. **(C)** Violin plot of Nur77^{GFP+} TCR3^{Rg} CD8^{+} T cells as a frequency of total Nur77^{GFP} TCR3^{Rg} CD8^{+} T cells in mice from (B) at 10 d.p.c..

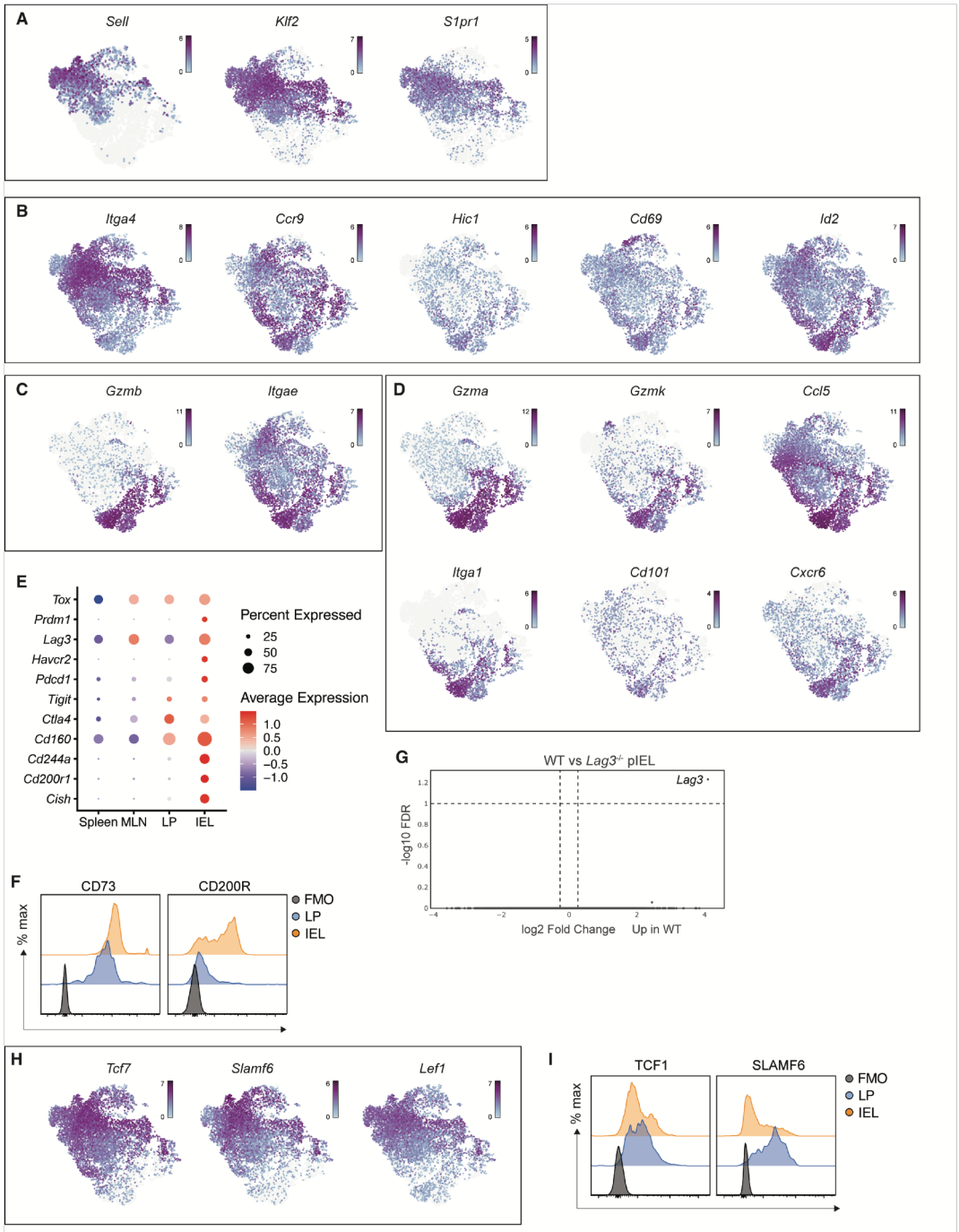

Fig. S4. **(A)** Uniform manifold approximation and projection (UMAP) plots showing log2 normalized expression of indicated secondary lymphoid organ homing genes, **(B)** gut homing genes, **(C)** pIEL associated genes, **(D)** effector genes, and **(E)** co-inhibitory receptor genes from 10x scRNAseq analysis of sorted TCR3^{Rg} CD8^{+} T cells from the spleen, MLN, ileum LP and IEL of Jax mice 11 d.p.c. and T cell transfer. Data were generated from cells pooled from 10 mice. **(F)** Protein expression of selected inhibitory receptors on TCR3^{Rg} CD8^{+} T cells from LP and IEL cells from Jax mice 14 d.p.c. and T cell transfer. **(G)** Volcano plot of differentially regulated genes from bulk RNA sequencing comparing sorted activated WT or *Lag3*$^{-/-}$ CD8αβ^{+} pIEL from mixed bone marrow chimeras colonized with eSFB 28 days prior to analysis. **(H)** UMAP plots showing log2 normalized expression of indicated stem-like associated genes. **(I)** Protein expression of selected inhibitory receptors on TCR3^{Rg} CD8^{+} T cells from LP and IEL cells from Jax mice 14 d.p.c. and T cell transfer.

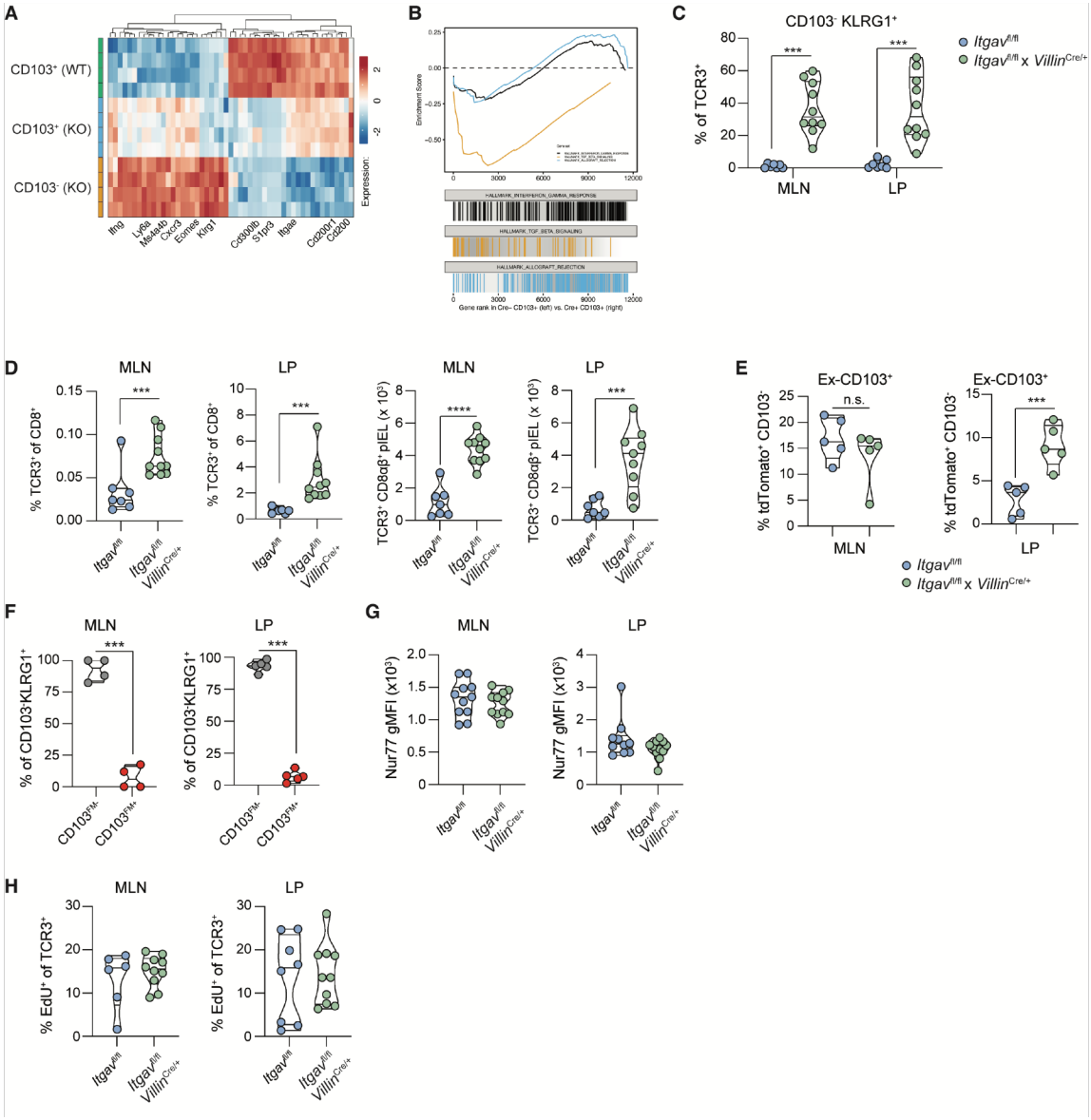

Fig. S5. **(A)** Heat map of normalized expression of top 30 differentially up- and down- regulated genes between TCR3^{Rg} CD8^{+} T cells that are CD103^{+} from *Itgav*$^{fl/fl}$mice and CD103^{+} and CD103^{-} from *Itgav*$^{fl/fl}$ *Villin*$^{Cre/+}$ littermate mice 14 d.p.c. and T cell transfer. **(B)** Gene set enrichment analysis (GSEA) of MSigDB hallmark gene sets indicated between CD103^{+} from *Itgav*$^{fl/fl}$ and CD103^{-} from *Itgav*$^{fl/fl}$ *Villin*$^{Cre/+}$ cells from (A). **(C)** Violin plots of CD103^{-}KLRG1^{+} TCR3^{Rg} CD8^{+} T cells from MLN and LP as a frequency of total TCR3^{Rg} pIEL from *Itgav*$^{fl/fl}$ *Villin*$^{Cre/+}$ or *Itgav*$^{fl/fl}$ littermate control mice 28 d.p.c. and T cell transfer, n=7-10 per group pooled from three independent experiments. **(D)** Violin plots of TCR3^{Rg} CD8^{+} T cells in MLN and LP plotted as total cells and as a frequency of total T cells from mice in (C). **(E)** Violin plots of CD103^{-}tdTomato^{+} cells from *Itgav*$^{fl/fl}$ *Villin*$^{Cre/+}$ or *Itgav*$^{fl/fl}$ littermate control mice in MLN and LP from CD103-CreERT2 fatemapping CD8^{+} T cells transduced *ex vivo* with TCR3 prior to transfer into *Itgav*$^{fl/fl}$ *Villin*$^{Cre/+}$ or *Itgav*$^{fl/fl}$ littermate control mice. Mice were given 4mg tamoxifen every other day starting 12 d.p.c. and T cell transfer and analyzed day 21, n=5 per group. **(F)** Violin plot of frequency of CD103^{-}KLRG1^{+} TCR3^{Rg} CD8^{+} T cells that are tdTomato^{-} or tdTomato^{+} from MLN and LP from *Itgav*$^{fl/fl}$ *Villin*$^{Cre/+}$ mice from (E). **(G)** Violin plot of the geometric mean fluorescence intensity (gMFI) of GFP from Nur77^{GFP} TCR3^{Rg} CD8^{+} T cells from MLN and LP of *Itgav*$^{fl/fl}$ *Villin*$^{Cre/+}$ or *Itgav*$^{fl/fl}$ littermate control mice 28 d.p.c and T cells transfer, n=11-12 per group pooled from two independent experiments. **(H)** Violin plot of EdU^{+} TCR3^{Rg} CD8^{+} T cells from MLN and LP as a frequency of total TCR3^{Rg} CD8^{+} T cells from *Itgav*$^{fl/fl}$ *Villin*$^{Cre/+}$ or *Itgav*$^{fl/fl}$ littermate control mice 28 d.p.c and T cells transfer, n=7-9 per group pooled from two independent experiments. P values were calculated using (C and E) two-way ANOVA with Šídák's multiple comparisons, (D, F-I) unpaired t test. Statistical significance denoted as not significant (ns), *** P <0.001, and **** P <0.0001.

TCR_name	cloneIdTcrGraphClonalExpansion	nCellsInClonotype	nCellsWithSequence	chain	cdr3	v_gene	v_gene_annotated	d_gene	j_gene	j_gene_annotated	c_gene
TCR1a	WT-Mouse-2_clone240	483	214	TRA	CAMRGYSNTNKVVF	TRAV16*01	TRAV16*06		TRAJ34	TRAJ34*02	TRAC
TCR2a	WT-Mouse-2_clone240	483	302	TRA	CGASSSFSKLVF	TRAV5-4	TRAV5-4*02		TRAJ50	TRAJ50*01	TRAC
TCR1b/2b	WT-Mouse-2_clone240	483	478	TRB	CASSQTANSDYTF	TRBV12-2	TRBV12-2*01		TRBJ1-2	TRBJ1-2*01	TRBC1
TCR3a	H2-M3KO-Mouse-1_clone21	373	330	TRA	CAASSGGSNYKLTF	TRAV14D-1	TRAV14D-1*01		TRAJ53	TRAJ53*01	TRAC
TCR4a	H2-M3KO-Mouse-1_clone21	373	129	TRA	CATDRGSGGSNYKLTF	TRAV8D-1	TRAV8D-1*01		TRAJ53	TRAJ53*01	TRAC
TCR3b/4b	H2-M3KO-Mouse-1_clone21	373	352	TRB	CASSQETGGYEQYF	TRBV5	TRBV5*01	TRBD1	TRBJ2-7	TRBJ2-7*01	TRBC2
TCR5a	H2-M3KO-Mouse-1_clone294	206	155	TRA	CAMREYTNTGKLTF	TRAV16D-DV11	TRAV16D-DV11*02 OR TRAV16*01		TRAJ27	TRAJ27*01	TRAC
TCR5b	H2-M3KO-Mouse-1_clone294	206	196	TRB	CASSLGGNSDYTF	TRBV12-2	TRBV12-2*01		TRBJ1-2	TRBJ1-2*01	TRBC1
TCR6a	WT-Mouse-1_clone29	198	156	TRA	CAASYGNEKITF	TRAV10	TRAV10*01		TRAJ48	TRAJ48*01	TRAC
TCR6b	WT-Mouse-1_clone29	198	191	TRB	CASSPGQGNSDYTF	TRBV29	TRBV29*01	TRBD1	TRBJ1-2	TRBJ1-2*01	TRBC1
TCR7a	WT-Mouse-1_clone248	185	142	TRA	CAMRDYTNTGKLTF	TRAV16N	TRAV16N*01		TRAJ27	TRAJ27*01	TRAC
TCR7b	WT-Mouse-1_clone248	185	185	TRB	CASSGTANSDYTF	TRBV12-2	TRBV12-2*01		TRBJ1-2	TRBJ1-2*01	TRBC1
TCR8a	H2-M3KO-Mouse-2_clone37	173	131	TRA	CALDYNQGKLIF	TRAV6D-4	TRAV6D-4*01		TRAJ23	TRAJ23*01	TRAC
TCR8b	H2-M3KO-Mouse-2_clone37	173	170	TRB	CASSDWGEYEQYF	TRBV13-1	TRBV13-1*02		TRBJ2-7	TRBJ2-7*01	TRBC2
TCR12a	WT-Mouse-1_clone242	172	93	TRA	CAMREYTNTGKLTF	TRAV16D-DV11	TRAV16*01 OR TRAV16D-DV11*02		TRAJ27	TRAJ27*01	TRAC
TCR12b	WT-Mouse-1_clone242	172	163	TRB	CASSLGGNSDYTF	TRBV12-2	TRBV12-2*01		TRBJ1-2	TRBJ1-2*01	TRBC1
TCR13a	WT-Mouse-1_clone333	172	154	TRA	CALGSYTNTGKLTF	TRAV6N-7	TRAV6N-7*01 OR TRAV6N-7*04		TRAJ27	TRAJ27*01	TRAC
TCR13b	WT-Mouse-1_clone333	172	166	TRB	CASSRTGDYAEQFF	TRBV12-2	TRBV12-2*01	TRBD1	TRBJ2-1	TRBJ2-1*01	TRBC2
	Note for some clonally expanded TCRs, a full length sequence was not able to be generated using Stitchr software due to missing IMGT annotation and were omitted from analysis										

Table S1. CDR3 and V(D)J sequences of CD8αβ$^+$ pIEL from mice colonized with eSFB

Name	Sequence (5'-3')*	Purpose
UDI-ClassI-Fwd-Mix-1	ACACTCTTTCCCTACACGACGCTCTTCCGATCTTGGCCTGCTTTGTTTGC	PCR1
UDI-ClassI-Fwd-Mix-2	ACACTCTTTCCCTACACGACGCTCTTCCGATCTGGCCTGCTTTGTTTGCC	PCR1
UDI-ClassI-Fwd-Mix-3	ACACTCTTTCCCTACACGACGCTCTTCCGATCTCCTGCTTTGTTTGCCGTG	PCR1
UDI-ClassI-Rev-Mix-1	GTGACTGGAGTTCAGACGTGTGCTCTTCCGATCTCCTCCACCACCGCTACCTC	PCR1
UDI-ClassI-Rev-Mix-2	GTGACTGGAGTTCAGACGTGTGCTCTTCCGATCCTTCCTCCACCACCGCTACC	PCR1
UDI-ClassI-Rev-Mix-3	GTGACTGGAGTTCAGACGTGTGCTCTTCCGATCGCTTCCTCCACCACCGCTAC	PCR1
UDI-Index1 F	AATGATACGGCGACCACCGAGATCTACACagcgctagACACTCTTTCCCTACACGACGCTCTTCCGATCT	PCR2 index and adaptors
UDI-Index2 F	AATGATACGGCGACCACCGAGATCTACACgatatcgaACACTCTTTCCCTACACGACGCTCTTCCGATCT	PCR2 index and adaptors
UDI-Index3 F	AATGATACGGCGACCACCGAGATCTACACcgcagacgACACTCTTTCCCTACACGACGCTCTTCCGATCT	PCR2 index and adaptors
UDI-Index4 F	AATGATACGGCGACCACCGAGATCTACACtatgagtaACACTCTTTCCCTACACGACGCTCTTCCGATCT	PCR2 index and adaptors
UDI-Index5 F	AATGATACGGCGACCACCGAGATCTACACaggtgcgtACACTCTTTCCCTACACGACGCTCTTCCGATCT	PCR2 index and adaptors
UDI-Index1 R	CAAGCAGAAGACGGCATACGAGATaaccgcggGTGACTGGAGTTCAGACGTGTGCTCTTCCGATC	PCR2 index and adaptors
UDI-Index2 R	CAAGCAGAAGACGGCATACGAGATggttataaGTGACTGGAGTTCAGACGTGTGCTCTTCCGATC	PCR2 index and adaptors
UDI-Index3 R	CAAGCAGAAGACGGCATACGAGATccaagtccGTGACTGGAGTTCAGACGTGTGCTCTTCCGATC	PCR2 index and adaptors
UDI-Index4 R	CAAGCAGAAGACGGCATACGAGATttggacttGTGACTGGAGTTCAGACGTGTGCTCTTCCGATC	PCR2 index and adaptors
UDI-Index5 R	CAAGCAGAAGACGGCATACGAGATcagtggatGTGACTGGAGTTCAGACGTGTGCTCTTCCGATC	PCR2 index and adaptors
UDI-Index6 F	AATGATACGGCGACCACCGAGATCTACACgaacatacACACTCTTTCCCTACACGACGCTCTTCCGATCT	PCR2 index and adaptors
UDI-Index7 F	AATGATACGGCGACCACCGAGATCTACACacatagcgACACTCTTTCCCTACACGACGCTCTTCCGATCT	PCR2 index and adaptors
UDI-Index8 F	AATGATACGGCGACCACCGAGATCTACACgtgcgataACACTCTTTCCCTACACGACGCTCTTCCGATCT	PCR2 index and adaptors
UDI-Index9 F	AATGATACGGCGACCACCGAGATCTACACccaacagaACACTCTTTCCCTACACGACGCTCTTCCGATCT	PCR2 index and adaptors
UDI-Index10 F	AATGATACGGCGACCACCGAGATCTACACttggtgagACACTCTTTCCCTACACGACGCTCTTCCGATCT	PCR2 index and adaptors
UDI-Index6 R	CAAGCAGAAGACGGCATACGAGATtgacaagcGTGACTGGAGTTCAGACGTGTGCTCTTCCGATC	PCR2 index and adaptors
UDI-Index7 R	CAAGCAGAAGACGGCATACGAGATctagcttgGTGACTGGAGTTCAGACGTGTGCTCTTCCGATC	PCR2 index and adaptors
UDI-Index8 R	CAAGCAGAAGACGGCATACGAGATtcgatccaGTGACTGGAGTTCAGACGTGTGCTCTTCCGATC	PCR2 index and adaptors
UDI-Index9 R	CAAGCAGAAGACGGCATACGAGATcctgaactGTGACTGGAGTTCAGACGTGTGCTCTTCCGATC	PCR2 index and adaptors
UDI-Index10 R	CAAGCAGAAGACGGCATACGAGATGACCTGAAGTGACTGGAGTTCAGACGTGTGCTCTTCCGATC	PCR2 index and adaptors

Table S2. Oligo sequences used for SABR epitope discovery insertion amplification.

Flow Cytometry				
Target	**Clone**	**Fluor/conjugation**	**Vendor**	**Catalog #**
b2-microglobulin	A16041A	PE	Biolegend	154503
CD103	2E7	PE	Biolegend	121406
CD103	2E7	BV510	Biolegend	121423
CD200R (OX2R)	OX-110	PE	Biolegend	123907
CD25	PC61	PE	BioLegend	102007
CD39	Duha59	PE-Cy7	Biolegend	143805
CD4	RM4-5	BUV737	BD Horizon	612843
CD4	RM4-5	PerCP/Cyanine5.5	Biolegend	100540
CD44	IM7	biotin	Biolegend	103003
CD44	IM7	Alexa Fluor 700	Thermo Scientific	56-0441-82
CD45	30-F11	BUV395	BD	564279
CD45	30-F11	APC-eFluor 780	Thermo Scientific	47-0451-82
CD45.1	A20	BUV395	BD	565212
CD45.2	104	BV510	BioLegend	109838
CD45.2	104	APC	BioLegend	109814
CD62L	MEL-14	BV421	BioLegend	104436
CD69	H1.2F3	eFluor 450	Thermo	48-0691-82
CD69	H1.2F3	APC	Thermo Scientific	17-0691-82
CD73	TY/11.8	PE-Cy7	Biolegend	127223
CD8a	53-6.7	Alexa Fluor 700	Thermo Scientific	56-0081-82
CD8b	H35-17.2	BV605	BD	740387
CD8b	YTS156.7.7	PE	BioLegend	126608
H2-Db	KH95	PE	BioLegend	111507
H2-Kb	AF6-88.5	FITC	BioLegend	116505
human CD69	FN50	PE-Cy7	Biolegend	310911
IFNg	XMG1.2	eFluor 450	Thermo Scientific	48-7311-82
KLRG1	MAFA	APC	Biolegend	138412
KLRG1	MAFA	FITC	BioLegend	138410
Lag3 (CD223)	C9B7W	PE	BioLegend	125208
Ly108 (SLAMF6)	330 AJ	APC	Biolegend	134609
NGFR (CD271)	ME20.4	APC	Biolegend	345108
NGFR (CD271)	ME20.4	PE	Biolegend	345106
PD-1 (CD279)	RMP1-30	PE-Cy7	BioLegend	109110
PD-1 (CD279)	J43	APC	Thermo	17-9985-82
TCF1	S33-966	PE	BD	564217
TCRb	H57-597	PerCP/Cyanine5.5	Thermo Scientific	45-5961-82
Thy1.1 (CD90.1)	OX-7	Alexa Fluor 700	BioLegend	202528
Thy1.1 (CD90.1)	OX-7	APC	BioLegend	202526
Thy1.2 (CD90.2)	30-H12	BV765	Biolegend	105331
Tim-3 (CD366)	RMT3-23	APC	Biolegend	119705
Tox	TXRX10	eFluor 660	ThermoFisher	50-6502-80
Live/Dead		UV excited/V emissi	Thermo	L34962
Other				
Target	**Clone**	**Fluor/conjugation**	**Vendor**	**Catalog #**
CD3 (activation)	17A2	NA	ThermoFisher	14-0032-85
Thy1.2 (CD90.2) (depletion)	30-H12	biotin	Biolegend	105304
Imaging				
Target	**Clone**	**Fluor/conjugation**	**Vendor**	**Catalog #**
Ep-CAM (CD326)	G8.8	Alexa Fluor 488	BioLegend	118210
Thy1.1 (CD90.1)	OX-7	Alexa Fluor 647	Biolegend	202508
Sequencing Hashatgs				
Target	**Clone**	**Fluor/conjugation**	**Vendor**	**Catalog #**
TotalSeq™-C0301 anti-mouse Hashtag 1 Antibody		oligo	Biolegend	155861
TotalSeq™-C0302 anti-mouse Hashtag 2 Antibody		oligo	BioLegend	155863
TotalSeq™-C0303 anti-mouse Hashtag 3 Antibody		oligo	Biolegend	155865
TotalSeq™-C0304 anti-mouse Hashtag 4 Antibody		oligo	Biolegend	155867
TotalSeq™-C0309 anti-mouse Hashtag 9 Antibody		oligo	Biolegend	155877
TotalSeq™-C0310 anti-mouse Hashtag 10 Antibody		oligo	BioLegend	155879
TotalSeq™-C0313 anti-mouse Hashtag 13 Antibody		oligo	Biolegend	155885
TotalSeq™-C0314 anti-mouse Hashtag 14 Antibody		oligo	Biolegend	155887
TotalSeq™-C0315 anti-mouse Hashtag 15 Antibody		oligo	Biolegend	155889
TotalSeq™-C0316 anti-mouse Hashtag 16 Antibody		oligo	Biolegend	155891
TotalSeq™-C0317 anti-mouse Hashtag 17 Antibody		oligo	Biolegend	113931
TotalSeq™-C0318 anti-mouse Hashtag 18 Antibody		oligo	BioLegend	113929

Table S3. List of antibodies used throughout the paper.

References

1. Belkaid Y, Harrison OJ. Homeostatic Immunity and the Microbiota. *Immunity*. 2017;46(4):562-576. doi:10.1016/J.IMMUNI.2017.04.008
2. Overacre-Delgoffe AE, Hand TW. Regulation of tissue-resident memory T cells by the Microbiota. *Mucosal Immunol*. 2022;15(3):408-417. doi:10.1038/S41385-022-00491-1
3. Ansaldo E, Farley TK, Belkaid Y. Control of Immunity by the Microbiota. *Annu Rev Immunol*. 2021;39:449-479. doi:10.1146/ANNUREV-IMMUNOL-093019-112348
4. Earley ZM, Lisicka W, Sifakis JJ, et al. GATA4 controls regionalization of tissue immunity and commensal-driven immunopathology. *Immunity*. 2023;56(1):43-57.e10. doi:10.1016/J.IMMUNI.2022.12.009
5. Nutsch KM, Hsieh CS. T cell tolerance and immunity to commensal bacteria. *Curr Opin Immunol*. 2012;24(4):385-391. doi:10.1016/J.COI.2012.04.009
6. Ostadmohammadi S, Nojoumi SA, Fateh A, Siadat SD, Sotoodehnejadnematalahi F. Interaction between Clostridium species and microbiota to progress immune regulation. *Acta Microbiol Immunol Hung*. 2022;69(2):89-103. doi:10.1556/030.2022.01678
7. Nishio J, Honda K. Immunoregulation by the gut microbiota. *Cell Mol Life Sci*. 2012;69(21):3635-3650. doi:10.1007/S00018-012-0993-6
8. Xu M, Pokrovskii M, Ding Y, et al. c-MAF-dependent regulatory T cells mediate immunological tolerance to a gut pathobiont. *Nature*. 2018;554(7692):373-377. doi:10.1038/NATURE25500
9. Matharu KS, Mizoguchi E, Cotoner CA, et al. Toll-like receptor 4-mediated regulation of spontaneous Helicobacter-dependent colitis in IL-10-deficient mice. *Gastroenterology*. 2009;137(4). doi:10.1053/J.GASTRO.2009.07.004
10. Bousbaine D, Fisch LI, London M, et al. A conserved Bacteroidetes antigen induces anti-inflammatory intestinal T lymphocytes. *Science*. 2022;377(6606):660-666. doi:10.1126/SCIENCE.ABG5645
11. Bilate AM, London M, Castro TBR, et al. T Cell Receptor Is Required for Differentiation, but Not Maintenance, of Intestinal CD4+ Intraepithelial Lymphocytes. *Immunity*. 2020;53(5):1001-1014.e20. doi:10.1016/J.IMMUNI.2020.09.003
12. Ansaldo E, Slayden LC, Ching KL, et al. Akkermansia muciniphila induces intestinal adaptive immune responses during homeostasis. *Science*. 2019;364(6446):1179-1184. doi:10.1126/SCIENCE.AAW7479
13. Bae M, Cassilly CD, Liu X, et al. Akkermansia muciniphila phospholipid induces homeostatic immune responses. *Nature*. 2022;608(7921):168-173. doi:10.1038/S41586-022-04985-7
14. Didriksen BJ, Eshleman EM, Alenghat T. Epithelial regulation of microbiota-immune cell dynamics. *Mucosal Immunol*. 2024;17(2):303-313. doi:10.1016/J.MUCIMM.2024.02.008
15. Chung H, Pamp SJ, Hill JA, et al. Gut immune maturation depends on colonization with a host-specific microbiota. *Cell*. 2012;149(7):1578-1593. doi:10.1016/J.CELL.2012.04.037
16. Tanoue T, Morita S, Plichta DR, et al. A defined commensal consortium elicits CD8 T cells and anti-cancer immunity. *Nature*. 2019;565(7741):600-605. doi:10.1038/S41586-019-0878-Z

17. Flannigan KL, Denning TL. Segmented filamentous bacteria-induced immune responses: a balancing act between host protection and autoimmunity. *Immunology*. 2018;154(4):537-546. doi:10.1111/IMM.12950
18. Harrison OJ, Linehan JL, Shih HY, et al. Commensal-specific T cell plasticity promotes rapid tissue adaptation to injury. *Science*. 2019;363(6422). doi:10.1126/SCIENCE.AAT6280
19. Naik S, Bouladoux N, Linehan JL, et al. Commensal-dendritic-cell interaction specifies a unique protective skin immune signature. *Nature*. 2015;520(7545):104-108. doi:10.1038/NATURE14052
20. Enamorado M, Kulalert W, Han SJ, et al. Immunity to the microbiota promotes sensory neuron regeneration. *Cell*. 2023;186(3):607-620.e17. doi:10.1016/J.CELL.2022.12.037
21. Cheroutre H, Lambolez F, Mucida D. The light and dark sides of intestinal intraepithelial lymphocytes. *Nat Rev Immunol*. 2011;11(7):445-456. doi:10.1038/NRI3007
22. Boland BS, He Z, Tsai MS, et al. Heterogeneity and clonal relationships of adaptive immune cells in ulcerative colitis revealed by single-cell analyses. *Sci Immunol*. 2020;5(50). doi:10.1126/SCIIMMUNOL.ABB4432
23. Duong HG, Choi EJ, Hsu P, et al. Identification of CD8 + T-Cell-Immune Cell Communications in Ileal Crohn's Disease. *Clin Transl Gastroenterol*. 2023;14(5). doi:10.14309/CTG.0000000000000576
24. Casalegno Garduño R, Däbritz J. New Insights on CD8+ T Cells in Inflammatory Bowel Disease and Therapeutic Approaches. *Front Immunol*. 2021;12. doi:10.3389/FIMMU.2021.738762
25. Fan X, Rudensky AY. Hallmarks of Tissue-Resident Lymphocytes. *Cell*. 2016;164(6):1198-1211. doi:10.1016/J.CELL.2016.02.048
26. Heeg M, Goldrath AW. Insights into phenotypic and functional CD8+ TRM heterogeneity. *Immunol Rev*. 2023;316(1):8-22. doi:10.1111/IMR.13218
27. Milner JJ, Goldrath AW. Transcriptional programming of tissue-resident memory CD8+ T cells. *Curr Opin Immunol*. 2018;51:162-169. doi:10.1016/J.COI.2018.03.017
28. Buck MD, Sowell RT, Kaech SM, Pearce EL. Metabolic Instruction of Immunity. *Cell*. 2017;169(4):570-586. doi:10.1016/J.CELL.2017.04.004
29. Crowl JT, Heeg M, Ferry A, et al. Tissue-resident memory CD8+ T cells possess unique transcriptional, epigenetic and functional adaptations to different tissue environments. *Nat Immunol*. 2022;23(7):1121-1131. doi:10.1038/S41590-022-01229-8
30. McDonald BD, Jabri B, Bendelac A. Diverse developmental pathways of intestinal intraepithelial lymphocytes. *Nat Rev Immunol*. 2018;18(8):514-525. doi:10.1038/S41577-018-0013-7
31. Lockhart A, Mucida D, Bilate AM. Intraepithelial Lymphocytes of the Intestine. *Annu Rev Immunol*. 2024;42(1):289-316. doi:10.1146/ANNUREV-IMMUNOL-090222-100246
32. Cheroutre H, Lambolez F. Doubting the TCR coreceptor function of CD8alphaalpha. *Immunity*. 2008;28(2):149-159. doi:10.1016/J.IMMUNI.2008.01.005
33. Madakamutil LT, Christen U, Lena CJ, et al. CD8alphaalpha-mediated survival and differentiation of CD8 memory T cell precursors. *Science*. 2004;304(5670):590-593. doi:10.1126/SCIENCE.1092316

34. Weiss ES, Hirai T, Li H, et al. Epidermal resident memory T cell fitness requires antigen encounter in the skin. *Elife*. 2025;14. doi:10.7554/ELIFE.107096
35. Obers A, Poch T, Rodrigues G, et al. Retinoic acid and TGF-β orchestrate organ-specific programs of tissue residency. *Immunity*. 2024;57(11):2615-2633.e10. doi:10.1016/J.IMMUNI.2024.09.015
36. Christo SN, Evrard M, Park SL, et al. Discrete tissue microenvironments instruct diversity in resident memory T cell function and plasticity. *Nat Immunol*. 2021;22(9):1140-1151. doi:10.1038/S41590-021-01004-1
37. von Hoesslin M, Kuhlmann M, de Almeida GP, et al. Secondary infections rejuvenate the intestinal CD103+ tissue-resident memory T cell pool. *Sci Immunol*. 2022;7(77). doi:10.1126/SCIIMMUNOL.ABP9553
38. Ivanov II, Atarashi K, Manel N, et al. Induction of intestinal Th17 cells by segmented filamentous bacteria. *Cell*. 2009;139(3):485-498. doi:10.1016/J.CELL.2009.09.033
39. Yang Y, Torchinsky MB, Gobert M, et al. Focused specificity of intestinal TH17 cells towards commensal bacterial antigens. *Nature*. 2014;510(7503):152-156. doi:10.1038/NATURE13279
40. Verma S, Dufort MJ, Olsen TM, et al. Antigen-level resolution of commensal-specific B cell responses can be enabled by phage display screening coupled with B cell tetramers. *Immunity*. 2024;57(6):1428-1441.e8. doi:10.1016/J.IMMUNI.2024.04.014
41. Gaboriau-Routhiau V, Rakotobe S, Lécuyer E, et al. The key role of segmented filamentous bacteria in the coordinated maturation of gut helper T cell responses. *Immunity*. 2009;31(4):677-689. doi:10.1016/J.IMMUNI.2009.08.020
42. Bunker JJ, Flynn TM, Koval JC, et al. Innate and Adaptive Humoral Responses Coat Distinct Commensal Bacteria with Immunoglobulin A. *Immunity*. 2015;43(3):541-553. doi:10.1016/J.IMMUNI.2015.08.007
43. Guan J, Peske JD, Manoharan Valerio M, Park C, Robey EA, Sadegh-Nasseri S. Commensal bacteria maintain a Qa-1b-restricted unconventional CD8+ T population in gut epithelium. *Elife*. 2023;12. doi:10.7554/ELIFE.90466
44. Kerksiek KM, Busch DH, Pilip IM, Allen SE, Pamer EG. H2-M3-restricted T cells in bacterial infection: rapid primary but diminished memory responses. *J Exp Med*. 1999;190(2):195-204. doi:10.1084/JEM.190.2.195
45. Xu H, Chun T, Choi HJ, Wang B, Wang CR. Impaired response to Listeria in H2-M3-deficient mice reveals a nonredundant role of MHC class Ib-specific T cells in host defense. *J Exp Med*. 2006;203(2):449-459. doi:10.1084/JEM.20051866
46. Bettini ML, Bettini M, Nakayama M, Guy CS, Vignali DAA. Generation of T cell receptor-retrogenic mice: improved retroviral-mediated stem cell gene transfer. *Nat Protoc*. 2013;8(10):1837-1840. doi:10.1038/NPROT.2013.111
47. Baldwin TA, Sandau MM, Jameson SC, Hogquist KA. The timing of TCR alpha expression critically influences T cell development and selection. *J Exp Med*. 2005;202(1):111-121. doi:10.1084/JEM.20050359
48. Manoharan Valerio M, Arana K, Guan J, et al. The promiscuous development of an unconventional Qa1b-restricted T cell population. *Front Immunol*. 2023;14. doi:10.3389/FIMMU.2023.1250316

49. Joglekar A V., Leonard MT, Jeppson JD, et al. T cell antigen discovery via signaling and antigen-presenting bifunctional receptors. *Nat Methods*. 2019;16(2):191-198. doi:10.1038/S41592-018-0304-8
50. Zdinak PM, Arshad S, Makani VKK, Joglekar A V. T Cell Antigen Discovery Using Cell-Based Epitope Libraries. *Methods Mol Biol*. 2026;2990:19-38. doi:10.1007/978-1-0716-4997-8_2
51. Zdinak PM, Trivedi N, Grebinoski S, et al. De novo identification of CD4+ T cell epitopes. *Nat Methods*. 2024;21(5):846-856. doi:10.1038/S41592-024-02255-0
52. Cruz AR, Wimmer BH, Teo TH, et al. Segmented filamentous bacteria undergo a structural transition at their adhesive tip during unicellular to filament development. *Nat Commun*. 2025;17(1). doi:10.1038/S41467-025-66892-5
53. Pamp SJ, Harrington ED, Quake SR, Relman DA, Blainey PC. Single-cell sequencing provides clues about the host interactions of segmented filamentous bacteria (SFB). *Genome Res*. 2012;22(6):1107-1119. doi:10.1101/GR.131482.111
54. Matsumoto S, Setoyama H, Umesaki Y. Differential induction of major histocompatibility complex molecules on mouse intestine by bacterial colonization. *Gastroenterology*. 1992;103(6):1777-1782. doi:10.1016/0016-5085(92)91434-6
55. Tuganbaev T, Mor U, Bashiardes S, et al. Diet Diurnally Regulates Small Intestinal Microbiome-Epithelial-Immune Homeostasis and Enteritis. *Cell*. 2020;182(6):1441-1459.e21. doi:10.1016/J.CELL.2020.08.027
56. Fung HY, Teryek M, Lemenze AD, Bergsbaken T. CD103 fate mapping reveals that intestinal CD103- tissue-resident memory T cells are the primary responders to secondary infection. *Sci Immunol*. 2022;7(77). doi:10.1126/SCIIMMUNOL.ABL9925
57. Malo CS, Huggins MA, Goddery EN, et al. Non-equivalent antigen presenting capabilities of dendritic cells and macrophages in generating brain-infiltrating CD8 + T cell responses. *Nat Commun*. 2018;9(1). doi:10.1038/S41467-018-03037-X
58. Cawthon AG, Lu H, Alexander-Miller MA. Peptide requirement for CTL activation reflects the sensitivity to CD3 engagement: correlation with CD8alphabeta versus CD8alphaalpha expression. *J Immunol*. 2001;167(5):2577-2584. doi:10.4049/JIMMUNOL.167.5.2577
59. Huleatt JW, Pilip I, Kerksiek K, Pamer EG. Intestinal and splenic T cell responses to enteric Listeria monocytogenes infection: distinct repertoires of responding CD8 T lymphocytes. *J Immunol*. 2001;166(6):4065-4073. doi:10.4049/JIMMUNOL.166.6.4065
60. Ebert EC. Inhibitory effects of transforming growth factor-beta (TGF-beta) on certain functions of intraepithelial lymphocytes. *Clin Exp Immunol*. 1999;115(3):415-420. doi:10.1046/J.1365-2249.1999.00824.X
61. Street K, Risso D, Fletcher RB, et al. Slingshot: cell lineage and pseudotime inference for single-cell transcriptomics. *BMC Genomics*. 2018;19(1). doi:10.1186/S12864-018-4772-0
62. Eksteen B, Mora JR, Haughton EL, et al. Gut homing receptors on CD8 T cells are retinoic acid dependent and not maintained by liver dendritic or stellate cells. *Gastroenterology*. 2009;137(1):320-329. doi:10.1053/J.GASTRO.2009.02.046

63. Hammerschmidt SI, Ahrendt M, Bode U, et al. Stromal mesenteric lymph node cells are essential for the generation of gut-homing T cells in vivo. *J Exp Med*. 2008;205(11):2483-2490. doi:10.1084/JEM.20080039
64. Qiu Z, Khairallah C, Chu TH, et al. Retinoic acid signaling during priming licenses intestinal CD103+ CD8 TRM cell differentiation. *J Exp Med*. 2023;220(5). doi:10.1084/JEM.20210923
65. Chung HK, Liu C, Battu A, et al. Atlas-guided discovery of transcription factors for T cell programming. *Nature*. 2026;651(8107). doi:10.1038/S41586-025-09989-7
66. Sun Q, Dong C. Regulators of CD8+ T cell exhaustion. *Nat Rev Immunol*. 2026;26(2). doi:10.1038/S41577-025-01221-X
67. Wherry EJ. T cell exhaustion. *Nat Immunol*. 2011;12(6):492-499. doi:10.1038/NI.2035
68. Zhang ZF, Zhang Y, Chen YW, et al. CD200R blockade enhances anti-tumor immunity by unleashing NK and CD8+ T cells in tumor. *Acta Pharmacol Sin*. 2025;46(10):2835-2848. doi:10.1038/S41401-025-01556-0
69. Guittard G, Dios-Esponera A, Palmer DC, et al. The Cish SH2 domain is essential for PLC-γ1 regulation in TCR stimulated CD8+ T cells. *Sci Rep*. 2018;8(1). doi:10.1038/S41598-018-23549-2
70. Tang Y, Liu W, Kadu S, et al. Exploiting the CD200-CD200R immune checkpoint axis in multiple myeloma to enhance CAR T-cell therapy. *Blood*. 2024;143(2):139-151. doi:10.1182/BLOOD.2022018658
71. Su Y, Yamazaki S, Morisue R, et al. Tumor-Infiltrating T Cells Concurrently Overexpress CD200R with Immune Checkpoints PD-1, CTLA-4, and TIM-3 in Non-Small-Cell Lung Cancer. *Pathobiology*. 2021;88(3):218-227. doi:10.1159/000511557
72. Grebinoski S, Zhang Q, Cillo AR, et al. Autoreactive CD8+ T cells are restrained by an exhaustion-like program that is maintained by LAG3. *Nat Immunol*. 2022;23(6):868-877. doi:10.1038/S41590-022-01210-5
73. Man K, Duarte da Silva VA, Potemkin N, et al. Stem-like tissue-resident memory T cells control functional heterogeneity and reactivation of T cell memory in the intestine. *Sci Immunol*. 2025;10(112). doi:10.1126/SCIIMMUNOL.ADW1992
74. Zhang N, Bevan MJ. Transforming growth factor-β signaling controls the formation and maintenance of gut-resident memory T cells by regulating migration and retention. *Immunity*. 2013;39(4):687-696. doi:10.1016/J.IMMUNI.2013.08.019
75. Zhang N, Bevan MJ. TGF-β signaling to T cells inhibits autoimmunity during lymphopenia-driven proliferation. *Nat Immunol*. 2012;13(7):667-673. doi:10.1038/NI.2319
76. Bauché D, Marie JC. Transforming growth factor β: a master regulator of the gut microbiota and immune cell interactions. *Clin Transl Immunology*. 2017;6(4). doi:10.1038/CTI.2017.9
77. Biancheri P, Giuffrida P, Docena GH, MacDonald TT, Corazza GR, Di Sabatino A. The role of transforming growth factor (TGF)-β in modulating the immune response and fibrogenesis in the gut. *Cytokine Growth Factor Rev*. 2014;25(1):45-55. doi:10.1016/J.CYTOGFR.2013.11.001

78. Reina-Campos M, Monell A, Ferry A, et al. Tissue-resident memory CD8 T cell diversity is spatiotemporally imprinted. *Nature*. 2025;639(8054):483-492. doi:10.1038/S41586-024-08466-X
79. Hegazy AN, West NR, Stubbington MJT, et al. Circulating and Tissue-Resident CD4+ T Cells With Reactivity to Intestinal Microbiota Are Abundant in Healthy Individuals and Function Is Altered During Inflammation. *Gastroenterology*. 2017;153(5):1320-1337.e16. doi:10.1053/J.GASTRO.2017.07.047
80. Martin JC, Chang C, Boschetti G, et al. Single-Cell Analysis of Crohn's Disease Lesions Identifies a Pathogenic Cellular Module Associated with Resistance to Anti-TNF Therapy. *Cell*. 2019;178(6):1493-1508.e20. doi:10.1016/J.CELL.2019.08.008
81. Uchida AM, Boden EK, James EA, Shows DM, Konecny AJ, Lord JD. Escherichiacoli-Specific CD4+ T Cells Have Public T-Cell Receptors and Low Interleukin 10 Production in Crohn's Disease. *Cell Mol Gastroenterol Hepatol*. 2020;10(3):507-526. doi:10.1016/J.JCMGH.2020.04.013
82. Livanos AE, Dunn A, Fischer J, et al. Anti-Integrin αvβ6 Autoantibodies Are a Novel Biomarker That Antedate Ulcerative Colitis. *Gastroenterology*. 2023;164(4):619-629. doi:10.1053/J.GASTRO.2022.12.042
83. Del Zotto B, Mumolo G, Pronio AM, Montesani C, Tersigni R, Boirivant M. TGF-beta1 production in inflammatory bowel disease: differing production patterns in Crohn's disease and ulcerative colitis. *Clin Exp Immunol*. 2003;134(1):120-126. doi:10.1046/J.1365-2249.2003.02250.X
84. Marafini I, Laudisi F, Salvatori S, et al. Diagnostic value of anti-integrin αvβ6 antibodies in ulcerative colitis. *Digestive and Liver Disease*. 2024;56(1):55-60. doi:10.1016/j.dld.2023.06.024
85. Fasano KJ, Yoshida AE, Madden JF, et al. UC-associated autoantibodies to αvβ6 inhibit mucosal TGFβ activation and predispose to intestinal inflammation. *bioRxiv*. Published online March 15, 2026. doi:10.64898/2026.03.12.709585
86. Rydell N, Ekoff H, Hellström PM, Movérare R. Measurement of Serum IgG Anti-Integrin αvβ6 Autoantibodies Is a Promising Tool in the Diagnosis of Ulcerative Colitis. *J Clin Med*. 2022;11(7). doi:10.3390/jcm11071881
87. Bez P, Scapolan M, Ribaldone DG, et al. Antibodies against integrin αvβ6 have high diagnostic accuracy for ulcerative colitis. *Front Immunol*. 2025;16. doi:10.3389/FIMMU.2025.1641329
88. El-Asady R, Yuan R, Liu K, et al. TGF-{beta}-dependent CD103 expression by CD8(+) T cells promotes selective destruction of the host intestinal epithelium during graft-versus-host disease. *J Exp Med*. 2005;201(10):1647-1657. doi:10.1084/JEM.20041044
89. Schwartzkopff S, Woyciechowski S, Aichele U, et al. TGF-β downregulates KLRG1 expression in mouse and human CD8(+) T cells. *Eur J Immunol*. 2015;45(8):2212-2217. doi:10.1002/EJI.201545634
90. Liebmann M, Hucke S, Koch K, et al. Nur77 serves as a molecular brake of the metabolic switch during T cell activation to restrict autoimmunity. *Proc Natl Acad Sci U S A*. 2018;115(34):E8017-E8026. doi:10.1073/PNAS.1721049115/-/DCSUPPLEMENTAL

91. Guy C, Mitrea DM, Chou PC, et al. LAG3 associates with TCR-CD3 complexes and suppresses signaling by driving co-receptor-Lck dissociation. *Nat Immunol*. 2022;23(5):757-767. doi:10.1038/S41590-022-01176-4
92. Nelson CE, Thompson EA, Quarnstrom CF, et al. Robust Iterative Stimulation with Self-Antigens Overcomes CD8+ T Cell Tolerance to Self- and Tumor Antigens. *Cell Rep*. 2019;28(12):3092-3104.e5. doi:10.1016/J.CELREP.2019.08.038
93. Buck J, Iyer NR, Fagerberg E, et al. CD8 T cells mediate immunosurveillance for neoantigen+ epithelial stem cells in the colon. *bioRxiv*. Published online October 19, 2025. doi:10.1101/2025.10.19.683142
94. Fischer MA, Jia L, Edelblum KL. Type I IFN Induces TCR-dependent and -independent Antimicrobial Responses in γδ Intraepithelial Lymphocytes. *The Journal of Immunology*. 2024;213(9):1380-1391. doi:10.4049/jimmunol.2400138
95. Païdassi H, Acharya M, Zhang A, et al. Preferential expression of integrin αvβ8 promotes generation of regulatory T cells by mouse CD103+ dendritic cells. *Gastroenterology*. 2011;141(5):1813-1820. doi:10.1053/J.GASTRO.2011.06.076
96. Worthington JJ, Czajkowska BI, Melton AC, Travis MA. Intestinal dendritic cells specialize to activate transforming growth factor-β and induce Foxp3+ regulatory T cells via integrin αvβ8. *Gastroenterology*. 2011;141(5):1802-1812. doi:10.1053/J.GASTRO.2011.06.057
97. Schnupf P, Gaboriau-Routhiau V, Gros M, et al. Growth and host interaction of mouse segmented filamentous bacteria in vitro. *Nature*. 2015;520(7545):99-103. doi:10.1038/NATURE14027
98. Ramirez Reyes B, Madden S, Meyer KA, et al. Homeostatic antiviral protection of the neonatal gut epithelium by interferon lambda. *Cell Rep*. 2025;44(2). doi:10.1016/J.CELREP.2025.115243
99. Jiang HQ, Bos NA, Cebra JJ. Timing, localization, and persistence of colonization by segmented filamentous bacteria in the neonatal mouse gut depend on immune status of mothers and pups. *Infect Immun*. 2001;69(6):3611-3617. doi:10.1128/IAI.69.6.3611-3617.2001
100. Umesaki Y, Okada Y, Matsumoto S, Imaoka A, Setoyama H. Segmented filamentous bacteria are indigenous intestinal bacteria that activate intraepithelial lymphocytes and induce MHC class II molecules and fucosyl asialo GM1 glycolipids on the small intestinal epithelial cells in the ex-germ-free mouse. *Microbiol Immunol*. 1995;39(8):555-562. doi:10.1111/J.1348-0421.1995.TB02242.X
101. Umesaki Y, Setoyama H, Matsumoto S, Imaoka A, Itoh K. Differential roles of segmented filamentous bacteria and clostridia in development of the intestinal immune system. *Infect Immun*. 1999;67(7):3504-3511. doi:10.1128/IAI.67.7.3504-3511.1999
102. Jonsson H, Hugerth LW, Sundh J, Lundin E, Andersson AF. Genome sequence of segmented filamentous bacteria present in the human intestine. *Commun Biol*. 2020;3(1). doi:10.1038/S42003-020-01214-7
103. Oemcke LA, Anderson RC, Altermann E, Roy NC, McNabb WC. The Role of Segmented Filamentous Bacteria in Immune Barrier Maturation of the Small Intestine at Weaning. *Front Nutr*. 2021;8. doi:10.3389/FNUT.2021.759137

104. Yin Y, Wang Y, Zhu L, et al. Comparative analysis of the distribution of segmented filamentous bacteria in humans, mice and chickens. *ISME J*. 2013;7(3):615-621. doi:10.1038/ISMEJ.2012.128
105. Lanzoni A, Faustinelli I, Cristofori P, et al. Localization of Helicobacter spp. in the fundic mucosa of laboratory Beagle dogs: an ultrastructural study. *Vet Res*. 2011;42(1). doi:10.1186/1297-9716-42-42
106. Ho CH, Dippel MA, McQuade MS, et al. Genetic and epigenetic screens in primary human T cells link candidate causal autoimmune variants to T cell networks. *Nat Genet*. 2025;57(10):2536-2545. doi:10.1038/S41588-025-02301-3
107. Walker JM. *M E T H O D S I N M O L E C U L A R B I O L O G Y*. http://www.springer.com/series/7651
108. Qu J, Yang Z. Protocol to produce high-titer retrovirus for transduction of mouse bone marrow cells. *STAR Protoc*. 2021;2(2). doi:10.1016/J.XPRO.2021.100459
109. Srivastava S, Furlan SN, Jaeger-Ruckstuhl CA, et al. Immunogenic Chemotherapy Enhances Recruitment of CAR-T Cells to Lung Tumors and Improves Antitumor Efficacy when Combined with Checkpoint Blockade. *Cancer Cell*. 2021;39(2):193-208.e10. doi:10.1016/J.CCELL.2020.11.005
110. Urdahl KB, Sun JC, Bevan MJ. Positive selection of MHC class Ib-restricted CD8(+) T cells on hematopoietic cells. *Nat Immunol*. 2002;3(8):772-779. doi:10.1038/NI814
111. Dickson BC, Streutker CJ, Chetty R. Coeliac disease: an update for pathologists. *J Clin Pathol*. 2006;59(10):1008-1016. doi:10.1136/JCP.2005.035345
112. Heather JM, Spindler MJ, Alonso MH, et al. Stitchr: stitching coding TCR nucleotide sequences from V/J/CDR3 information. *Nucleic Acids Res*. 2022;50(12):e68. doi:10.1093/NAR/GKAC190
113. Hao Y, Stuart T, Kowalski MH, et al. Dictionary learning for integrative, multimodal and scalable single-cell analysis. *Nat Biotechnol*. 2024;42(2):293-304. doi:10.1038/S41587-023-01767-Y
114. Xia L, Lee C, Li JJ. Statistical method scDEED for detecting dubious 2D single-cell embeddings and optimizing t-SNE and UMAP hyperparameters. *Nat Commun*. 2024;15(1):1753. doi:10.1038/S41467-024-45891-Y
115. Chen S, Zhou Y, Chen Y, Gu J. fastp: an ultra-fast all-in-one FASTQ preprocessor. *Bioinformatics*. 2018;34(17):i884-i890. doi:10.1093/BIOINFORMATICS/BTY560
116. Dobin A, Davis CA, Schlesinger F, et al. STAR: ultrafast universal RNA-seq aligner. *Bioinformatics*. 2013;29(1):15-21. doi:10.1093/BIOINFORMATICS/BTS635
117. Anders S, Pyl PT, Huber W. HTSeq--a Python framework to work with high-throughput sequencing data. *Bioinformatics*. 2015;31(2):166-169. doi:10.1093/BIOINFORMATICS/BTU638
118. Andrews S. FastQC: A Quality Control Tool for High Throughput Sequence Data. https://www.bioinformatics.babraham.ac.uk/projects/fastqc/).
119. Bolger AM, Lohse M, Usadel B. Trimmomatic: a flexible trimmer for Illumina sequence data. *Bioinformatics*. 2014;30(15):2114-2120. doi:10.1093/BIOINFORMATICS/BTU170
120. Robinson MD, Oshlack A. A scaling normalization method for differential expression analysis of RNA-seq data. *Genome Biol*. 2010;11(3). doi:10.1186/GB-2010-11-3-R25

121. Ritchie ME, Phipson B, Wu D, et al. limma powers differential expression analyses for RNA-sequencing and microarray studies. *Nucleic Acids Res*. 2015;43(7):e47. doi:10.1093/NAR/GKV007
122. Liberzon A, Birger C, Thorvaldsdóttir H, Ghandi M, Mesirov JP, Tamayo P. The Molecular Signatures Database (MSigDB) hallmark gene set collection. *Cell Syst*. 2015;1(6):417-425. doi:10.1016/J.CELS.2015.12.004
123. Subramanian A, Tamayo P, Mootha VK, et al. Gene set enrichment analysis: a knowledge-based approach for interpreting genome-wide expression profiles. *Proc Natl Acad Sci U S A*. 2005;102(43):15545-15550. doi:10.1073/PNAS.0506580102

CHAPTER 3: Uncovering other mechanisms of commensal-specific CD8αβ$^+$ T cell induction and regulation in the intestine

Introduction

From the discoveries made in Chapter 2, and other experiments conducted during my studies, we are reasonably confident that commensal microbial antigens are acquired in the intestines and trafficked to the MLN where naïve CD8$^+$ T cells are activated and imprinted for gut-homing. Upon arrival in the gut tissue, microbiota-reactive CD8$^+$ T cells first migrate through the LP and then encounter IECs where they engage with pMHC and receive other epithelial-derived signals that instruct their differentiation to bone fide IEL. The extent of movement between the LP and IEL for gut-resident CD8$^+$ T cells is unknown, though there are some indications that TCR$\gamma\delta^+$ IELs can move between these niches[1], suggesting localization is not strictly limited to one compartment. However, the degree of cellular recirculation or turnover among commensal-specific CD8$^+$ T cells has not been addressed directly. In Chapter 2, we found that proliferation and TCR engagement of microbiota-specific CD8$^+$ T cells remained high even at stable timepoints post commensal colonization. This suggests that either these cells are undergoing robust proliferation in the tissue as the TCR is engaged, or they have proliferated elsewhere and new IELs continuously arrive. The details here are worth digging into further as they have implications for the treatment of intestinal immune pathologies. However, in either case, it is clear that commensal-specific CD8$^+$ T cells' interaction with IECs is critical for instructing their identity as IELs and the restrained phenotype that contributes to commensal tolerance.

In the following Chapter, I will explore what is known about the initiation of T cell responses in the gut and discuss where antigen could be acquired in the case of SFB-specific CD8$^+$ T cells. I will move on to discuss both intrinsic and extrinsic cellular factors that may play additional roles in instructing commensal-specific IEL fate/identity. And finally, I will include a short discussion about the possible function of IEL and compare commensal-specific IEL and pathogen-specific IEL, finishing with short concluding remarks.

Outstanding Questions

How are commensal-specific CD8$^+$ T cell responses primed?

As briefly touched upon in Chapter 1, conventional naïve T cell priming after pathogen infection takes place in a well characterized signaling cascade starting with the activation of an APC in the tissue. Naïve T cells are optimally activated in the lymph node by an APC when three conditions are met: 1) the TCR engages MHCI (CD8$^+$) or MHCII (CD4$^+$) presenting cognate peptide, 2) TCR:pMHC is accompanied by co-stimulating molecules like CD80/CD86 upregulated by an activated APC, and 3) cytokines are secreted by the APC to enforce activation and instruct the appropriate naïve T cell differentiation and response. This process is particularly well described for CD4$^+$ T helper cell activation[2,3]. Which so called "first order cytokines" are secreted by the activated APC (IL-6, IL-12 or IL-4 for instance), depends on the inflammatory milieu encountered at the site of homeostatic disturbance and sets the course for the type of T cell responses. Once a naïve T cell has been primed in the lymph node, massive clonal expansion takes place and effector or helper T cells migrate and home to the site of inflammation where they can encounter further TCR:pMHC engagement and produce second order cytokines such as IFNγ, IL-5/13, or IL-17, which go on to effect the local myeloid and non-immune cell subsets resulting in robust inflammation and eventual pathogen clearance[2,3].

The type of APC also influences the type of T cell response that is primed in the lymph node. In the case of most pathogen infections, professional APCs are primarily conventional dendritic cells (cDCs) which consist of several subsets both expressing high levels of MHCII and CD11c: cDC1s are adept at taking up extracellular antigen and priming CD8$^+$ T cell responses, while cDC2s are specialized for taking up all types of foreign antigens and priming CD4$^+$ T cell responses[4,5]. In some unconventional settings of immune activation, such as cancer where inflammation may be limited, the types of APCs involved can also be unconventional, where plasmacytoid DCs (pDCs) and innate-like lymphoid cells 2 (ILC2s) have been shown to prime CD8$^+$ T cell responses via cross-presentation instead of traditional DCs[6,7]. Another

unconventional way $CD8^+$ T cells can be primed is via “cross-dressing” where pMHC produced by another cell is taken up and presented by a specialized DC subset to prime naïve T cells[8].

Yet another site where conventionally accepted means of T cell priming has seen a paradigm shift in recent years is the intestine[9–12]. Indeed, there are several specialized APC subsets, including $CD103^+$ DCs, found in the gut that favor the induction of Tregs as they can activate latent TGFβ.[11] More recently, it has been shown that $ROR\gamma t^+$ APCs can be responsible for priming commensal-specific Tregs in the colon while the cDC2s prime Th1, Th17, and T follicular helper $CD4^+$ responses to commensal microbes[9,10,13]. The characteristics of the microbe that dictate which T helper cell subset is induced has not been fully elucidated. It is interesting to speculate that this could be due to the route by which microbial antigen is made available for APC uptake or the extent to which innate immune sensors are engaged upon colonization.

Underscoring the observation that immunogenic microbes tend to be those that interact closely or directly with IECs is the intriguing hypothesis that positions IECs as intermediate APCs during commensal colonization, acting as shuttles for microbial antigen to move from the lumen to the basolateral side of the epithelial layer via exosomes or other means[14]. Indeed, IEC-specific deletion of MHCII results in reduced gut Treg frequencies and less microbial-bound IgA[14,15]. Other modes of antigen uptake include the sampling of luminal antigen through M cells of Peyer’s patches in the small intestine and also through epithelial “flossing” of $TCR\gamma\delta^+$ and double negative $TCR\alpha\beta^+CD8\alpha\beta^-CD4^-$ IEL which can slip between IECs to sample from the luminal space[16–18].

What APC primes commensal-specific $CD8^+$ T cells in the small intestine? The answer, unfortunately, is an open question though we may be able to infer likely candidates. $CD8^+$ IELs have been primarily characterized for pathogen-specific responses that induce significant inflammation and tissue damage, presumably leading to wide-spread antigen availability and uptake by cDC1s that can cross-present as previously stated. This was also the case in a mouse model of the intraepithelial pathogen *Cryptosporidium*[19]. In settings of low inflammation, like

exogenous expression of a model antigen in IECs, CD103^{+}CD11b^{lo} DCs were responsible for cross-presenting and priming CD8^{+} T cells.[19] The latter is the most likely candidate for priming SFB-specific CD8^{+} IEL responses as SFB antigen is known to be trafficked directly into the cytoplasm of IECs via microbial-adhesion-triggered-endocytosis (MATE)-vesicles[20]. Whether IEC-derived pMHC is also involved in antigen hand-off to motile APCs during CD8^{+} T cell priming in the gut is yet another open question worth pursuing. Until then, we shall remain in the dark and be comforted knowing CD8^{+} T cells are indeed induced by commensal colonization, regardless of the APC or mechanism responsible.

How other factors may shape commensal-specific CD8^{+} T cells at steady state

As identified in Chapter 2, IEC expression of pMHCI and αvβ6 is essential for IEL accumulation and functional restraint, providing both the cue for retention and immune-dampening IEC-activated TGFβ. However, tucked away in our sequencing data are other hits that may also help define the unique characteristics of commensal-specific CD8^{+} IEL, namely other IEL-IEC interactions and the restraint of their potent effector potential without crossing over to exhaustion. Here, I will focus on the most interesting hits we found, while, admittedly, ignoring transcripts identified by others or that are universal features of IELs already identified in Chapter 2. To recap, we sought to identify the signals contributing to local immune regulation of IEL by comparing transcripts found in these populations compared to those in cells isolated from the LP or MLN, by performing scRNAseq of TCR3^{Rg} CD8αβ^{+} T cells from the spleen, MLN, LP, and IEL of SFB-colonized mice **(Chapter 2, Fig. 4B-C)**. Simple volcano plot analysis between LP and IEL revealed increased expression of *Gzmb*, *Gzma*, and *Ifng* as well as the TF *Heyl* and its transcription co-factor *Cited4* **(Fig. 6A)**. Additionally, though not highlighted in the volcano plot, the TF *Lyl1* is also up in IEL versus LP **(Fig. 6A).** Beyond this simple gene enrichment analysis, we also performed single-cell regulatory network inference and clustering (SCENIC) analysis to predict differentially active transcription factors (TFs) between tissues[21,22]. SCENIC analysis

integrates known transcription factor binding sites with gene expression to determine “TF regulons” giving us a sense of which TFs are on or off in a given cell, making this a powerful tool to understand functional differences. Applying this approach to our scRNAseq data confirmed the significance of *Heyl* and *Lyl1* regulons as well as known IEL regulons such as *Hic1* **(Fig. 6B).** It also revealed a *Jund* regulon, a difference between IEL and LP that was overlooked in our volcano plot since *Jund* is widely expressed across tissues in TCR3^{Rg} CD8αβ^{+} T cells, though it appears another layer of regulation keeps this TF from turning on target genes (not shown). So what function might these hits have in SFB-specific CD8^{+} IEL?

Heyl, Notch, and TGFβ?

Heyl is a transcriptional repressor upregulated downstream of Notch signaling[23]. Notably, other Notch effectors, such as *Hey1* and *Hes1* which are upregulated during T cell development,

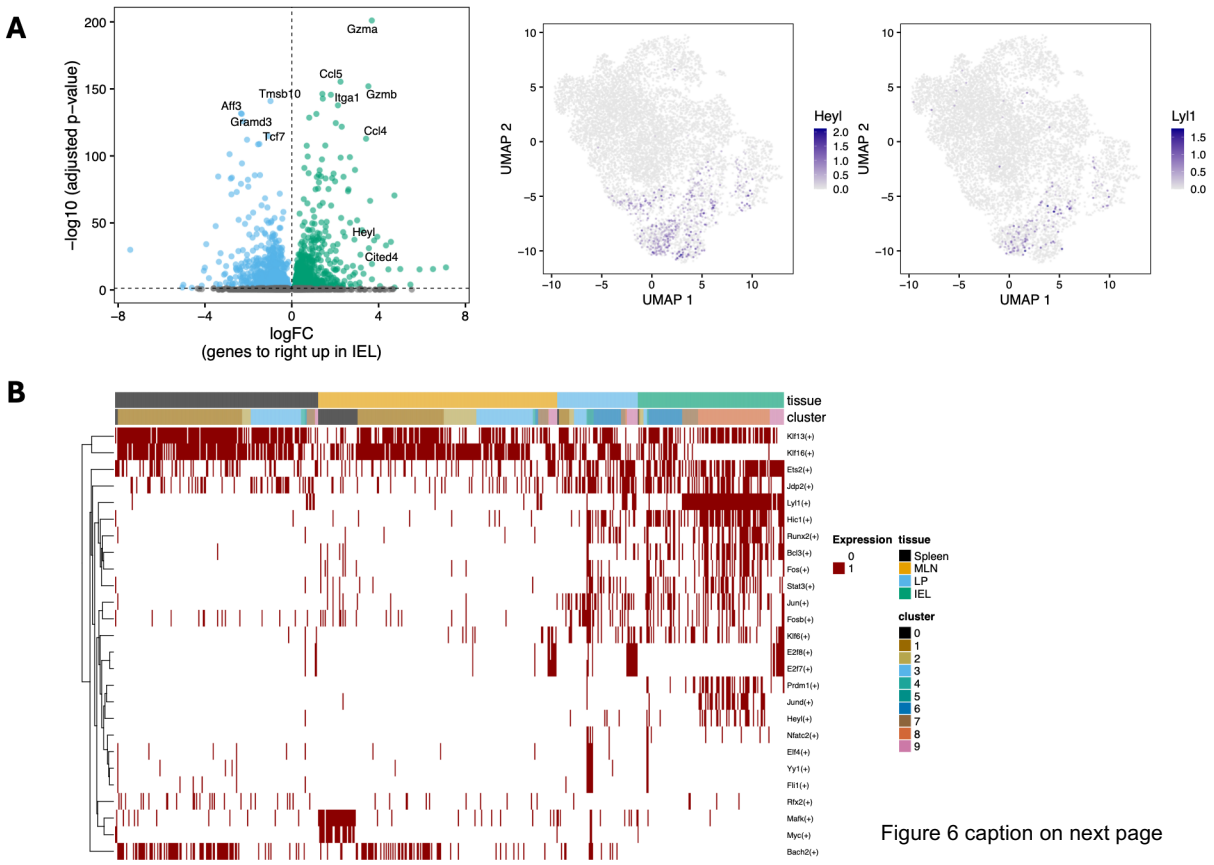

Figure 6 caption on next page

Figure 6: Distinct gene transcriptional and functional differences in commensal-specific CD8αβ$^+$ pIEL and LP. **(A)** Volcano plot of differential transcripts between LP and IEL with highlighted UMAP plots of select genes from 10x scRNAseq analysis of sorted TCR3^{Rg} CD8$^+$ T cells from the spleen, MLN, ileum LP and IEL of Jax mice 11 d.p.c. and T cell transfer. Data were generated from cells pooled from 10 mice. **(B)** SCENIC TF regulon analysis of cells from (A) sorted by tissue type.

are not present in SFB-specific CD8$^+$ pIEL (not shown). The types of effectors upregulated during Notch signaling have been shown to be dictated by upstream ligand-Notch1 receptor engagement where DLL1 provides pulsing interactions leading to *Hes1* expression and DLL4 provides sustained activation leading to *Heyl* expression[24], though both are expressed by IECs in the small intestine[25,26]. Mediated exclusively through cell-to-cell contact, Notch signaling in general is a context-dependent signaling pathway that directs developmental cell fate decisions, and it has been implicated in modulating the activity of peripheral T cells in addition to its importance in thymic T cell development. As a Notch effector, *Heyl* has been canonically associated with the epithelial-to-mesenchymal transition in cardiac tissue[27], is required for cell-fate decisions in neural progenitor cells[28], and is upregulated in multiple tumor types[29,30]. However, the role for *Heyl* in T cells has not been directly investigated.

What makes the discovery of *Heyl* expression in pIEL particularly interesting is the connection between Notch, *Heyl* expression, and TGFβ signaling. This manifests as Notch signaling directly inhibiting TGFβ through Heyl interactions with Smad proteins downstream of TGFβR ligation, blunting signal transduction[31]. In human keratinocytes, a similar signaling crosstalk takes places between Notch and TGFβ leading to regulation of cell-contact growth inhibition[32]. And in mouse prostate stem/progenitor cells TGFβ signaling and Notch are in balance to support stem cell dormancy[33]. An interesting hypothesis emerges suggesting dual Notch and TGFβ signaling in IEL maintains functional potential while avoiding T cell exhaustion from constant TCR engagement. Further supporting this notion is that over-expression of *Heyl* can be found in several tumor types, including from increased Notch signaling observed in T cell acute lymphoblastic leukemia (T-ALL)[29,34,35], and Notch pre-conditioning of CAR T cells has been shown to protect their functional capacity[36]. Other Notch components, like Numb and Numblike, appear to localize with TCR signaling machinery at the cell surface suggesting a role for TCR signaling

regulation for Notch in peripheral T cells that could be important to consider in the context of pIEL[37].

Given this overview, and the fact that commensal-specific CD8$^+$ pIEL, in contact with IECs, display constant TCR engagement and TGFβ signaling while expressing *Heyl* provides a compelling argument for investigating the contribution of Notch signaling in regulating TGFβ signal integration and may explain, in part, how these cells escape terminal exhaustion.

Lyl1 and T cell stemness?

The other potentially interesting hit we found is the helix-loop-helix transcription factor *Lyl1*. *Lyl1* is a well described oncogene and its overexpression results in B/T lymphoma in mice[38,39]. Given this, it is probably not surprising that it was later described as an important TF in maintaining early T cell progenitor cells and hematopoietic stem cell lymphoid lineages[40,41]. *Lyl1* expression wanes during development and is almost entirely absent in mature T cells, though it is expressed in other mature immune cell populations like B cells, mast cells and some myeloid cells to varying degrees[42]. It is interesting, then, that commensal-specific CD8$^+$ pIEL, which we have already discussed balance chronic TCR engagement with preservation of effector potential, express high levels of *Lyl1*; the obvious hypothesis being that *Lyl1* expression enables commensal-specific CD8$^+$ pIEL to proliferate and maintain function in the face of antigenic burden. Though not highlighted above, c*Kit*, is another stemlike gene upregulated in pIEL worth investigating further as it has important roles in T cell priming and has already been found to potentiate CAR-T cell function in solid tumors[43,44].

Jund in T cells

Jund is a well described AP-1 family member transcription factor responsible for myriad T cell functions including, proliferation[45,46] and regulating aspects of T cell stemness where higher levels of *Jund* (and lower levels of *Bach2*) are found in neonatal CD8$^+$ T cells[47]. This is consistent

with our SCENIC analysis which does not identify a *Bach2* regulon but shows a strong *Jund* regulon **(Fig. 6B)**. The observation that *Jund* functions in neonatal T cells and is involved in stemness-properties makes elucidating its role in commensal-specific $CD8^+$ T cell biology in the intestine worthwhile.

What is the function of commensal-specific $CD8^+$ T cell in the intestine and how do they differ to pathogen-specific IEL?

How the immune system maintains antigen-experienced T cells at sites of continuous microbial antigen exposure without causing tissue damage has been a longstanding question in mucosal immunology. As touched upon in Chapter 2, the function of commensal-specific $CD8^+$ T cells in homeostasis has not been fully defined. Though IEC-directed cytotoxicity by $CD8^+$ pIEL has demonstrated that expression of neoepitopes from IECs can result in robust IEC death without overt pathology[48]. Using similar models of IEC-overexpression of model antigens, breaking tolerance to IEC-derived peptides required many heterologous infections of pathogens expressing the same protein to elicit a pathological IEL response[49].

In fact, in conversation with others who study IEL responses, getting IELs to respond as canonical cytotoxic $CD8^+$ T cells by relieving the effects of inhibitory receptors using immune checkpoint blockade (ICB), either alone or in combination, did not result in loss of tolerance in mice. Furthermore, data from enteric infection models show that pathogen-specific IELs are unable to kill target cells or respond to secondary challenge[50–52]. From this, it is tempting to posit that one of the functions of $CD8^+$ pIEL is to *not* respond and their quiescence is a feature, not a flaw. Perhaps, where we should look for indications on the homeostatic function of commensal-specific $CD8^+$ IEL is $TCR\gamma\delta^+$ IEL which are present at birth and are replaced by $CD8^+$ IEL overtime through colonization and infection. $TCR\gamma\delta^+$ IEL have been shown to facilitate epithelial shedding via CD103-IEC interactions and extracellular granzyme release and importantly type I interferons

can lower their TCR-dependent activation thresholds[53,54]. The latter suggests that perhaps, for commensal-specific CD8$^+$ IEL or IEL specific to IEC-derived peptides without infection, inflammatory conditions may license IEL to respond and reveal their latent cytolytic or cytokine producing function. I would like to stress that lack of evidence for a functional role does not rule out the possible presence of one.

It is worth noting again that the TCR-responsiveness and the continued proliferation we observe in SFB-specific CD8$^+$ IEL has not been observed in either commensal-specific CD4$^+$CD8αα$^+$ pIEL nor in virus- or bacteria-specific CD8$^+$ IEL (see Chapter 2). To more directly compare virus- and commensal-specific CD8$^+$ IEL, we combined existing scRNAseq data from an LCMV infection model in Crowl *et al*. 2022[55] with our own scRNAseq data (designated P627) and analyzed differential gene expression between spleen and IEL **(Fig. 7A)**. Crowl *et al*. transferred naïve LCMV-specific CD8$^+$ T cells into mice and allowed virus to be cleared, such that memory CD8$^+$ T cells remained at 35 days post infection and sequenced cells from a variety of tissues[55–57]. LCMV infects a wide array of cells and elicits robust systemic immunity[57]. Since SFB does not cause systemic immunity, it is not surprising, then, that we observe differences between cells in each dataset where splenocytes from LCMV-infected mice exhibit higher levels of *Gzma* and *Ccl5* transcripts **(Fig. 7B)**.

We then looked more specifically at differences among the three hits that came out of our own dataset (*Heyl*, *Lyl1*, and *Jund*) to evaluate if virus-specific CD8$^+$ IEL showed similar phenotypes. In fact, neither *Heyl* nor *Lyl1* transcripts were detectable to a significant degree in virus-specific IEL **(Fig. 7C)**, leading to the exciting hypothesis that these are uniquely expressed in commensal-specific CD8$^+$ IEL. There were slight differences in *Jund* expression in both spleen and IEL. Though, as we saw in our own dataset, *Jund* is widely expressed so SCENIC analysis would need to be performed to validate functional differences in its regulon. Overall, though we cannot rule out differences in batch effects between the datasets or tissue or data QC, the difference in *Heyl* and *Lyl1* warrants investigation and validation.

Continued…

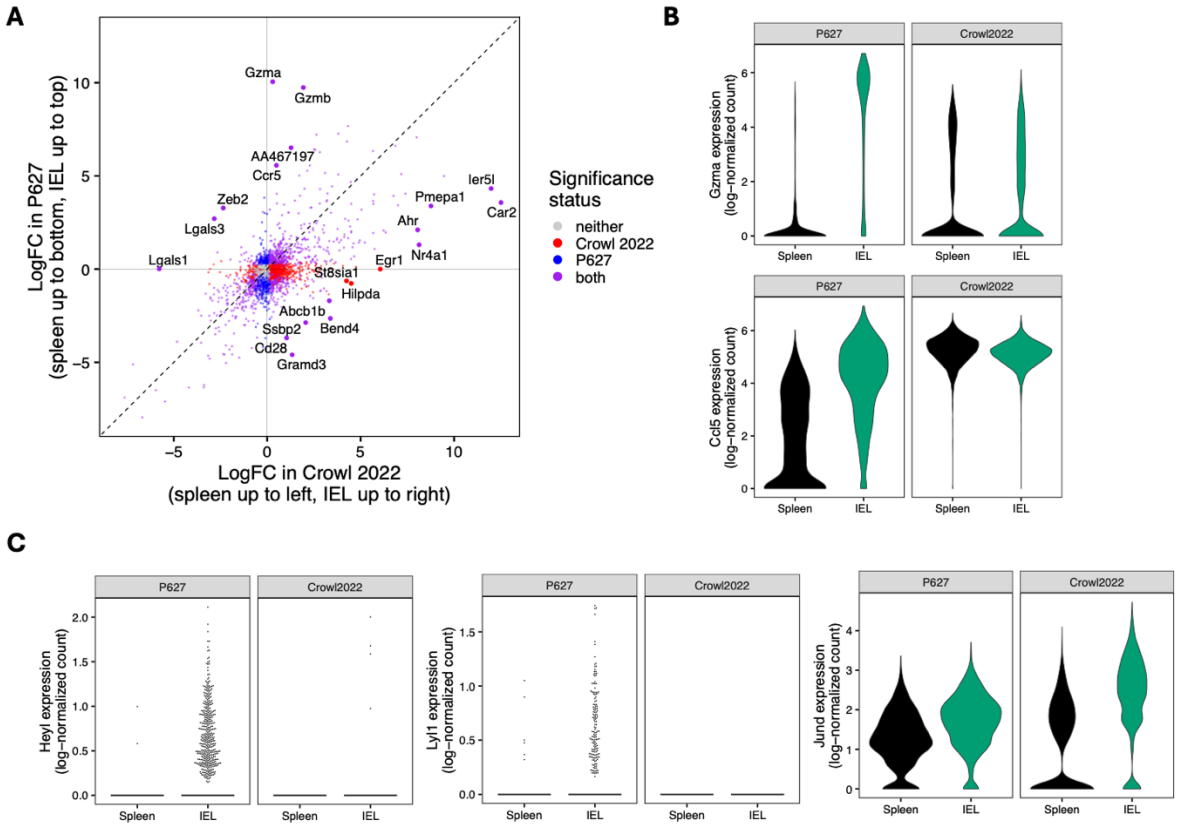

Figure 7: Transcriptional differences between virus- and commensal-specific CD8αβ⁺ spleen and IEL. **(A)** Volcano plot of differential transcripts between spleen and IEL comparing data from Crowl *et al.* 2022 10x scRNAseq from P14 cells day 35 post LCMV infection and P627 (10x scRNAseq of sorted TCR3^{Rg} CD8^{+} T cells from the spleen, MLN, ileum LP and IEL of Jax mice 11 d.p.c. and T cell transfer). **(B)** Violin plots of *Gzma* and *Ccl5* and **(C)** Beeswarm plots of *Heyl* and *Lyl1*, and violin plot of *Jund*.

Concluding Remarks

Many things in biology remain vestiges of past function or usage, whether these are remnants of bones no longer needed for land ambulation or molecular remnants of past evolutionary selective pressure, they remain as historical records. On the other hand, investigating pathways without an obvious function does not mean they are not still useful to the host or interesting biologically. I mention this because one of the criticisms for studying commensal-specific CD8^{+} IEL has been their lack of apparent function and, much to my benefit, is perhaps one of the main reasons they have largely gone unstudied. What is the point in studying something without a use? I will rejoin that that refrain lacks imagination. Based on what you have

read so far, I am sure you can fill in the rest of my answer to that question. To put it somewhat lamely: when you study new things, you learn new things. And perhaps problems in other fields of biology begin to make more sense.

One such field is cancer biology. In fact, many of the same settings in cancer and commensal colonization run parallel to one another: in solid tumors, there is often a highly immunosuppressive environment both from the myeloid population during T cell activation and from tissue-activated TGFβ concomitant with pMHC from widely available antigen as well as reduced inflammation at the site of T cell ingress. The main difference here is our perspective. In one setting, cancer, we would like for these cells to continue destroying the tumor, while in the intestine, continued optimal T cell activation leads to tissue damage and we would like these cells to not continue on a destructive path. Though as we have seen, the integration of molecular cues provided to IEL in the intestine protects them from exhaustion while maintaining functional potential. Perhaps we can learn to manipulate engineered T cells to mimic those cues found to develop more effective solid tumor therapies.

Additionally, there is obvious benefit, as described in Chapter 2, in studying these ancient biological responses since we cannot escape them bar significant, detrimental antibiotic usage. Thus, understanding how disrupted commensal-host interactions are initiated or propagate can help us treat “pseudo-autoimmune” disorders (a term I just invented describing dysregulated anti-commensal immunity rather than strictly self-specific responses), which can contribute to type 1 diabetes, rheumatoid arthritis, and IBD, among others[58,59].

Beyond the obvious benefits in applying what we have learned to improve cancer therapeutics or define the etiology of “pseudo-autoimmune” disorders, we can start to get a better picture of $CD8^+$ T cell biology more generally by studying new settings of $CD8^+$ T cell immunity. We know that without the right cues, inflammation and persistent antigen leads to T cell exhaustion. We also know that inflammation accompanied by antigen clearance leads to T effector responses that lead to tissue resident memory formation. Here, I submit anot Continued…

when inflammation is highly localized and accompanied by persistent antigen with contextual tissue cues, the result is neither a restrained nor a fully functional CD8$^+$ T cell, but rather a “T restrained” cell as we have described in Chapter 2 and others have described for auto-reactive CD8$^+$ T cells[60] **(Table 1)**. This state may allow for homeostatic functions like silent killing and immune surveillance or reactivation during heterologous immune challenge. Future work will be required and establish these roles.

	Cleared Antigen	Persistent Antigen
Systemic Inflammation	Teff, Tcm, Trm	Tex
Local inflammation	Trm	Teff, Tex+
Local Inflammation Tissue Context	Trm	Trm with homeostatic function (Tres)

Table 1: Inflammation, antigen and CD8+ T cell responses. Tex: T exhausted cell, Tcm: T central memory cell, Trm: Tissue resident memory cell, Tres: T restrained cell, a cell with possible homeostatic function, does not lead to overt pathogy but whose function is maintained, presumably by local tissue cues.

Finally, I hope that this work will lead to a reinvigorated interest in understanding CD8$^+$ commensal-specific immunity, and lead to a deeper understanding of the interactions between IEL and IECs **(Schematic 2)**. The features of microbes that induce CD4$^+$ T cell responses will most likely also induce a CD8$^+$ T cell response. Since CD8$^+$ T cell responses are usually confined to the IEL, researchers studying commensal-specific CD4$^+$ responses in the LP will almost necessarily overlook commensal-induced CD8$^+$ T cell responses as they bleach their IEL fraction. Far from being a fringe immune response, I think the more researchers look for commensal-specific CD8$^+$ T cell responses, the more they will find, if only they look in the right places.

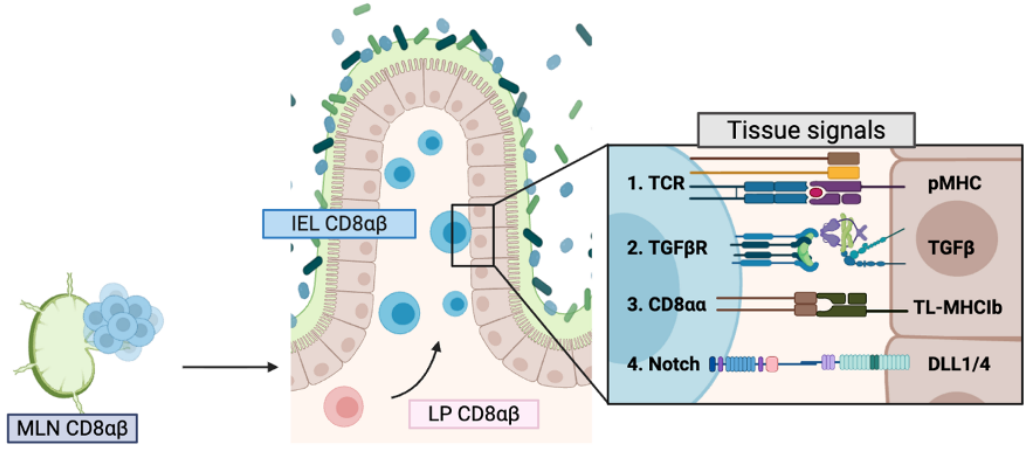

Schematic 2: From MLN to IEL and the potential tissue signals instructing them.

References

1. Fischer MA, Golovchenko NB, Edelblum KL. γδ T cell migration: Separating trafficking from surveillance behaviors at barrier surfaces. *Immunol Rev*. 2020;298(1):165-180. doi:10.1111/IMR.12915
2. Li L, Yao Z. Modes of the initiation of T cell-mediated immune responses. *Medical Review*. 2026;6(1):83. doi:10.1515/MR-2025-0066
3. Annunziato F, Romagnani C, Romagnani S. The 3 major types of innate and adaptive cell-mediated effector immunity. *Journal of Allergy and Clinical Immunology*. 2015;135(3):626-635. doi:10.1016/J.JACI.2014.11.001
4. Luri-Rey C, Teijeira Á, Wculek SK, et al. Cross-priming in cancer immunology and immunotherapy. *Nat Rev Cancer*. 2025;25(4):249-273. doi:10.1038/S41568-024-00785-5
5. Tatsumi N, Kumamoto Y. Role of mouse dendritic cell subsets in priming naive CD4 T cells. *Curr Opin Immunol*. 2023;83. doi:10.1016/J.COI.2023.102352
6. van der Sluis RM, García-Rodríguez JL, Nielsen IH, et al. Distinctive CD8+ T cell activation by antigen-presenting plasmacytoid dendritic cells compared to conventional dendritic cells. *Cell Rep*. 2025;44(3). doi:10.1016/J.CELREP.2025.115413
7. Kim J, Song SG, Park S, et al. Antigen Cross-Presentation by Type-2 Innate Lymphoid Cells Facilitates the Activation of Antitumor CD8+ T Cells. *Cancer Res*. 2025;85(14):2659-2678. doi:10.1158/0008-5472.CAN-24-4194
8. Li J, Kim S, Herndon JM, et al. Cross-dressed CD8α+/CD103+ dendritic cells prime CD8+ T cells following vaccination. *Proc Natl Acad Sci U S A*. 2012;109(31):12716-12721. doi:10.1073/PNAS.1203468109
9. Kedmi R, Littman DR. Antigen-presenting cells as specialized drivers of intestinal T cell functions. *Immunity*. 2024;57(10):2269-2279. doi:10.1016/J.IMMUNI.2024.09.011
10. Kedmi R, Najar TA, Mesa KR, et al. A RORγt+ cell instructs gut microbiota-specific Treg cell differentiation. *Nature*. 2022;610(7933):737-743. doi:10.1038/S41586-022-05089-Y
11. Grainger JR, Askenase MH, Guimont-Desrochers F, da Fonseca DM, Belkaid Y. Contextual functions of antigen-presenting cells in the gastrointestinal tract. *Immunol Rev*. 2014;259(1):75-87. doi:10.1111/IMR.12167
12. Ulezko Antonova A, Fachi JL, Gilfillan S, Colonna M. The thin line between conventional dendritic cells (cDCs) and group 3 innate lymphoid cells (ILC3s) in the gut. *Int Immunol*. 2023;35(3):107-121. doi:10.1093/INTIMM/DXAC054
13. Carroll SL, Ly A, Liu AK, et al. Identification of distinct cDC2 subpopulations that direct microbiota-specific T cell differentiation. *bioRxiv*. Published online November 5, 2025. doi:10.1101/2025.11.04.686414
14. Stephens WZ, Kubinak JL, Ghazaryan A, et al. Epithelial-myeloid exchange of MHC class II constrains immunity and microbiota composition. *Cell Rep*. 2021;37(5). doi:10.1016/J.CELREP.2021.109916
15. Heuberger C, Pott J, Maloy KJ. Why do intestinal epithelial cells express MHC class II? *Immunology*. 2021;162(4):357-367. doi:10.1111/IMM.13270

16. Mabbott NA, Donaldson DS, Ohno H, Williams IR, Mahajan A. Microfold (M) cells: important immunosurveillance posts in the intestinal epithelium. *Mucosal Immunol*. 2013;6(4):666-677. doi:10.1038/MI.2013.30
17. Hoytema van Konijnenburg DP, Reis BS, Pedicord VA, Farache J, Victora GD, Mucida D. Intestinal Epithelial and Intraepithelial T Cell Crosstalk Mediates a Dynamic Response to Infection. *Cell*. 2017;171(4):783-794.e13. doi:10.1016/J.CELL.2017.08.046
18. Nemoto Y, Morikawa R, Yonemoto Y, et al. Intestinal CD4-CD8αβ-TCRαβ+ T cells function as tolerogenic antigen presenting cells in mice. *Nat Commun*. 2025;16(1). doi:10.1038/S41467-025-62089-Y
19. Cerovic V, Houston SA, Westlund J, et al. Lymph-borne CD8α+ dendritic cells are uniquely able to cross-prime CD8+ T cells with antigen acquired from intestinal epithelial cells. *Mucosal Immunol*. 2015;8(1):38-48. doi:10.1038/MI.2014.40
20. Ladinsky MS, Araujo LP, Zhang X, et al. Endocytosis of commensal antigens by intestinal epithelial cells regulates mucosal T cell homeostasis. *Science (1979)*. 2019;363(6431). doi:10.1126/science.aat4042
21. Aibar S, González-Blas CB, Moerman T, et al. SCENIC: single-cell regulatory network inference and clustering. *Nat Methods*. 2017;14(11):1083-1086. doi:10.1038/NMETH.4463
22. Bravo González-Blas C, De Winter S, Hulselmans G, et al. SCENIC+: single-cell multiomic inference of enhancers and gene regulatory networks. *Nat Methods*. 2023;20(9):1355-1367. doi:10.1038/S41592-023-01938-4
23. HEYL Gene - GeneCards. Accessed August 15, 2026. https://www.genecards.org/card/HEYL
24. Nandagopal N, Santat LA, LeBon L, Sprinzak D, Bronner ME, Elowitz MB. Dynamic Ligand Discrimination in the Notch Signaling Pathway. *Cell*. 2018;172(4):869-880.e19. doi:10.1016/J.CELL.2018.01.002
25. Biton M, Haber AL, Rogel N, et al. T Helper Cell Cytokines Modulate Intestinal Stem Cell Renewal and Differentiation. *Cell*. 2018;175(5). doi:10.1016/j.cell.2018.10.008
26. Intestinal Stem Cell - Single Cell Portal. Accessed August 15, 2026. https://singlecell.broadinstitute.org/single_cell/study/SCP241/intestinal-stem-cell?genes=H2-K1&hiddenTraces=Epithelial%2CMonocyte%20%28cycling%29%2CNK%2CPlasma%20cell%2CNeutrophil%2CB%20cell#study-visualize
27. Fischer A, Steidl C, Wagner TU, et al. Combined loss of Hey1 and HeyL causes congenital heart defects because of impaired epithelial to mesenchymal transition. *Circ Res*. 2007;100(6):856-863. doi:10.1161/01.RES.0000260913.95642.3B
28. Jalali A, Bassuk AG, Kan L, et al. HeyL promotes neuronal differentiation of neural progenitor cells. *J Neurosci Res*. 2011;89(3):299-309. doi:10.1002/JNR.22562
29. Han L, Korangath P, Nguyen NK, et al. HEYL Regulates Neoangiogenesis Through Overexpression in Both Breast Tumor Epithelium and Endothelium. *Front Oncol*. 2021;10. doi:10.3389/FONC.2020.581459
30. Weber S, Koschade SE, Hoffmann CM, et al. The notch target gene HEYL modulates metastasis forming capacity of colorectal cancer patient-derived spheroid cells in vivo. *BMC Cancer*. 2019;19(1). doi:10.1186/S12885-019-6396-4

31. Han L, Diehl A, Nguyen NK, et al. The Notch pathway inhibits TGFβ signaling in breast cancer through HEYL-mediated crosstalk. *Cancer Res*. 2014;74(22):6509-6518. doi:10.1158/0008-5472.CAN-14-0816
32. Xu Y, Xue S, Zhou J, Voorhees JJ, Fisher GJ. Notch and TGF-β pathways cooperatively regulate receptor protein tyrosine phosphatase-κ (PTPRK) gene expression in human primary keratinocytes. *Mol Biol Cell*. 2015;26(6):1199-1206. doi:10.1091/MBC.E14-12-1591
33. Valdez JM, Zhang L, Su Q, et al. Notch and TGFβ form a reciprocal positive regulatory loop that suppresses murine prostate basal stem/progenitor cell activity. *Cell Stem Cell*. 2012;11(5):676-688. doi:10.1016/J.STEM.2012.07.003
34. Le Lay ASG, Oravecz A, Mastio J, et al. The tumor suppressor Ikaros shapes the repertoire of notch target genes in T cells. *Sci Signal*. 2014;7(317). doi:10.1126/SCISIGNAL.2004545
35. Zheng R, Li M, Wang S, Liu Y. Advances of target therapy on NOTCH1 signaling pathway in T-cell acute lymphoblastic leukemia. *Exp Hematol Oncol*. 2020;9(1). doi:10.1186/S40164-020-00187-X
36. Kondo T, Morita R, Okuzono Y, et al. Notch-mediated conversion of activated T cells into stem cell memory-like T cells for adoptive immunotherapy. *Nat Commun*. 2017;8. doi:10.1038/NCOMMS15338
37. Anderson AC, Kitchens EA, Chan SW, et al. The Notch regulator Numb links the Notch and TCR signaling pathways. *J Immunol*. 2005;174(2):890-897. doi:10.4049/JIMMUNOL.174.2.890
38. Meng YS, Khoury H, Dick JE, Minden MD. Oncogenic potential of the transcription factor LYL1 in acute myeloblastic leukemia. *Leukemia*. 2005;19(11):1941-1947. doi:10.1038/SJ.LEU.2403836
39. Zhong Y, Jiang L, Hiai H, Toyokuni S, Yamada Y. Overexpression of a transcription factor LYL1 induces T- and B-cell lymphoma in mice. *Oncogene*. 2007;26(48):6937-6947. doi:10.1038/SJ.ONC.1210494
40. Zohren F, Souroullas GP, Luo M, et al. The transcription factor Lyl-1 regulates lymphoid specification and the maintenance of early T lineage progenitors. *Nat Immunol*. 2012;13(8):761-769. doi:10.1038/NI.2365
41. Souroullas GP, Goodell MA. A new allele of Lyl1 confirms its important role in hematopoietic stem cell function. *Genesis*. 2011;49(6):441-448. doi:10.1002/DVG.20743
42. Heng TSP, Painter MW, Elpek K, et al. The Immunological Genome Project: networks of gene expression in immune cells. *Nat Immunol*. 2008;9(10):1091-1094. doi:10.1038/NI1008-1091
43. Frumento G, Zuo J, Verma K, et al. CD117 (c-Kit) Is Expressed During CD8+ T Cell Priming and Stratifies Sensitivity to Apoptosis According to Strength of TCR Engagement. *Front Immunol*. 2019;10(MAR). doi:10.3389/FIMMU.2019.00468
44. Xiong Y, Taleb M, Misawa K, et al. c-Kit signaling potentiates CAR T cell efficacy in solid tumors by CD28- and IL-2-independent co-stimulation. *Nat Cancer*. 2023;4(7):1001-1015. doi:10.1038/S43018-023-00573-4

45. Meixner A, Karreth F, Kenner L, Wagner EF. JunD regulates lymphocyte proliferation and T helper cell cytokine expression. *EMBO J*. 2004;23(6):1325-1335. doi:10.1038/SJ.EMBOJ.7600133
46. Ruppert SM, Chehtane M, Zhang G, Hu H, Li X, Khaled AR. JunD/AP-1-mediated gene expression promotes lymphocyte growth dependent on interleukin-7 signal transduction. *PLoS One*. 2012;7(2). doi:10.1371/JOURNAL.PONE.0032262
47. Watson NB, Patel RK, Kean C, et al. The gene regulatory basis of bystander activation in CD8+ T cells. *Sci Immunol*. 2024;9(92). doi:10.1126/SCIIMMUNOL.ADF8776
48. Buck J, Iyer NR, Fagerberg E, et al. CD8 T cells mediate immunosurveillance for neoantigen+ epithelial stem cells in the colon. *bioRxiv*. Published online October 19, 2025. doi:10.1101/2025.10.19.683142
49. Nelson CE, Thompson EA, Quarnstrom CF, et al. Robust Iterative Stimulation with Self-Antigens Overcomes CD8+ T Cell Tolerance to Self- and Tumor Antigens. *Cell Rep*. 2019;28(12):3092-3104.e5. doi:10.1016/J.CELREP.2019.08.038
50. Huleatt JW, Pilip I, Kerksiek K, Pamer EG. Intestinal and Splenic T Cell Responses to Enteric Listeria monocytogenes Infection: Distinct Repertoires of Responding CD8 T Lymphocytes . *The Journal of Immunology*. 2001;166(6):4065-4073. doi:10.4049/jimmunol.166.6.4065
51. Fung HY, Teryek M, Lemenze AD, Bergsbaken T. CD103 fate mapping reveals that intestinal CD103- tissue-resident memory T cells are the primary responders to secondary infection. *Sci Immunol*. 2022;7(77). doi:10.1126/SCIIMMUNOL.ABL9925
52. von Hoesslin M, Kuhlmann M, de Almeida GP, et al. Secondary infections rejuvenate the intestinal CD103+ tissue-resident memory T cell pool. *Sci Immunol*. 2022;7(77). doi:10.1126/SCIIMMUNOL.ABP9553
53. Hu MD, Golovchenko NB, Burns GL, et al. γδ Intraepithelial Lymphocytes Facilitate Pathological Epithelial Cell Shedding Via CD103-Mediated Granzyme Release. *Gastroenterology*. 2022;162(3):877-889.e7. doi:10.1053/J.GASTRO.2021.11.028
54. Fischer MA, Jia L, Edelblum KL. Type I IFN Induces TCR-dependent and -independent Antimicrobial Responses in γδ Intraepithelial Lymphocytes. *The Journal of Immunology*. 2024;213(9):1380-1391. doi:10.4049/jimmunol.2400138
55. Crowl JT, Heeg M, Ferry A, et al. Tissue-resident memory CD8+ T cells possess unique transcriptional, epigenetic and functional adaptations to different tissue environments. *Nat Immunol*. 2022;23(7):1121-1131. doi:10.1038/s41590-022-01229-8
56. Dangi T, Chung YR, Palacio N, Penaloza-MacMaster P. Interrogating Adaptive Immunity Using LCMV. *Curr Protoc Immunol*. 2020;130(1). doi:10.1002/CPIM.99
57. Nicklas W, Bleich A, Mähler M. Viral Infections of Laboratory Mice. *The Laboratory Mouse*. Published online 2012:427. doi:10.1016/B978-0-12-382008-2.00019-2
58. De Luca F, Shoenfeld Y. The microbiome in autoimmune diseases. *Clin Exp Immunol*. 2019;195(1):74-85. doi:10.1111/CEI.13158
59. Adawi M. The role of gut microbiota in autoimmune disease progression and therapy: a comprehensive synthesis. *Frontiers in microbiomes*. 2025;4. doi:10.3389/FRMBI.2025.1553243

60. Grebinoski S, Zhang Q, Cillo AR, et al. Autoreactive CD8+ T cells are restrained by an exhaustion-like program that is maintained by LAG3. *Nat Immunol*. 2022;23(6):868-877. doi:10.1038/s41590-022-01210-5